



University
of Glasgow

Fisher, John (1986) *Design development and evaluation of an improved pericardial bioprosthetic heart valve.*

PhD thesis

<http://theses.gla.ac.uk/3994/>

Copyright and moral rights for this thesis are retained by the author

A copy can be downloaded for personal non-commercial research or study, without prior permission or charge

This thesis cannot be reproduced or quoted extensively from without first obtaining permission in writing from the Author

The content must not be changed in any way or sold commercially in any format or medium without the formal permission of the Author

When referring to this work, full bibliographic details including the author, title, awarding institution and date of the thesis must be given

DESIGN DEVELOPMENT AND EVALUATION OF AN IMPROVED
PERICARDIAL BIOPROSTHETIC HEART VALVE

Volumes I and II

VOLUME I

John Fisher BSc MIMechE CENG ©

Degree of Doctor of Philosophy

University of Glasgow

Department of Cardiac Surgery
and
Department of Clinical Physics and BioEngineering

Faculty of Medicine

September 1986

TABLE OF CONTENTS

	Page
SUMMARY	16
Chapter 1: <u>INTRODUCTION</u>	19
1.1 Function of natural valves	
1.2 History of valve replacement	
1.3 Current valve developments	
1.4 Outline of the project	
Chapter 2: <u>LABORATORY TEST METHODS</u>	29
2.1 Laboratory tests	
2.2 Review of test methods and apparatus	
2.3 Theory of fluid flow	
2.4 Function test methods	
2.5 Standard test conditions	
2.6 Accelerated fatigue tests	
2.7 Fatigue test methods	
2.8 Summary	
Chapter 3: <u>EVALUATION OF THREE LEAFLET PERICARDIAL HEART VALVES</u>	44
3.1 Three leaflet pericardial valves	
3.2 Methods used to analyse valve designs and geometries	
3.3 Valve designs and descriptions	
3.4 Valve function tests	
3.5 Fatigue tests	
3.6 Discussion	

	Page
Chapter 4: <u>BOVINE PERICARDIAL TISSUE</u>	60
4.1 Introduction	
4.2 Bovine pericardial sac	
4.3 Mechanical properties of fresh tissue	
4.4 Mechanical properties of fixed tissue	
4.5 Fixation of tissue with glutaraldehyde	
4.6 Chemistry of aqueous glutaraldehyde	
4.7 Thermal denaturation temperature of fixed pericardium	
4.8 Discussion	
Chapter 5: <u>VALVE DESIGN</u>	83
5.1 Introduction	
5.2 Frame design	
5.3 Covering materials	
5.4 Leaflet design and configurations	
5.5 Discussion	
Chapter 6: <u>VALVE DEVELOPMENT I</u>	97
6.1 Introduction	
6.2 Frame development	
6.3 Leaflet geometry A and B	
6.4 Leaflet geometry C and D	
6.5 Discussion	

	Page
Chapter 7: <u>VALVE DEVELOPMENT II and</u>	112
<u>FINAL SPECIFICATION</u>	
7.1 Introduction	
7.2 Covering materials for the frames	
7.3 Closure of the leaflets at the posts	
7.4 Final specification	
7.5 Manufacture	
7.6 Discussion	
Chapter 8: <u>LABORATORY EVALUATION</u>	127
8.1 Introduction	
8.2 Hydrodynamic function tests	
8.3 Fatigue tests	
8.4 Discussion	
Chapter 9: <u>ANIMAL TESTS</u>	142
9.1 Introduction	
9.2 Methods	
9.3 General description of explanted valves	
9.4 Pathology of explanted valves	
9.5 Discussion	
Chapter 10: <u>DISCUSSION AND FURTHER WORK</u>	151
APPENDIX I: Standard conditions for function testing	157
APPENDIX II: List of publications	161
REFERENCES:	191
APPENDIX III: Microcomputer data acquisition system	214
APPENDIX IV: Calculation of energy loss	227

LIST OF TABLES AND ILLUSTRATIONS

VOLUME II

- Figure 1.1 Pressure signals for the left heart
- Figure 1.2 Starr Edwards ball and cage valve
- Figure 1.3 Bjork Shiley tilting disc valve
- Figure 1.4 Duromedics bileaflet valve
- Figure 1.5 Carpentier-Edwards porcine valve
- Figure 1.6 Ionescu-Shiley pericardial valve
- Figure 1.7 Explanted Hancock porcine valve
- Figure 1.8 Explanted Carpentier-Edwards porcine valve
- Figure 1.9 Explanted Ionescu-Shiley pericardial valve
- Figure 1.10 Explanted Carpentier-Edwards valve
- Figure 1.11 Six explanted Ionescu-Shiley low profile valves
- Figure 1.12 Two explanted Hancock pericardial valves
-
- Figure 2.1 Flow through an orifice plate
- Figure 2.2 Pulsatile flow test apparatus
- Figure 2.3 Mitral and aortic valve test sections
- Figure 2.4 Flow time waveforms of the pump
- Figure 2.5 Steady flow and column test apparatus
- Figure 2.6 Rowan Ash accelerated fatigue tester
- Figure 2.7 Test chamber of the Rowan Ash instrument
- Figure 2.8 Differential pressure waveforms in the fatigue tester

- Figure 2.9 Closing characteristics of the Ionescu-Shiley Low Profile valves
- Figure 3.1 Geometry of a three-leaflet valve
- Table 3.1 Key dimensions of three-leaflet valves
- Figure 3.2 Three dimensional plot of the leaflet geometry
- Figure 3.3 Size 29 mm pericardial valves
- Figure 3.4 Mean pressure difference plotted against RMS forward flow for pericardial valves
- Figure 3.5 Regurgitant volumes for pericardial valves
- Figure 3.6 Energy losses across pericardial valves
- Figure 3.7 Closed Ionescu-Shiley valves in the test apparatus
- Figure 3.8 Geometries of the open valve leaflets
- Figure 3.9 Results of accelerated fatigue tests for pericardial valves
- Figure 3.10 Four failed Ionescu-Shiley Low Profile valves
- Figure 3.11 Leaflets from failed valves
- Figure 3.12 Failed Ionescu-Shiley Standard valve
- Figure 3.13 Three failed Hancock Pericardial valves
- Figure 3.14 Two failed Mitral Medical valves
- Figure 4.1 Cast of the bovine heart

- Figure 4.2 Bovine pericardial membrane
- Figure 4.3 Frame of reference for the pericardial membrane
- Table 4.1 Thickness measurements for the membrane
- Figure 4.4 Polarised light micrograph of pericardium
- Figure 4.5 Orientation of the fibrils in the membrane
- Figure 4.6 Uniaxial force extension curves for fresh tissue
- Table 4.2 First load extension for fresh tissue
- Figure 4.7 Uniaxial force extension curves for fixed tissue
- Table 4.3 First load points for fixed tissue
- Figure 4.8 Absorbance spectra for glutaraldehyde
- Table 4.4 Absorbance of glutaraldehyde at 280 nm and 235 nm
- Table 4.5 Absorbance of glutaraldehyde at 280 nm for varying dilutions
- Figure 4.9 Variation in absorbance of glutaraldehyde solutions with time
- Figure 4.10 Absorbance of glutaraldehyde solutions with tissue added
- Figure 4.11 Variation in tissue shrinkage temperature with fixation time
- Figure 4.12 Stratographic analysis of tissue shrinkage temperature
- Figure 5.1 Design option 1

- Figure 5.2** Design option 2
- Figure 5.3** Design option 3
- Figure 5.4** Design option 4
- Figure 5.5** Design option 5
- Figure 5.6** Leaflet geometry A
- Figure 5.7** Leaflet geometry B
- Figure 5.8** Leaflet geometry C
- Figure 5.9** Leaflet geometry D
- Figure 5.10** Section through a closed leaflet
-
- Figure 6.1** Inner and outer valve frames
- Figure 6.2** Dimensions of pins, studs and washers
- Figure 6.3** Force-extension graphs for fixed tissue
- Figure 6.4** Leaflet template
- Figure 6.5** Shape of the valve frame posts
- Figure 6.6** Valve configuration A in the test apparatus
- Figure 6.7** Valve configuration B1 in the test apparatus
- Figure 6.8** Extension of the leaflet under pressure
- Figure 6.9** Valve configuration B3 in the test apparatus
- Figure 6.10** Size 27 mm mould
- Figure 6.11** Force-extension graphs for moulded tissue

- Figure 6.12** Leaflet configurations C1 and C2
- Figure 6.13** Valve configuration C1 in the test apparatus
- Figure 6.14** Valve configuration D1 in the test apparatus
- Figure 6.15** Valve configuration D2 in the test apparatus
-
- Figure 7.1** Cloth covered outer frame
- Figure 7.2** pericardial covered inner frame
- Figure 7.3** Fatigue test results for valves with different frame coverings
- Figure 7.4** Failed valves 27.1 and 27.2 after fatigue tests
- Figure 7.5** Leaflets from fatigued valves 27.1 and 27.4
- Figure 7.6** Valves 27.4 and 27.5 after fatigue tests
- Figure 7.7** Vertical section through open valve leaflets
- Figure 7.8** Horizontal section through the leaflets at the posts
- Figure 7.9** Stitch configurations A and B
- Figure 7.10** Closed valve in the test apparatus with and without stitches
- Figure 7.11** Open valve in the test apparatus with stitches

- Figure 7.12** Fatigue test results for valves with stitch configurations A and B
- Figure 7.13** Valves 27.6 to 27.9 after the fatigue tests
- Figure 7.14** Valves 31.1 and 31.3 after the fatigue tests
- Figure 7.15** Three dimensional diagram of the leaflet geometry
- Figure 7.16** Critical dimension for implantation of the valve
- Table 7.1** Key dimensions for the Glasgow valve
- Figure 7.17** Size 27 mm mitral valve
- Figure 7.18** Size 25 mm aortic valve
-
- Table 8.1** Critical dimensions for pericardial valves
- Figure 8.1** Leaflet movements in the test apparatus
- Figure 8.2** Valves in the steady flow test apparatus
- Figure 8.3** Size 25 mm valves in the test apparatus
- Figure 8.4** Graphs of mean pressure difference and RMS flow
- Table 8.2** Variation in EOA with flow
- Table 8.3** Comparison of calculated and actual orifice areas
- Table 8.4** Variation in mean pressure difference across ten size 25 mm valves
- Figure 8.5** Comparison of mean pressure difference across pericardial valves

- Figure 8.6** Regurgitant volumes for the Glasgow valve
- Figure 8.7** Comparison of regurgitant volumes for pericardial valves
- Figure 8.8** Comparison of energy losses across pericardial valves
- Figure 8.9** Fatigue test results for prototype valves manufactured to the final specification
- Figure 8.10** Failed valve 29.1 after fatigue tests
- Figure 8.11** Valves 29.2 to 2.5 after fatigue tests
- Figure 8.12** Valves 31.1 to 31.6 and 29.6 after fatigue tests
- Table 8.5** Hydrodynamic function before and after fatigue tests
- Figure 9.1** Explanted valve 1
- Figure 9.2** Explanted valve 2
- Figure 9.3** Explanted valve 3
- Figure 9.4** Explanted valve 4
- Figure 9.5** Explanted valve 5
- Figure 9.6** Explanted valve 6
- Figure 9.7** Explanted valve 7
- Figure 9.8** X-ray film of explanted valves
- Figure 9.9** X-ray film of explanted valve leaflets
- Table 9.1** Function test results for explanted valves
- Figure 9.10** Histological sections of valve leaflets before implant and after explant

- Figure A1.1** Pressure and flow waveforms in the test apparatus
- Figure A1.2** Variation in mean pressure difference for different time intervals
- Figure A1.3** Mean pressure difference for different pressure tappings
- Figure A1.4** Time reference points on pressure and flow waveforms
- Figure A1.5** Variation in regurgitation with valve orientation

ACKNOWLEDGEMENTS

This research work was funded by the Scottish Development Agency, Glasgow University, Biomedical Systems, Ltd., Bothwell, and the Greater Glasgow Health Board. I would like to acknowledge the encouragement, support and supervision given by Professor DJ Wheatley and Dr D J Wyper, and the technical assistance provided by Mr GR Jack, Miss L Cathcart, Mr I Douglas, Mrs AM Howie and Mr R Marshall. Advice and assistance with the scientific work was provided by Dr SD Gorham, Dr AL Evans, Mr IM Macdonald, Professor JC Barbenel, Mr P Zioupos, Dr C McCartney, Mr IJ Reece, Mr JM Anderson, and Mr TJ Spyt. Photography was performed by Mr F Spiers, Mr S Palmer and Mr P Harris at Glasgow Royal Infirmary, and the manuscript was typed by Mrs M Tosh.

WORK CARRIED OUT BY THE AUTHOR

The design and development of the heart valve function test apparatus was carried out by the author and the manufacture of the components for the test equipment was closely supervised by the author. The computer software for the test equipment was designed by Dr AL Evans and Mr I Macdonald to the author's specification. The author carried out the laboratory evaluation of commercial prosthetic valves and studies of failure modes and macroscopic pathology in explanted clinical valves. The author designed, developed, constructed and tested the prototype valves. Manufacture of the valve components and assembly of later prototypes was supervised by the author. The animal implants were carried out by Professor DJ Wheatley and Mr TJ Spyt, the function and macroscopic pathology of explanted animal valves were studied by the author, and microscopic pathology performed by Mr J Anderson. The author has also produced detailed design and manufacturing specifications for the valve and has supervised the establishment of production facilities for clinical valves. The author carried out or supervised investigations of the fixation conditions for the pericardial tissue, and macroscopic studies of the pericardial sac. Professor JC Barbenel and Mr P Zioupos (Strathclyde University) carried out biaxial and uniaxial studies of the mechanical properties of the tissue. Cloth for the valve was developed by Ms M Grimsley to the author's specifications.

During the course of this study the author has visited heart valve research facilities at the University of Sheffield; University of Edinburgh; Cardiac Development Laboratory, Victoria BC, Canada;

University of Washington, St Louis; Albert Einstein College of Medicine, New York; College of Technology, Atlanta (all USA), and the Helmholtz Institute of BioEngineering, Aachen, West Germany.

Publications relevant to this work and abstracts of papers presented at Meetings are listed in Appendix II.

SUMMARY

Pericardial bioprosthetic valves have shown good long-term clinical follow-up results over a period of 13 years with a low incidence of thrombo-embolism and calcification, and good haemodynamic function. However, doubts remain about the long-term durability of these valves and a significant incidence of primary tissue failure has been reported and this has been observed in our clinical series in Glasgow. I have identified tears in leaflets of explanted valves close to the edge of the cloth-covered stent which have caused prolapsed leaflets and large regurgitation.

The performances of four pericardial valves, the Ionescu-Shiley Standard, Ionescu-Shiley Low Profile, Hancock and Mitral Medical pericardial valves have been evaluated in my test apparatus in an attempt to gain understanding of the mechanisms of these primary tissue failures. A hydrodynamic function test apparatus has been developed which allowed pressure difference, regurgitation and energy loss across the valve to be measured, and leaflet dynamics to be studied. Durability tests were carried out with Rowan Ash accelerated fatigue testers. The valve function and leaflet dynamics were dependent on the method of leaflet fixation, and the leaflet geometries and the coaption sutures used to close the leaflets together at the top of the posts. These could also affect the durability of the valves. However, accelerated fatigue test results showed premature failure for all four types of valves with tears in the leaflets caused by abrasion at the edge of the cloth-covered frames. In the Ionescu-Shiley Standard valve, tears were also seen

at the commissure stitches. Although in these laboratory tests the mechanism of failure was abrasion and thinning of the leaflets as they were pulled over the edge of the cloth-covered frame, care has to be taken when extrapolating these results to clinical practice as biological effects, such as blood deposits on the cloth and tissue ingrowth, can reduce the abrasion to the leaflets at the edge of the frame. These processes are variable and leaflet abrasion on the cloth-covered frames remains the major cause of primary tissue failure in clinically explanted valves.

The new three leaflet pericardial valve which I have developed has improved durability and comparable function in vitro to existing valves. The valve is based on a unique twin frame design. The inner support frame is covered with a single piece of bovine pericardium to reduce abrasion to the leaflets at the edge of the frame and has an array of radially-projecting pins and studs onto which the leaflets are mounted. The outer frame is covered with polyester cloth and this is located over the same radial pins to retain the leaflets in position. The assembled valve is secured with a fine locking ring in the base of the valve. The sewing ring is constructed from polyester cloth and can be positioned towards the inflow aspect of the valve in the aortic position to give a supra-annular configuration and away from the inflow aspect in the mitral position to reduce the length of post projecting into the ventricle. The posts on the outer frame are rounded to reduce the risk of damage of the ventricular wall, and a protective suture can be placed across the top of the posts to reduce the risk of suture-snaring during implantation in the mitral position.

The mechanical properties of the pericardial tissue used for the leaflets have been investigated and fixation conditions analysed to produce uniform cross-linking throughout the tissue. Prototype valves have been tested with different leaflet geometries and differing methods of leaflet fixation, and an optimal leaflet geometry has been developed. The flexing position of the leaflet was moulded during fixation in a shape defined by two cylindrical surfaces which intersect in a spherical surface in the centre of the leaflet. This gave a stable closed position with deep coaption between the leaflets and synchronous movement of the leaflets to a uniform open position. Prototype valves have been manufactured in sizes 19 to 31 mm.

Hydrodynamic tests on the prototype valves have shown comparable pressure difference, regurgitation and energy loss to other pericardial valves. Accelerated fatigue testers have shown greatly improved durability with eight out of nine valves cycled to over 400 million cycles, the equivalent of 10 years without failure. Implantation of size 25 mm valves in the mitral position in seven sheep for over three months has shown good short-term in vivo function. A randomised clinical trial is planned comparing a porcine valve with this improved pericardial valve.

CHAPTER 1

INTRODUCTION

1.1 The function of natural heart valves

The four natural heart valves perform a similar but important mechanical function in allowing the blood to flow in one direction only. The mitral and tricuspid valves (atrio-ventricular valves) allow blood to flow into the ventricles from the left and right atria, whilst the aortic and pulmonary valves (the ventriculo-arterial valves) allow blood to flow out of the ventricles into the arterial systems. The sequence of the valves' opening and closing in the left ventricle is shown in Figure 1.1. As the muscular ventricle contracts, the pressure rises and the atrio-ventricular valve closes under the back pressure. Subsequently, the ventriculo-arterial valve opens to allow forward flow into the arterial system. At the end of systole, the ventricle relaxes and the ventriculo-arterial valve closes under the back pressure from the arterial system. As the ventricular pressure falls to almost zero, the atrio-ventricular valve opens to allow the ventricle to fill with blood from the atrium.

A normal valve has little resistance to forward flow and closes rapidly with little reverse flow. A valve will not function correctly if it becomes obstructive to forward flow (stenotic) or it fails to close correctly, allowing significant regurgitation. There are several causes of valve malfunction. Rheumatic fever is often followed by a chronic fibrosing reaction in the valve leaflets, causing stenosis due to stiffening of the leaflets and/or regurgitation. Infective endocarditis can cause a rapid degeneration

of the valve leaflets producing holes and tears and a large regurgitation. Stenosis of the valve leaflets can also be caused by calcification or, in a few cases, by congenital abnormalities in which the leaflets are not correctly formed.

The valves in the left heart are replaced most frequently. Stenosis and regurgitation in the mitral valve causes increased pressure in the atrium and pulmonary veins which results in lung congestion. Stenosis of the aortic valve causes an increase in the ventricular pressure during systole, left ventricular hypertrophy, and ultimately, ventricular failure. Aortic regurgitation also causes left ventricular hypertrophy, dilation of the ventricle and rapid loss of arterial pressure during diastole (1). These conditions can be detected by listening to the heart sounds, by radiology, nuclear medicine imaging, echocardiography, or by cardiac catheterisation.

1.2 History of valve replacement

Valve replacement first became feasible in 1954 when man-made materials were placed in the descending aorta (2) and extracorporeal circulation was developed (3). The first mechanical aortic valve was successfully implanted in 1960 (4) and this was soon followed by a mitral valve replacement (5). The first homograft tissue valves were implanted in 1962 (6,7) and at this early stage in valve surgery the division between mechanical valves and tissue valves was already established. Following the success of the ball and cage valve, a tilting disc mechanical valve was developed in 1968 (8) and a bileaflet valve was subsequently produced in 1976 (9). There have

also been significant developments in tissue valves. In the late sixties valves were fabricated from dura mater and fascia lata (10). The first bioprosthetic valve was produced in 1970 when a porcine aortic valve was chemically treated with glutaraldehyde and mounted inside a cloth-covered frame (11). In 1976 a three leaflet valve fabricated from glutaraldehyde-treated pericardium was developed (12). There are currently over twenty different valves available commercially. The majority of these fall into five main categories, three types of mechanical valves and two types of tissue valves (13).

The ball and cage valves were the first mechanical valves implanted. The Starr-Edwards valve (Figure 1.2) has been the most widely-used ball and cage valve. It has shown good durability and has the largest clinical follow-up (14). The valve has been improved by changing the material used for the ball and also the covering material on the struts. Its main disadvantages are that it is very obstructive to forward flow, it can cause haemolysis, and thrombus can build up on the struts.

The tilting disc valve shown in Figure 1.3 was designed to give less obstruction to forward flow than the ball and cage valve and to reduce the profile height of the valve (8). It has since been improved with the introduction of a pyrolytic carbon disc and an increased opening angle of 70° (15). There has been an occasional mechanical failure due to strut fracture, but overall the valve has a good clinical follow-up (16). Other tilting disc valves use different mechanisms for pivoting and retention of the disc.

The bileaflet mechanical valve (Figure 1.4) was developed in 1976 to give an improved forward flow pattern through the valve (17).

This valve has shown good clinical follow-up (18). The durability of all three types of mechanical valves is good, with only occasional cases of mechanical failure due to poor design or manufacture, or valve dysfunction caused by tissue ingrowth or clot formation. The main disadvantage of all these mechanical valves is that there is a significant incidence of thrombosis and haemolysis, and the patients require long-term anticoagulation therapy (19). These problems are caused by the central rigid occluder causing highly disturbed flow patterns and the use of synthetic materials which do not have ideal blood compatibility.

There are two types of bioprosthetic tissue currently in use. The porcine valve consists of a three-leaflet porcine aortic valve which has been chemically-treated with glutaraldehyde and sutured inside a cloth-covered support frame (Figure 1.5). The glutaraldehyde treatment cross-links the collagen in the valve leaflets, reduces its antigenicity and prevents biological degradation (20). More recently it has been shown that glutaraldehyde treatment can alter the mechanical properties of the tissue (21). Two valves, the Carpentier-Edwards and the Hancock porcine valves, have shown good long-term clinical results (22,23). As the whole porcine valve is mounted inside a support frame the orifice of the valves is rather small. This gives higher pressure drops during forward flow. The valve performance has been improved slightly with low pressure fixation of the leaflets which give greater tissue extensibility and modification to the orifice to remove the muscle shelf on the right coronary leaflet (24).

The second type of tissue valve is the three-leaflet pericardial

valve (Figure 1.6). The leaflets are fabricated from bovine pericardium, which has been treated with glutaraldehyde, and are sutured onto the outside of a cloth-covered frame (25). This gives a larger orifice for forward flow than the porcine valves (26). The long-term clinical follow-up on these valves has been reported to be good (27) but there has been a significant incidence of leaflet failure due to tearing close to the edge of the cloth-covered frame in both the mitral (28,29) and aortic (30) positions. Unpredictable durability is the main disadvantage of both types of tissue valves. Figure 1.7 shows a Hancock porcine valve explanted after eight years with a tear in the belly of one leaflet, and Figure 1.8 shows a Carpentier-Edwards valve explanted after five years with a tear at the commissure causing a prolapsed leaflet. An Ionescu-Shiley pericardial valve explanted after four years with a tear in the leaflet at the top of a post is shown in Figure 1.9. Tissue ingrowth can also cause problems by obstructing the valve orifice (Figure 1.7). Calcification can seriously reduce the lifetime of a tissue valve by making the leaflets less flexible and obstructive and this can also result in leaflet tears. Figure 1.10 shows a heavily calcified Carpentier-Edwards valve explanted after six years. An additional disadvantage of tissue valves is that variation in the biological tissue and the precision required in valve assembly can cause high rejection rates in production. These disadvantages have to be compared with the disadvantages of mechanical valves (19). It is clear that the ideal heart valve prosthesis does not exist (31,32).

1.3 Current developments in valve technology

There have been few new developments in mechanical valve design since the introduction of the bileaflet valve in 1978 (18). The Bjork-Shiley valve has been modified recently to eliminate mechanical weakness in the struts. There have however been significant developments with tissue valves (33). Anticalcification treatments have been developed (34,35) which are currently being tested in clinical trials for both porcine and pericardial valves. As calcification is a long-term failure mode, the results of these trials will not be available for several years. Although several new porcine valves have been developed (36) the designs show little improvement over clinically-proven valves. Low pressure fixation of the tissue has been used to improve pressure gradients, and to improve durability and modified orifice, supra-annular and composite valves have also been developed. Major improvements in this type of valve may be dependent on finding a more durable valve from a different animal (37).

There have been significant changes in valves fabricated from pericardium. Four new pericardial valves have been commercially developed since 1980; the Ionescu-Shiley Low Profile (ISLP), the Hancock Pericardial valve (HP), the Mitral Medical valve (MM) and the Edwards Pericardial valve (EP). All the valves have undergone initial clinical trials with up to three years follow-up in some cases (38). These valves have a lower post height or profile than the original Ionescu-Shiley valve which reduces the risk of damage to the ventricular wall from the tips of the posts in the atrio-ventricular

position. The Ionescu-Shiley Low Profile, Hancock, and Mitral Medical valves mount the pericardial leaflets by suturing them to the outside of a cloth-covered frame. There are significant differences between these three valves in the design of the frames and leaflets, and also in the technique used for preparing tissue. The Edwards Pericardial is fundamentally different to the other valves as the leaflets are sutured inside and underneath an egiloy wire frame. The in vitro function of all four valves is reported to be similar (39) but initial results in clinical trials show that there are significant differences in the performance of these valves. In a clinical trial in Glasgow of 105 Ionescu-Shiley Low Profile and 98 Hancock Pericardial valves started in 1982 (40,41 - Appendix II) there have been six Ionescu-Shiley Low Profile valves explanted due to primary tissue failure and two Hancock valves explanted due to primary tissue failure. Five of the Ionescu-Shiley Low Profile valves explanted had torn leaflets adjacent to the top of the post and the sixth valve had a leaflet which stretched abnormally circumferentially at the free edge (Figure 1.11). In all six cases the damaged leaflets were prolapsed below the other two leaflets causing large regurgitation. Close examination of these explanted valves did not reveal any clear indication of the cause of the primary tissue failure. The Hancock group showed two similar failures with tears in the leaflets adjacent to the top of the posts causing the leaflet to prolapse (Figure 1.12). Primary tissue failures have been reported from other clinical centres (42) with this valve. The clinical experience with the Mitral Medical valve is limited but one Centre has shown no primary tissue failure with three years follow-up (43).

Likewise, with the Edwards pericardial valve, limited clinical trials have shown no valve failures (30,44,45).

Some laboratory investigations have been carried out into the mode of failure of pericardial valves using accelerated fatigue testers. Gabbay has shown early failures in fatigue testers (46) with the Standard Ionescu-Shiley valves and has compared his results with his clinical experience (47). Similar failures have been reported by other Centres (27,48). Gabbay proposes that abrasion of the leaflets on the cloth is the main cause of the failures. This may be an explanation for early failures in vitro, but may not be true in vivo if blood deposits and host tissue smooth over the cloth, or if host tissue reinforces the leaflets. Walker and Scotten have also identified similar failures in vitro in the Ionescu-Shiley and Mitral Medical valves (49,50). In each case tissue failure close to the edge of the frame was the common factor. Cosgrove (30) proposes that tissue failure with the Ionescu-Shiley valve in the aortic position originates from the commissure stitches close to the top of the posts, whereas Martin proposes failures due to abrasion on the buttress on the outside of the post (51). Shiley Incorporated have indicated that two dimensional flexion of the leaflet close to the edge of the frame, or bending of the tissue around the top of the post, may cause mechanical tears (52). This would be consistent with some theoretical stress analysis (53). More recently, however, Ionescu has reported improved durability of the Ionescu-Shiley Low Profile valve over the Standard Ionescu-Shiley valve (27). He also describes further developments with a Mark 3 Ionescu-Shiley valve which uses pericardial patches to cover over the cloth at the edge of the frame

in the area over which the leaflet flexes. This new valve has shown improvement in durability and has undergone restricted clinical trials (54). In a bicuspid pericardial valve, Black et al have shown that placement of sutures close to areas of tissue flexion can significantly reduce the durability of the tissue (55). A new bicuspid pericardial (56) and monocusp (57) valve are also under development.

The general clinical experience of the new pericardial valves is good and they show better haemodynamic (26) and hydrodynamic (39) function than the porcine valves. Several reports have suggested that their long-term clinical durability is variable but laboratory tests have been unable to predict clinical lifetimes (27,58,59). In particular, leaflets are likely to fail close to the edge of the frame. Three possible causes have been suggested - abrasion of the leaflets on the cloth-covered frame, tears originating from sutures, and bending or flexion stresses at the edge of the leaflet. In addition, failures have been seen clinically due to abnormal extension of the tissue. The variable durability seen in vivo and in vitro between the different types of valves is probably due to the differences in design and construction and may also vary with valve size and the position in which the valve is used. The failure modes require further investigation and analysis in order that a more durable pericardial valve can be developed.

1.4 Outline

The design, construction and function of existing pericardial valves will be investigated with particular reference to their mechanical function and durability. The function of the valves will be investigated in detail in a pulsatile flow test apparatus and the construction, design, and tissue preparation methods used will be analysed. This information will be used in an attempt to explain the failures seen clinically in Glasgow and other Centres and also the results of fatigue studies being carried out in Glasgow and elsewhere.

These studies will form the basis for the design construction and evaluation of an improved three-leaflet pericardial valve which will have better mechanical durability than existing valves. The new valve design will be tested in the pulsatile flow test apparatus and fatigue testers in the laboratory, and will undergo animal studies.

CHAPTER 2

LABORATORY TEST METHODS

2.1 Laboratory tests

Laboratory tests have been carried out primarily to assess the mechanical function and durability of prosthetic heart valves. The function of existing commercial valves has been assessed in a number of centres by measuring pressure difference across the valve during forward flow, regurgitant volumes and energy losses under pulsatile and steady flow conditions (60,61,62). Fluid velocity fields around prosthetic valves have also been studied using flow visualisation and laser doppler anemometry (63,64) in attempts to predict areas of thrombus formation and haemolysis. High speed ciné photography has also been used to study valve dynamics (65,66). Accelerated fatigue tests have been used to study the mechanical durability of valves and some mechanisms of failure have been identified (51). Conditions for these tests have not been standardised, and different approaches have been used to simulate complex physiological cardiovascular mechanics. However, little effort has been directed towards incorporating biological effects into these tests (67). Materials used in prostheses have been assessed for biocompatibility, thrombogenicity, antigenicity, toxicity and calcification, and animal tests have been used for final assessment of the prostheses prior to clinical implantation (68).

The laboratory tests can give very detailed information about valve performance and are an important stage in the development of a

new prosthesis. The test methods and apparatus which I have developed to analyse valve function and durability are described in this chapter.

2.2 Review of function test apparatus and methods

The apparatus and methods currently used to test the function of prosthetic heart valves have become more sophisticated than the initial test rigs developed in the 1960's (69,70). Current test apparatus can be considered in four sections.

- i Pump
- ii Test sections and valve chambers simulating the left atrium, ventricle and aortic root
- iii Afterload simulating the aorta, systemic and peripheral circulation.
- iv Measuring instruments and data processing

Two different types of pulsatile pump have been used to drive the test rigs, neither of which perfectly models the complex pumping action of the left ventricle (71). Positive displacement pumps have been used to produce flows in the rig which are independent of load, whereas pressure generators have been used to control the ventricular pressure, but the volume displaced is always dependent on the load. The ventricle can be considered a combination of both these systems, as during systole the source impedance is about ten times the load so can be approximated by a positive displacement pump (72), whereas

during diastole, flow through the mitral valve is primarily controlled by the atrial pressure. The displacement pumps used have varied from simple reciprocating sinusoidal pumps (73,74,75,76) to servo-controlled piston pumps (77,78) which can be programmed to simulate physiological flow waveforms. The pressures generated by these pumps are dependent on the load and dynamic characteristics of the test apparatus. Pressure generators have produced physiological pressure waveforms (79,80,81,82) but the flow through the valve under test is difficult to control. Elastic components have been introduced into some positive displacement pump chambers (83,84) whilst other systems have allowed positive displacement pumps to fill under static pressure (85,86).

The chambers used for testing the valves are a critical part of the apparatus. Geometry affects both the boundary conditions for flow and inertia and resistance of the fluid flow, which combined with the compliance in the system determine the dynamic pressure or flow waveforms produced in the test rig. Cylindrical rigid test sections have been widely used (79,80,87) and only the geometry close to the valve has been modelled on physiological data. Uniform flow patterns are produced by flow straighteners upstream of the valve under test. These systems have the following advantages:

They provide reproducible flow patterns; an electromagnetic flowmeter can be used to measure instantaneous flow through the valve; and there is good visibility of the valve under test:

while the main disadvantages are that flow patterns in the left ventricle are not modelled and the inertia of the fluid in the rigid tubes can distort the pressure waveforms.

The ventricle has been modelled with a shaped rigid chamber (74,88) or a flexible ventricle (78,81,89,90). In both these cases it is more difficult to determine the flow through the valve under test.

A simple lumped parameter afterload has been used to simulate the arterial system and peripheral circulation (91,92,93). A compliant aorta (62,72), curved aorta (94) and branching arterial tree (95) have all been modelled in different studies. A 4% water glycerine solution has been used to match the density and viscosity of blood but it can affect the mechanical properties of some tissue valves. It has been shown that viscous losses are small (94,80) and that a physiological saline can produce satisfactory results.

Microcomputers have been extensively used to digitise, store and analyse pressure and flow signals from the test rigs (63,77,96). The mean pressure difference across the valve during forward flow is a more reproducible measurement than peak pressure (97) and this should be plotted as a function of root mean square (RMS) forward flow (63,98). Root mean square (RMS) flow is used as the pressure difference across an orifice is proportional to the flow squared. The mean pressure difference across large valves is low (typically 1 to 2 mmHg) and has to be measured while the pressure in the ventricle oscillates up to 150 mmHg. Pulsatile flow pressure measurements have been supplemented with steady flow pressure measurements which can be made with greater accuracy (89,99,100). Similarly, the leakage

through a closed valve is small (1 to 5 ml.s⁻¹) and can often be measured more accurately under a static back pressure (61). The position of the pressure measurements, area of the test sections and valve orientation can all affect the pressure measurements (88,100). The flow through the valve has been measured directly with an electromagnetic flow probe (61,80,87) but can also be derived from the pump signal (62). If the flow is measured directly the regurgitation while the valve is closing and when the valve is closed, and the energy losses across the valve, can be calculated (78,80).

Most test rigs have been manufactured from polished acrylic to allow good visibility of valve dynamics, and high speed ciné and still photography (65,79) have been used to record valve movements. Small particles, gas bubbles or dye injection, have been used for flow visualisation (79) and laser doppler anemometry has been used to measure fluid velocity fields downstream of valves (63,64,101,102, 103).

2.3 Theory of fluid flow

The relationship between the pressure across and flow through heart valves and also the flow patterns and dynamic forces which affect opening and closure of the valves have been described in detail. In engineering studies the pressure differences across orifices of known geometry has been accurately predicted for a range of flows in order that flow can be metered from the pressure measurements. For a simple orifice plate in a pipe (Figure 2.1) assuming steady streamline flow and an incompressible inviscid fluid

with no loss of mechanical energy, the pressure difference between points 1 and 2 can be predicted from Bernoulli's equation (104).

$$P_1 - P_2 = \frac{1}{2} \rho \frac{Q^2}{A_2^2} \left\{ 1 - \frac{A_2^2}{A_1^2} \right\} \quad 1$$

P_1, P_2 are the pressure at points 1 and 2, Q is flow, ρ is density of the fluid and A_1, A_2 is the cross sectional area of flow. If A_0 is the orifice area then $A_2 = C_c A_0$, $C_c < 1$.

Loss of static pressure is due to conversion of potential energy to kinetic energy. If small viscous losses occur and an empirical constant C_v (which is less than one) is used to account for these losses, then

$$P_1 - P_2 = \frac{1}{2} \frac{\rho Q^2}{C_v^2 C_c^2 A_0^2} \left\{ 1 - \frac{C_c^2 A_0^2}{A_1^2} \right\} \quad 2$$

If $A_1 \gg A_0$ and a discharge coefficient is defined as

$C_d = C_v C_c$ then

$$P_1 - P_2 = \frac{1}{2} \rho \frac{Q^2}{C_d^2 A_0^2} \quad 3$$

Downstream of the orifice the pressure is more difficult to predict as there is significant turbulence and energy loss. Equation

3 has been used to predict the area A_0 of stenotic mitral valves (105,106). However, several assumptions have to be made to calculate the discharge coefficient for in vivo measurements.

Under pulsatile flow conditions the pressure difference across a test valve has been described by equation 4 (90,98,107,108,109)

$$P_1(t) - P_2(t) = \frac{\rho Q^2}{2 C_d^2 A_0^2} + \rho B \frac{dQ}{dt} \quad 4$$

where B is a constant dependent on the inertia of the fluid between the pressure measurement points. The pressure at point 3 downstream of the aortic valve has also been predicted (110).

Equation 4 reduces to equation 3 if pressure and flow measurements are made at the time of peak flow ($dQ/dt = 0$) or if a time average of the signals is taken between the points of zero flow. Under either of these conditions the area of the valve can be expressed as:

$$A_0 = \frac{Q}{C_d \sqrt{\frac{2(P_1 - P_2)}{\rho}}} \quad 5$$

Unlike the fixed geometry of an orifice plate where C_d can be defined precisely, the discharge coefficient will vary from valve to valve. This is eliminated if an effective orifice area is used (87).

$$EOA = C_d A_o = \frac{Q}{\frac{\sqrt{2(P_1 - P_2)}}{\rho}} \quad 6$$

In tissue valves A_o increases with flow as the increased pressure difference forces the leaflets to open wider (62) in these cases.

$$P_1 - P_2 = A Q^c \quad 7$$

$$1.5 < c < 2$$

The inertial forces shown as (BdQ/dt) in equation 4 play an important role in the closure of the valve. During the deceleration phase of forward flow this term becomes negative and P_2 becomes greater than P_1 . This reverse pressure starts the closure of the valve whilst there is still forward flow (111,112) so reducing the amount of dynamic regurgitation. This early closure has also been attributed to vortex formation within the sinuses of the aortic valve (113,114) but this has been contradicted by experimental evidence (112).

2.4 Function test methods

The pulsatile flow test apparatus which has been developed has been described in detail elsewhere (115, Appendix 2) and is shown in Figure 2.2. Essential features of the apparatus were:

The pulsatile flow was produced by a servo-controlled piston pump [Cardiac Development Laboratories] (78) which was controlled by a programmable waveform generator.

The flow through either valve was measured with an electromagnetic flowmeter (Gould SP2201) which was modified to give a frequency response of -6dB at 100 Hz.

The valves were mounted in rigid test chambers and pressure measurement ports were positioned every 25 mm downstream and upstream of the valves (Figure 2.3).

The mean differential pressure across the valve under test was measured with a differential transducer (Gaeltec 3CT special) and direct pressure measurements were made on the atrial, ventricular and aortic test sections to establish the correct test conditions.

The fluid medium used for all tests was physiological saline (0.9% sodium chloride solution).

Five different flow conditions were used for the tests which varied from a stroke volume of 60 ml and rate of 60 min⁻¹ to a stroke volume of 80 ml and 120 min⁻¹ (Figure 2.4). These correspond to cardiac outputs of between 3 and 8.5 l min⁻¹.

Seven signals (four pressure, flow and the displacement and velocity of the pump) were collected for a period of 20 seconds on an Apple 11 computer. Details of the computer software will be reported

elsewhere (116, Appendix III)). The computer calculated the average waveform for each of the seven signals. These were stored on a floppy disk and plotted on an Anadex printer.

The computer calculated the mean pressure difference, mean forward flow and root mean square forward flow (RMS) and effective orifice area for different time intervals during forward flow. It also calculated the volume of fluid passing through the valve during forward flow, and the regurgitant volumes (dynamic regurgitation while the valve was closing, static regurgitation while the valve was closed). The energy loss during each phase of the cycle was also calculated as described in Appendix IV.

Visual recordings of valve movements were made from a Panasonic AI video camera, JCV video cassette recorder CR 6650 and Barco colour monitor. Valves were viewed from the end and the side of the test sections and movements analysed with still frames every 20 ms. Valve movements were also recorded using synchronised flash photography. An electronic delay unit triggered from the pump signal was used to fire an electronic flash gun linked to a 35 mm SLR camera. This allowed still photographs to be taken every five ms while the valve was opening or closing.

Pulsatile flow measurements were supplemented by steady flow pressure difference measurements and static back pressure leakage measurements. The test apparatus used for the tests is shown in Figure 2.5. The steady flow test rig was a modification of the pulsatile flow test rig. The pump produced a static pressure difference between the two reservoirs which in turn produced a steady flow through the two valves. In the column test apparatus, a static

back pressure of 100 mmHg was applied to the valve and the leakage measured by collecting the fluid leaking through the closed valve.

2.5 Standard test conditions

Variation in results from different test apparatus show that condition of the test can significantly affect the results. The main factors affecting the forward flow pressure difference results are time interval during forward flow used to average the signal, position of the pressure measurements and valve orientation, whereas the regurgitant volumes are affected by definition of the dynamic regurgitation, valve orientation and shape of the pressure waveform. Experiments were carried out to determine the affect of these variables on the results (Appendix 1). From these tests the following standard set of test conditions were specified:

- i Mean differential pressure and RMS flow measured during the pressure flow and pressure-pressure intervals.
- ii Upstream pressure measurements were made 25 mm from the mitral valve and 50 mm from the aortic valve, and the downstream measurements were made 50 mm from both valves.
- iii Pressure measurements were made in the minor orifice of tilting disc valves, the major orifice of bileaflet valves and adjacent to the stent in tissue valves.
- iv The end of dynamic regurgitation was defined as the lowest negative flow, prior to the constant leakage.
- v Mechanical valves were tested with the discs or leaflets opening in the horizontal plane in order that gravity had no effect.

vi The valves were tested without compliance in the ventricular chamber.

The apparatus has been used to test the function of a range of prosthetic valves in both the mitral and aortic positions. The results of these studies have been published (117,118 - Appendix 2).

2.6 Accelerated fatigue tests

Accelerated fatigue testing remains the only way of assessing valve durability in a reasonable period of time prior to clinical implant. Valves have been tested at between 10 and 20 Hz which allow forty million cycles (equivalent of one year's lifetime) to be completed in 23 to 46 days. At these rates it is impossible to simulate physiological flows, volumes and pressure waveforms precisely. The cycle rate depends on the speed at which the valves can open and close. This is much lower in mechanical valves which have larger inertia in the moving parts (89). Although early fatigue studies were completed in 1964 (119,120) there has been little published data on valve durability. Recently, interest in the durability of bioprosthetic valves has increased (51) and four different test systems are currently being used. Test conditions have not been standardised and comparative studies of the durability of the same valves in different instruments have not been published.

Two fundamentally different principles have been used in the design of these instruments. In three of the four instruments the fluid is pulsed through a stationary valve, whilst in the fourth the valve is moved through a stationary column of fluid. In the

instrument developed by Swanson (48) and marketed by Dynatek, a rotating shaft with a small slot allows fluid from a high pressure reservoir to pulse through six valves simultaneously, whereas in the system developed by Haussinger (87,121) up to six valves are opened sequentially by a rotating slit disc. In the system manufactured by Shellhigh Co, fluid pulses are produced by a rotating cam acting on polyurethane bellows (46).

In the most widely used test instrument (Rowan Ash accelerated fatigue tester 51,122) the valves are oscillated through stationary columns of fluid. The displacement of the valve determines the flow and the back pressure on the closed valve is adjusted independently. This instrument was selected for our fatigue studies.

2.7 Fatigue test methods

The Rowan Ash accelerated fatigue tester is shown in Figure 2.6. The machine cycled up to six valves at rates between 10 and 20 Hertz. The principle of operation is shown in Figure 2.7. Each valve was mounted on a hollow piston which oscillated through a stationary column of fluid (0.2% buffered glutaraldehyde). On the upward stroke of the piston the valve closed and pushed fluid around the recirculation tube and the variable resistance was used to adjust the closing pressure on the valve. On the downward stroke the valve leaflets opened fully. The displacement of the piston was adjusted to give maximum opening of the valve and full closure. Typically the amplitude was set to 3 to 4 mm which corresponded to peak flows of 20 to 27 l min⁻¹ (330-450 ml s⁻¹). The valve movements were viewed

using a synchronised strobe light and photographed using a 35 mm SLR camera.

The pressure difference across the valve was measured with a Gaeltec 3CT special differential transducer, which was driven by a Gould (13 4615-85) pressure amplifier in a series 8000 recorder. The signal from the amplifier was linked to an oscilloscope and the pressure waveform photographed using a polaroid camera. The Gaeltec transducer had a volume displacement of $0.7 \text{ mm}^3/100 \text{ mmHg}$ which when connected to a rigid tube (diameter 2 mm, 100 mm long) gave a resonant frequency of 125 Hz. This was measured with reference to a catheter tip transducer using a Siemens pressure generator. The pressure signal was filtered electronically to give a flat response ($\pm 25\%$) up to 135 Hz. The peak closing pressure was set between 100 and 130 mmHg. This was achieved by gradually increasing the pressure during the initial 2 million cycles of the test. The valves were cycled at 12 Hz and viewed three times a week. Pressures were checked and adjusted every week (8 million cycles) and the machine stopped after every 160 million cycles or at valve failure and the valves taken out, inspected and photographed.

Differential pressure waveforms for two 29 mm ISLP valves are shown in Figure 2.8. The differences in the shape of the waveforms were caused by interactions between the valves and the machine. The rapid rise in pressure as the valve closed was due to the inertia of the fluid which was recirculated around the chamber. This was highest for the first valve to shut (Figure 2.8a) and was lower for the valve which shut last (Figure 2.8b). In this case the second peak was set to the maximum closing pressure by increasing the

resistance in the recirculation circuit. A catheter tip transducer placed in the chamber above the valve showed that there were high frequency pressure oscillations (greater than 100 Hz) which may cause localised pressure gradients greater than 130 mmHg.

At these accelerated rates the leaflet movements differed from the movements recorded in the function tester at normal heart rates. At normal rates the leaflets moved to the fully closed position in approximately 60 ms whilst in the fatigue tester closure occurred in about 10 to 20 ms. As the leaflet moved to the closed position in the fatigue tester the free edge of the leaflet lagged behind the belly causing a sharp bend or kink along the radial axis of the leaflet. This did not occur in the function tester. This is shown in Figure 2.9 for size 29 mm ISLP valves photographed just before full closure in the fatigue tester and function tester.

It is not known whether this abnormal leaflet action affects the valve durability or whether the different pressure waveforms described previously affect the results of the test.

2.8 Summary

Apparatus and methods have been developed to perform mechanical function and durability tests on prosthetic heart valves. The function tests allowed the mean pressure difference during forward flow, regurgitant volumes, energy losses, valve dynamics and flow visualisation to be studied under standard conditions. Results of these tests on commercial valves have been published. A commercially available fatigue tester (Rowan Ash) has been used for the durability studies.

CHAPTER 3

EVALUATION OF THREE-LEAFLET PERICARDIAL VALVES

3.1 Three leaflet pericardial valves

Current designs of three-leaflet pericardial valves have evolved from valves fabricated from pieces of fresh tissue such as fascia lata sutured onto cloth-covered frames (25). Three leaflets have been used to mimic the geometry of the natural aortic valve where the width of each leaflet at its free edge is approximately equal to the diameter (d) of the orifice which allows the leaflets to open to the full circumference of the orifice. Clinical results with commercial pericardial valves were described in Section 1.4. The first valve manufactured, the Ionescu-Shiley Standard (ISU) valve has 13 years clinical follow-up (38) and has shown a significant incidence of tissue failure (46) with tears adjacent to the cloth-covered frame. Early clinical results have shown similar primary tissue failure with two low profile pericardial valves, the Hancock Pericardial (HP) and Ionescu-Shiley Low Profile (ISLP) whilst two other pericardial valves, the Mitral Medical Mitroflow (MM) and Edwards pericardial (EP) have not shown tissue failures clinically. The MM valve has shown tissue failures in accelerated conditions in the laboratory (49). Various mechanisms for clinical tissue failure have been discussed but the precise reasons are not clear and correlations between clinical and laboratory studies are variable (46,47).

In this chapter the design, construction function and durability of four pericardial valves which were commercially available in 1984

have been studied (ISU, ISLP, HP, MM). In addition, the design features of two newer three-leaflet valves, EP and Ionescu-Shiley III (ISIII) and two new bileaflet valves are discussed. The results of function and durability tests and clinical experience with explanted valves have been used to identify key areas of design and construction in these valves.

3.2 Methods used to analyse valve designs and geometries

A considerable number of studies have been made of the geometry, leaflet dynamics and stress analysis of both fresh and glutaraldehyde-treated aortic valves, but few studies have been made of fabricated leaflet valves. The geometry of natural valves has been extensively described (123,125) and the material properties of the leaflets have also been studied (126-129). Simple membrane and thin shell theories have been used to analyse the stress in closed valve leaflets described by two principal radii of curvature (130,131) and by ellipsoids of revolution (132). Finite element stress analysis has also been used for the closed aortic valve (133-136). Membrane and bending stresses in both the closed and open positions have also been studied by Thubrikar (137,138). The results of this stress analysis were highly dependent on the anisotropic, non-linear visco-elastic leaflet properties, the leaflet geometry, the boundary conditions applied, the leaflet thickness and the method of analysis used. These studies have revealed a number of important features of the natural and glutaraldehyde-treated aortic valves.

i The leaflets grow in a complex shape with a variable radius of

curvature. The natural geometry is a prime determinant of the membrane stresses in the closed position. The leaflets coapt over a large area well below the top of the leaflets at the commissures.

- ii The leaflets grow radially outwards from the aortic wall and are thickest at the points of attachment particularly close to the commissures where the membrane tension is highest, and thinnest in the belly of the leaflet where the tissue undergoes maximum bending.
- iii The leaflet material is anisotropic and is more extensible radially than circumferentially, but shows a higher ultimate tensile strength circumferentially than radially. This gives a more stable closed position with increased coaption caused by additional radial extension, whilst the high circumferential stresses at the commissures act along the stiffer stronger axis. In transposing from the open to the closed position and vice versa, the increased radial extension allows the leaflet to buckle in a S shape along its radial axis as described by Swanson (124).
- iv The wall of the aorta expands during systole to create a larger orifice. This effectively straightens out some curvature in the leaflet giving a more stable open geometry.
- v The leaflet is not supported along its free edge and the radial stresses diminish rapidly towards the top of the leaflet, which produces high unidirectional stresses circumferentially towards the top of the commissures or posts. The magnitude of these stresses is highly dependent on the geometry of the leaflet

close to the coaption area.

- vi Fixation of tissue under tension reduces its extensibility and flexibility. This may cause increased bending stresses and tissue failure (126).

Designs of existing pericardial valves are considerably different to the natural valves and few detailed studies of their design have been published. An optimal geometry for a valve leaflet fabricated from synthetic material has been described using a shell defined by two principle radii of curvature (140-141) and the stresses in the leaflets of an ISU pericardial valve have been analysed by assuming a cylindrical geometry (53). These fixed geometries cannot account for changes in geometry caused by extension of the leaflet material under back pressure. Similarly, defining a fixed open geometry does not allow for changes in the geometry or strain caused by variable tissue properties.

The studies of natural aortic valves would indicate the following areas to be particularly important for pericardial valves:

- i The geometry of the unloaded leaflet (its natural shape). This is determined by the shape formed during fixation with glutaraldehyde and/or the shape formed in the leaflet when mounting it on the frame.
- ii The geometry of the leaflet under back pressure in the closed position. In particular the area of coaption between the leaflets when closed as this not only seals the valve but also affects the leaflet stability and stresses in the closed position.

- iii The geometry of the leaflet in the open position and the dynamics of moving between the open and closed, and closed and open positions.
- iv The mechanical properties of the leaflets (thickness and extensibility) which depend on selection of fresh tissue and fixation conditions.
- v The frame geometry and flexibility.
- vi The covering material used on the frame.
- vii The method of attachment of leaflet to frame.

It is also important to define a number of parameters to describe the valve geometry. The size of the valve quoted as the tissue annulus diameter (TAD) cannot always be related to a particular dimension of the valve. Figure 3.1 shows some key dimensions. The external diameter of the frame, D_o , should be defined at the base and the top of the posts for a tapered frame. The internal diameter of the frame, D_i , is measured in the base of the valve. The overall height of the valve is H and h is the height of the scallop over which the leaflets flex. W defines the width of the top of the posts and a radial view on post B indicates the shape of the post. The outline of the unloaded leaflet AOBC is shown with a dotted line, and a vertical section through OC defines the radial radius of curvature R_r . A vertical section through OB shows the area of coaption between the unloaded leaflets. The circumferential radii of curvature is defined by R_c . An additional parameter, H_i , is the implantation height for a mitral valve and is defined as the distance from the top of the sewing ring to the top of the posts.

A three dimensional plot of the leaflet can be generated by measuring vertical and horizontal sections every 2.5 mm through the unloaded leaflet. This is illustrated in Figure 3.2.

3.3 Valve designs and descriptions

i Ionescu-Shiley Standard Valve (ISU)

A photograph of a size 29 mm ISU mitral valve is shown in Figure 3.3 and has been described in (25,142-144). The three pronged frame was manufactured from rigid titanium and covered with a polyester cloth. The leaflets were manufactured from bovine pericardium, fixed in glutaraldehyde in its natural shape and stitched onto the outside of the cloth-covered frame. The key dimensions for a size 29 mm mitral valve are given in Table 3.1. The frame was slightly tapered and the outside diameter D_o was 1 mm greater at the top of the posts in the 29 mm valve. In the aortic valve the taper was greater with the outside diameter D_o increased from 23 to 27 mm in a 23 mm valve. The leaflets were sealed together with a coaption stitch inside the top of each post which also pulled the leaflets into the closed position. In addition, the valves were stored with spherical cotton balls restraining the leaflet in the closed position making the natural position of the unloaded leaflet closed. The tissue thickness was approximately 0.35 mm.

ii Ionescu-Shiley Low Profile Valve (ISLP)

This valve is shown in Figure 3.3 and described in (52). It had an improved design compared to the ISU valve with a flexible

cylindrical stent manufactured from acetal. The heights H and h of the stent and leaf were reduced by approximately 1 mm (Table 3.1) for the 29 mm valve, but the leaflets were no longer cut away towards the centre, so the height to the centre of the leaflet at the coaption depth remained similar to the ISU. As with the ISU valve, the tissue was fixed in its natural shape and then mounted on the frame. The main difference was in the design of the stent post and attachment of the leaflet at the top of the post. In the ISLP, the post projected into the orifice at the top of the post which allowed two coaption stitches to pass through the post and the leaflets. The new design was claimed to give improved durability over the ISU valve (38) and better hydrodynamic performance. The leaflet thickness varied from .55 to .35 mm in the size 29 mm valves.

iii Hancock Pericardial Valve (HP)

The HP valve is shown in Figure 3.3. The valve had a flexible stent manufactured from polypropylene with a low overall height, H (Table 3.1). The stent post profile differed from the Shiley stents in that the posts were a triangular shape tapering away to a rounded point at the top, which eliminated the parallel portion found at the top of the Shiley posts. The tissue projected about 1 mm above the top of the posts where the leaflets were sealed with a coaption stitch. A small stitch was also used to attach the tissue to the edge of the stent post. The shape of the stent and posts gave a low coaption depth, h_c , for the unloaded leaflets. Fresh tissue was sutured on to the cloth-covered stent and the leaflets fixed in the closed position

under a low pressure. This produced more curvature in the leaflets (Rc Rr approximately 15 mm), a sharp V shape in the centre of the leaflet at the free edge and a sharp bend in the tissue as it passes over the edge of the frame. The leaflets were thin (approximately 0.35 mm) in the size 29 mm valve.

iv **Mitral Medical (Mitroflow) valve (MM)**

The valve shown in Figure 3.3 had a cloth-covered flexible acetal stent. The stent height was similar to the HP valve but the post had a small parallel section at its tip. A single stitch placed over the top of the post restrained the leaflets but did not bring the leaflets into apposition inside the post in the unloaded position. A small triangular hole was also seen between the free edges in the centre of the valve in the unloaded position. The leaflets were moulded on a jig during fixation with glutaraldehyde into a geometry which nearly matched the closed position of the leaflet. This formed a natural curvature in the leaflet (Rc Rr approximately 15 mm) and fixed a sharp bend in the leaflet where it passes over the edge of the frame. The leaflet thickness, t , was approximately 0.5 mm in the size 29 mm valve.

v **Other valves under development**

Other pericardial valves under development include the Edwards Pericardial valve (EP), the Ionescu-Shiley III pericardial valve, and the Sheffield and Cardiac Development Laboratories Bileaflet valves. The Shiley III valve was constructed similar to other Shiley valves but had a strip of pericardial tissue along the edge of the frame (54). The EP valve mounted the tissue under a

wire frame in a similar manner to that proposed by Reul (145) and Davis (146). In this configuration the leaflets came into apposition inside the frame at the top of the post without the need for a commissure stitch (44). Effectively, the leaflets projected radially inwards from the frame taking a natural closed position without the need for moulding. A similar construction has been used in the Sheffield bileaflet valve (55,147) and a bileaflet valve has been developed with leaflets moulded in the closed position in the shape of a bubble surface (56).

There were considerable differences in the detailed design and construction of these valves which were investigated during valve function and durability tests. All the valves are difficult to manufacture, with considerable skill and precision required to suture the leaflets in place. This resulted in a high proportion of rejected valves after final assembly.

3.4 Valve function tests

Four size 29 mm valves were tested in the mitral position of the pulse duplicator and four size 23 mm valves were tested in the aortic position.

The mean pressure difference is plotted against RMS forward flow in Figure 3.4 for the 29 mm mitral valves and the 23 mm aortic valves. In the 29 mm mitral valves the ISU had the largest pressure difference whilst the MM had the lowest. In each case the valve orifice increased with flow rate and was determined by the free edge of the leaflets and not the internal diameter of the stent. The free

edges of the leaflets were restricted in opening to varying degrees by the coaption stitches at the top of the posts (Figure 3.3). This restriction was greatest in the ISU valve with the coaption stitch inside the post, and least in MM valve where the stitch was placed over the top and towards the outside of the post. The HP 23 mm aortic valve had the lowest gradient whilst the ISU and ISLP had similar gradients. The ISU valve was effectively a larger valve as dimension D_0 (Figure 3.1) at the top of the stent was 27 mm.

The regurgitation was similar in all four valves (Figure 3.5). In the mitral position the closing volume was higher than the closed regurgitation, due to the large volume swept back by the leaflets, the flexibility of the stent and extension of the leaflets, and short systolic time period. In the aortic position the closing volumes were lower, but the static regurgitation higher, due to the longer diastolic time period. Energy loss results (Figure 3.6) show that the regurgitant fraction was dominant at low flows in both sizes of valve, but at higher flows energy losses during forward flow dominated (particularly in the aortic position) and valves with the lowest pressure differences also had the lowest total energy loss.

The different valve designs also had a significant effect on leaflet dynamics. The closed position of the ISU and ISLP size 29 mm valves under 120 mm back pressure is shown in Figure 3.7. The flexible stent of the ISLP allowed the free edge of the leaflet to twist when closed indicating that the tissue was not under as much tension. This reduction in stress may improve durability (148). The effect of the tissue fixation method on the opening of the leaflets was shown by testing the 29 mm valves at low steady flows of

40, 80, 120, 160 ml.s⁻¹. All these leaflets opened at 40 ml.s⁻¹ for the ISU and ISLP valves, at 80 ml.s⁻¹ for the HP valve and 120 ml.s⁻¹ for the MM valve. All leaflets opened at the lowest flow in the pulsatile test (stroke volume 60 ml, rate 60 BP min) with a peak flow of 150 ml. s⁻¹, although the last leaf to open in the MM was slow taking an additional 50 ms to open. These tests confirmed that the fixation of the tissue could affect synchronous leaflet opening action and this was demonstrated more clearly in the valves with thicker leaflets. However, in all cases, the leaflets opened when the pressure difference across the valve was less than 1 mm Hg. The method in which the valves opened also differed. Synchronised photography at 10 ms intervals showed that the Shiley valves moved from the open to closed position by buckling across the leaflet forming an S shape in the circumferential direction whilst the HP and MM valves reversed their curvature in the base of the leaflet first forming an S shape in the radial direction. The opening action was the reverse of the closure. The leaflets took 30 to 60 ms to open depending on the flow waveform and 50 to 70 ms to close. Synchronous closure was good in all valves with the leaflets coming together within 10 ms. Although it has been suggested that asynchronous closure may place extra load on the leaflets that close first, this may not be significant as the high back pressure was not generated until all three leaflets were almost closed.

The geometry of the leaflet in the open position was also affected by the method of fixation. In the HP and MM valves fixed in the closed position the sharp curve fixed in the leaflet at the edge of the stent was not straightened out and when the leaflet opened this

produced an S profile at the edge of the stent on the base of the leaflet. In Shiley valves the leaflets opened up to a straight line (see Figure 3.8). This will affect bending stresses and perhaps tissue ingrowth in these areas. Alternatively, tissue ingrowth may change the open geometry of the Shiley valve over a period of time.

3.5 Fatigue studies

Fatigue studies were carried out on one ISU, four ISLP, three HP and 2 MM, size 29 mm mitral valves. The results of the tests will be published (149,150). The lifetimes of the valves to failure are shown in Figure 3.9. Failure was defined as a tear 3 mm long in order that the start of a tear could be isolated before it propagated through the leaflet. In all valves, failure occurred due to tears originating close to the edge of the stent. These tears were caused by abrasion of the leaflet as it flexed over the edge of the cloth-covered frames.

The four ISLP failed valves are shown in Figure 3.10. In three valves the tear started halfway up the post at the shoulder of the scallop and in one valve propagated to the free edge of the leaflet before the test was stopped. In the fourth valve the tear started after 315 million cycles at the top of the post where the post deepened and projected into the valve orifice. The tissue was intact around the coaption stitches in all four valves. All leaflets showed wear, abrasion and thinning along the edge of the cloth-covered frame (Figure 3.11). The one valve that failed after 20 million cycles had thinner leaflets. The ISU valve failed after 5 million cycles with a

tear in the leaflet which propagated from the shoulder of the stent scallop to the free edge (Figure 3.12). The opposite side of the same leaflet also had a short tear at the shoulder of the stent and the coaption stitches at two posts had pulled out through the tissue producing a small tear. As in the ISLP, all leaflets had abrasion and thinning around the edge of the frame.

The HP valves all failed in under 10 million cycles with tears adjacent to the stent (Figure 3.13). In two valves the tears started two thirds up the post and propagated to the free edge while in the third the tear occurred at the top of the post. In each case the torn leaflet prolapsed and all leaflets showed abrasion and thinning along the edge of the cloth-covered frame (Figure 3.11). The tears did not appear to originate from the coaption stitches.

The two MM valves failed at 15 and 54 million cycles with tears adjacent to the cloth-covered frames (Figure 3.14). As with all other valves, tears were caused by abrasion on the cloth-covered frames. Function tests were carried out on all the failed valves. These showed that where the tear had propagated to the free edge, the leaflet prolapsed below the other two leaflets giving a large regurgitation of between 25 and 45 ml for a stroke volume of 70 ml.

The mode of failure abrasion on the cloth-covered stent was similar in all valves although the lifetimes varied considerably. The early failure of the ISU compared to the ISLP may have been due to thinner leaflets or a rigid stent and has been predicted by other workers (27,49). Our results showed earlier failure of the HP valve than other centres (49). The abrasion was caused by the leaflet being pulled over the edge of the frame in the closed position and was

greatest where the tension in the leaflet was highest. The position of maximum tension may have been affected by the abnormal closing action of the valve in the fatigue tester discussed in Chapter 2. The effects of different leaflet designs and dynamics discussed in Section 3.4 are clearly overtaken by the premature failure due to abrasion.

These in vitro tests were artificially harsh for pericardial valves and did not predict clinical failure rates (typically 1% per patient year). In vivo blood deposits form rapidly on the cloth followed by host tissue ingrowth. These processes greatly reduce the abrasion of the leaflets on the cloth but do not eliminate it (46). Our clinical experience of six failed ISLP valves (Figure 1.11) and two explanted HP valves (Figure 1.12) show that clinically the tears appeared closer to the top of the posts than generally found in the fatigue tester. In the ISLP valve which failed in the fatigue tester after 315 million cycles, with a tear close to the top of the post, the mode of failure was more similar to the clinical valves. In both types of clinical valves endothelialisation and host tissue ingrowth reduced abrasion and reinforced the leaflets particularly in the base of the scallops. It is not clear whether the tears at the top of the stent posts were caused by abrasion or by the coaption stitches which passed through the leaflet close to the point of the tears. However, stress concentrations around the stitches in an area which was thinned and weakened by abrasion probably contributed to the tissue failure.

3.6 Discussion

Although pericardial valves have been used for over 13 years their clinical performance is not ideal and there is particular concern about longterm durability and calcification. Clinical experience with explanted valves has shown a characteristic failure mode with tears occurring close to the edge of the cloth-covered stent. Although extensive studies have been made of the function, design and dynamics of natural and glutaraldehyde-treated porcine valves few detailed studies have been made of the design, function and dynamics of pericardial valves. There was considerable variation in the detailed design of the four pericardial valves studied, in particular differing methods of tissue fixation, leaflet geometries, mechanical properties for the leaflets, methods of attachment to the stent and covering materials used. In all cases the methods of manufacture required skill and precision which resulted in a high rejection rate of finished valves. Standard hydrodynamic parameters were similar for all four valves although the pressure drop was dependent on the restricted opening of the free edges of the leaflet caused by coaption stitches. The leaflet dynamics were dependent on the method of fixation and the properties of the tissue used. Forming the leaflet in the closed position during fixation was seen to affect the synchronous opening of the leaflets, the method of buckling from the open to closed position, and the geometry of the open position. It is clear that the method of fixation, the changes induced in the material properties (126) and the varying geometries can affect the stresses in the leaflet (53).

The in vitro fatigue studies were not able to show differences in valve durability due to these differences in valve design, as abrasion of the leaflets on the cloth-covering at the edge of the stent caused premature tissue failure and tears in all but one of the valves. This confirms studies made in other centres (44,49). In these in vitro tests, tissue failure was not caused by flexion (145), tears from sutures (30) or by Dacron buttresses on the outside of the post (51) although in the ISU valve, coaption stitches did pull through the leaflets producing small tears, but these did not extend or cause leaflet prolapse. However, if the abrasion problem was overcome, alternative failure modes would be identified which could perhaps be attributed to differences in valve design, tissue fixation, etc.

Clinical results with two valves, HP and ISLP, showed that abrasion of the leaflets was greatly reduced by biological processes, such as endothelialisation and tissue ingrowth, but did occur especially close to the top of the posts where coaption stitches may also have contributed to the tears. It is clear that tissue abrasion on the cloth-covered stent and coaption stitches at the top of the post are the main factors affecting valve durability. Only after these failure modes have been eliminated will the effect of different leaflet designs and function on valve durability become apparent.

CHAPTER 4

BOVINE PERICARDIAL TISSUE

4.1 Introduction

Bovine pericardium is a complex biological material. Variations in the mechanical properties and structure of the tissue within sacs and between sacs from different animals, and changes induced in the tissue following treatment with glutaraldehyde pose considerable problems when studying the properties of tissue used in valve leaflets. A better understanding of these material properties is essential if current valve designs are to be improved.

There is considerable knowledge of the mechanical properties of biological materials such as skin and tendon (151-153) and also natural valve leaflets (154). Uni-axial testing of fresh aortic leaflets has shown them to be anisotropic and non-linear with an initial low modulus of elasticity followed by an abrupt transition to a much stiffer material. They are more extensible and have a lower ultimate tensile strength (UTS) radially than circumferentially (155). The anisotropy is caused by fibre orientation and the low initial modulus of the stress-strain curve (often described as the soft incubation period) has been attributed to the "waviness" or "crimp" in the collagen fibres (156). Fixation of the valve leaflets in a stressed condition can reduce or eliminate this "crimp" (157,158) and cause a less extensible material by modification of the soft incubation period on the stress-strain curve. These variations in the mechanical properties have been related to changes in function and

durability of glutaraldehyde-treated porcine aortic heart valves (159-163). The visco-elastic properties of fresh porcine leaflets have been illustrated using uni-axial testing (129) and have been attributed to movement of the collagen fibres through the viscous ground matrix. In this study, fixation with glutaraldehyde in a stressed condition produced a less extensible material (as above), but fixation at zero stress produced a more extensible material (164). This additional extensibility was associated with break-up of the ground substance matrix.

The structure of both human and bovine pericardium has been described by Ishihara (165,166). Three distinct layers were identified, the inner serosal surface of mesothelial cells, the middle fibrosa containing variously orientated layers of type 1 collagen fibrils and elastin fibres, and the epipericardial connective tissue layer containing random orientated collagen bundles up to 15 μM in diameter, blood vessels, nerves and adipose tissue cells. The collagen fibrils in the fibrosa are formed in bundles or layers approximately 5 μM thick, with the fibrils within each bundle or layer having similar orientation. The orientation of the fibrils may vary from layer to layer. The fibrils themselves are between 50 and 150 nM in diameter and are formed from aggregates of collagen pentafibrils (diameter 3.5 nM). A cross section through each pentafibril reveals five staggered tropocollagen molecules (each molecule being 290 nM long). This produces a characteristic banding every 67 nM in the tropocollagen molecules (167).

The layers or bundles of collagen fibrils in the fibrosa have a wavy appearance (period typically 20 μM) which is often referred to as

"crimp". The layers of fibrils are birefringent and the pattern of the "crimp" can be readily seen using polarised light microscopy. This is a simple way of identifying the orientation of the fibrils are running. The fibrils themselves are quite inelastic and extensibility of the tissue is due to the "crimp" of the fibrils, realignment of the fibrils in the ground substance, and the elastin fibres. It has been shown that the "crimp" disappears when the tissue is stretched. Mechanical testing of canine pericardium (168) has shown a non-linear visco-elastic material with an initial low modulus of elasticity and a much stiffer modulus at high strains. Shifts in the stress-strain curve were found after preconditioning. The viscous properties are related to rearrangement of the collagen fibres in the viscous ground substance (169). Although the tissue has been described as nearly isotropic, the ultimate tensile strength and tissue modulus were greater in the direction of the long axis of the heart than the circumferential direction. Bi-axial stress-strain testing of fresh canine pericardium has also indicated anisotropic properties (170,176). Van Noort has shown that fixation of bovine pericardium with glutaraldehyde modifies the stress curve with stiffening of the soft incubation period (171). The stress-strain curve is further modified and moves towards the origin if stress or strain is applied to the tissue during fixation (172). This correlates with loss of waviness in the collagen bundles. Trowbridge has shown that the abrupt stiffening of stress-strain curve found in fresh samples occurs more gradually in fixed tissue (174) and that the response to load in the unstrained state suggests fixed tissue is isotropic (174). There is however considerable difference in the stress-strain curves and

maximum extensibility for tissue taken from different areas of the sac and this has been attributed to the elastin content of the tissue (175). Stress-strain curves can also be affected by choice of gauge length (177).

The anatomy of the human pericardial sac has been described in detail (178) and compared to the bovine sac. The mechanical properties of the tissue, its thickness and ultimate strength, vary throughout the sac and are associated with the orientation of the layers of fibrils in the fibrosa. To select the best tissue for valve leaflets it is important to define more precisely the mechanical properties of both the fresh and fixed bovine tissue in different areas of the sac.

The properties of bovine pericardium taken from beef cattle aged 12 to 36 months have been studied. The gross structure and geometry of the sacs have been defined and I have established a frame of reference using the ligaments (sterno pericardiaca) and the tissue surrounding the inferior vena cava. The tissue thickness has been measured throughout the sac and the fibril orientation studied using polarised light microscopy. In one area of the sac with more uniform thickness, uni-axial and bi-axial tensile testing have been carried out. The mechanical properties of this area have also been studied after glutaraldehyde fixation.

In addition I have investigated the chemistry of glutaraldehyde fixation and have monitored the degree of crosslinking in the tissue by measuring the thermal denaturation temperature.

4.2 Pericardial sac

Pericardial sacs obtained from beef cattle aged 12 to 36 months have been studied as part of this thesis work. Sacs were harvested from animals by circumferential dissection around the top of the heart adjacent to the major vessels. Sacs were stored in physiological saline and transported to the laboratory. Fat was carefully removed from the epipericardial surface and the tissue washed thoroughly in saline. The approximate shape of one sac was determined by taking a plaster cast of the heart and is shown in Figure 4.1. The shape can be considered a truncated cone with the apex of the heart forming a spherical tip. Each sac was dissected down the posterior surface along the line of attachment to the pleural membrane. This line overlies the posterior descending coronary artery. This dissection line was continued around the apex to the two ligaments (sterno pericardiaca) on the lower anterior surface. This allowed the sac to be laid out as a flat membrane. Figure 4.2 shows a sac transilluminated on a light box and Figure 4.3 shows a diagram of a membrane. The circumferential dissection line made to remove the sac from the heart is shown as ACBEFA¹, and AB, A¹B¹ shows the dissection down the posterior surface to the ligaments BB¹. C shows the flap of tissue from around the inferior vena cava. Transillumination of the sac (Figure 4.2) showed two bands of thicker tissue extending over the anterior surface of the sac from the two ligaments. These were defined by lines BD and B¹E. The curvature of the sac did not allow it to lie smoothly on a single plane without some wrinkling. This occurred in areas of most curvature. Lines BC, BD and B¹E were used

as a frame of reference. The angle CBD was between 80° and 90° and the angle between BD and B^lE was approximately 30° . Ten sacs were studied and the tissue thickness measured at 26 points radiating from ligaments B and B^l (see Figure 4.3). The dimensions BB^l, BC, BD, BE, BF were also measured. The tissue thickness was measured with a Mitutoyo thickness gauge with 1 cm diameter pads and five seconds was allowed for tissue relaxation before each measurement was taken. The mean value and standard deviation for the thickness is given in Table 4.1. The tissue was significantly thicker at points 10 to 15, which lie on the bands originating from the ligaments, and also at points 3 close to the inferior vena cava (point C). It was marginally thicker at points 2, 3 and 23. In between the thick bands, points 24 and 25, the tissue was much thinner. Areas defined by points 4 to 9 and 16 to 22 had more uniform thickness.

The radii of curvature varied over the mould (see Figure 4.1). Circumferentially it was almost flat on the posterior surface, but had a much smaller radius of curvature over each ventricle ($r \approx 40$ cm). The radius of curvature was smaller close to the apex. In the direction parallel to the long axis of the heart there was little curvature over the midline of the ventricles, but there was significant curvature at the apex A and also in the area overlying the atrium producing a spherical surface.

Polarised light transmission microscopy was used to identify crimp or waviness in the collagen fibrils in the tissue, which can be used to define the orientation of the fibrils. An example of a micrograph of the epipericardial surface is shown in Figure 4.4. It was not clear whether the pattern relates to the top surface of the

tissue or was an averaging effect of the light passing through the tissue.

The pattern was difficult to identify in all areas of the sac, and in other areas the orientation of the fibrils was different from the two surfaces. Figure 4.5 shows the general direction of the fibrils on one sac studied. The fibrils ran along the long axis of the heart in thick bands BD, B¹E, but elsewhere they tended to run circumferentially around the heart.

Three areas shown in Figure 4.5 which were considered to have uniform thickness were possible sites for leaflet manufacture. Area 1 in the centre of the sac overlying the right ventricle was selected for further investigation using tensile testing and histological techniques. This area close to reference points 5 and 8 (Figure 4.3) also had uniform fibril orientation.

These investigations have been carried out as a joint research project with the BioEngineering Unit at Strathclyde University.

4.3 Mechanical properties of fresh pericardial tissue

Initial studies of the properties of fresh pericardial tissue have been carried out in area 1 of the sac (Figure 4.5) using biaxial inflation and uniaxial tensile tests. Biaxial inflation tests (179) have shown that the tissue was more extensible in the circumferential direction than along the long axis of the sac (axial direction). This anisotropy could have been due to geometrical or material properties. In the circumferential direction the sac had more natural curvature, R 40 mm, but this would only account for the

difference in extensibility of 4%. Microscopic examination of the tissue showed that in this area the fibrils predominantly ran circumferentially around the sac, so the additional extensibility could have been caused by the crimp or waviness seen in collagen fibrils, as suggested by other workers (172).

Initial uniaxial tensile tests have been carried out with tissue taken from area 1 of three sacs. The sacs were prepared as described previously and the predominant direction of the fibril orientation in area 1 identified with polarised light (Figure 4.4). Three parallel strips of tissue 70 mm x 3 mm were cut in the direction of the fibrils (circumferentially) and three parallel strips cut perpendicular to the fibrils (axially) in a T configuration. The strips were cut to allow a final gauge length of 15 mm to be used. This was selected so that the same size of strips could be cut from fabricated leaflets. In order to set the gauge length for the tissue, the tissue was floated onto a piece of glass under water and, when totally relaxed, a piece of paper was placed onto the tissue so that the tissue adhered to the paper. A 15 mm steel gauge was used to set the jaws of the Instron tester, and the paper and tissue set between the jaws at this length. The paper kept the tissue in an unstrained state and allowed the gauge length to be set. The specimen was bonded in position in the jaws of the test instrument using sandpaper and cyanoacrylate adhesive. The tissue was then mounted at its gauge length, the supporting paper removed by cutting and the initial gauge length recorded on the instrument. The tests were carried out in physiological saline with a cross head speed of 5 mm/min.

As well as defining the original gauge length, the first load

point was also determined at a force of 0.001 N (0.1 g) by increasing the sensitivity of the machine ten times. This was similar to the reference point defined by Trowbridge (174) where the specimen was extended to register a load of 1 gram, and then the tester reversed until no load was detected. In our case it was considered easier to define a very small first load 0.1 g.

Specimens were cycled five times to a load of 0.8N to condition the tissue. This corresponds to a stress of 0.8 N mm^{-2} induced by a pressure of 150 mmHg in a leaflet with a curvature R of 13 mm. The load-unload extension curves for the first and fifth pulls were recorded along with the first load point at 0.001N. After the fifth extension the tissue was extended to its ultimate breaking point and the extension curve recorded.

All the specimens showed typical non-linear force extension curves as described by other workers (172,174,175,177) with a soft incubation period and a greater modulus at higher extension ratios. The visco-elastic nature of the tissue was seen with the hysteresis in the load-unload curves as energy was dissipated and a reduction in the force at each extension point on the second to fifth pulls as the tissue was conditioned. The first load point (0.001 N) was within a few percent of the gauge length on the first extension for all the specimens. However, the first load point occurred at greater extension ratios on the conditioned specimens due to the creep caused by the visco-elastic nature of the tissue.

The graphs of the load extension curves for the fifth cycle and the final extension to the breaking point for six specimens from each sac tested are shown in Figures 4.6 a, b, c. Details of the tissue

thickness and the extension ratio for the first load points on the conditioned curves are shown in Table 4.2. Both force extension curves are plotted for the original gauge length and the first load point on the condition curves are also shown. The graphs are plotted for strips 1, 2, 3, cut in the direction of the long axis of the heart and strips 4, 5, 6, cut in the circumferential direction.

For each sac specimen 4, 5, 6 and 1, 2, 3 showed similar loading curves to 0.8 N, which confirms the uniformity of the tissue and the repeatability of the technique. For strips 1,2 and 3 the slope of the initial portion of the loading curve was less, the extension ratio of the first load point greater, and the transition to the higher modulus region more abrupt than for strips 4, 5 and 6. The extension ratio at 0.8 N was similar for all the strips from any one sac but varied between 1.3 to 1.5 for different sacs. These loading extension curves did not correlate with the biaxial tests which showed greater extensibilities in the circumferential direction parallel to the fibrils than in the axial direction.

The ultimate tensile strength was much greater for strips 4, 5, 6 than strips 1, 2, 3 in each sac (17 to 20 N compared with 1.5 to 5 N). In strips 4, 5 and 6 the breaking point was more abrupt which would be consistent with the breaking of the fibrils, while strips 1, 2 and 3 had a low ultimate tensile strength and more gradual transition which would be consistent with pulling the fibrils apart in the matrix.

In tissue where the fibrils tend to run in one direction (circumferentially in this case) cutting the tissue in thin strips across the direction of the fibrils, as in strips 1, 2 and 3, could

reduce the ultimate strength of the tissue compared to a larger piece of tissue where fibrils orientated at small angles to the average direction can give a much greater contribution to the strength in the normal direction. Similarly, this could have increased the extensibility of strips 1, 2 and 3 in uniaxial test which could explain the difference between the results of the uniaxial and biaxial test. It is also worth noting that if the extension curves were plotted from the first load point on the conditioned curves, the tissue would appear less extensible in the axial direction.

These initial studies suggest that the average orientation of the fibres in the circumferential direction in area 1 can cause different mechanical properties between the circumferential and axial directions in the fresh tissue.

4.4 Mechanical properties of glutaraldehyde treated tissue

The mechanical properties of tissue taken from area 1 of three sacs and treated with 0.25% glutaraldehyde has been investigated with uniaxial tensile tests. The sacs were prepared as described previously and dissected down the line BD. The tissue surrounding the right ventricle including area 1 was fixed in 0.25% buffered glutaraldehyde for seven days. The tissue was freely floated in the fixation bath so it was fixed in its unstrained state. Uniaxial tests were carried out as with the fresh tissue. The average orientation of the fibrils was identified optically and strips 4, 5 and 6 cut circumferentially in the direction of the fibrils and strips

1, 2 and 3 cut axially normal to the fibrils. The tissue was mounted in the Instron tester and cycled five times to 1.0N before being extended to its breaking point.

The force extension curves for the conditioned tissue on the fifth cycle are shown in Figures 4.7 a, b, c for the three sacs and the sixth cycle to determine the UTS is also plotted. The tissue thickness and first load point for the fifth cycle is shown in Table 4.3. As with the fresh tissue the specimen showed typical non-linear visco-elastic properties of soft tissues. The graphs were similar for specimens 1, 2, 3 and 4, 5, 6 in each sac showing the uniformity of the tissue on a localised area and the repeatability of the technique. There was some variation between sacs with an extension ratio at 1.0N varying between 1.20 and 1.35. All the loading curves showed a greater modulus in the initial incubation period than the fresh tissue and this had the effect of reducing the extension ratio of the first load point of the conditioned cycles to between 1.02 and 1.07. This also gave a more gradual transition to the fixed tissue curve which was probably caused by the crosslinks formed between or within fibrils during fixation. It was difficult to detect any difference in the loading curves to 1.0N between the circumferential and axial directions. The extension ratios for the fixed strips at 0.8 N were slightly less than for the fresh strips when taken from the gauge length, but were slightly greater when taken from the first load point. This confirms that the definition of the original gauge length can be a critical factor in interpreting the results (173).

As with the fresh tissue the UTS was much greater in the

circumferential direction (strips 4, 5, 6) than the axial direction (15 to 20 N compared with 1 to 5 N) and was primarily caused by the orientation of the fibrils. However, the loading curves to 1 N showed little difference between the circumferential and axial direction for the fixed tissue. This agreed with the findings of Trowbridge et al (173).

The structure and mechanical properties of both fixed and fresh tissue are complex. The conditioned force extension curves to 1 N, the first load point on the conditioned cycle which is the point to which the tissue returns to during cycling, and the variation found between specimens and between the different orientations, are particularly important in valve leaflet design.

4.5 Fixation of tissue with glutaraldehyde

Glutaraldehyde has been used for over 15 years to stabilise and crosslink tissue in bioprosthetic heart valves (180). The crosslinks reduce the biodegradability and antigenicity of the tissue (181), modify the mechanical properties (171) and may reduce its thrombogenicity (182,183). The complex reactions which occur between the glutaraldehyde and the primary amine groups (lysine, hydroxylisine and N terminal amino acid groups) which are all present in the protein molecule, are not fully understood (184). The complexity is due to the mixture of free aldehyde, mono and dihydrated monomeric glutaraldehyde, monomeric and polymeric cyclic hemiacetals and alpha and beta unsaturated polymers found in aqueous solution of

glutaraldehyde (185-187). The nature of the crosslinks has caused considerable controversy in the literature (188,189) but more recently a fuller description of the possible reactions has been given (190-193) with up to 12 different compounds being proposed. Under certain conditions fixation of the tissue may not be uniform or complete (191-193). Polymerisation of the glutaraldehyde during formation of the crosslinks may prevent penetration of the free monomer into the whole matrix of the tissue. Alternatively, polymerisation may occur on the outer surface of the fibrils themselves which would prevent penetration into the structure of the penta-fibrils. These effects depend on fixation conditions, glutaraldehyde purity, concentration, pH, temperature and time. If the tissue is not crosslinked completely, repeated cycling of the tissue in vivo, which gives rise to structural changes, may well expose areas of tissue which are not fully crosslinked. These would be sites for biological degradation, immunological reactions and possible calcification.

It is difficult to determine the sites in the microscopic structure onto which the crosslinks form or indeed the nature of the crosslinks. I have carried out two studies (described in the next two sections) in an attempt to ensure that the tissue is adequately and consistently fixed.

Firstly, ultraviolet spectroscopy has been used to monitor the purity and concentrations of commercially available aqueous glutaraldehyde solutions. Secondly, the shrinkage temperature (collagen denaturation temperature) of the fixed tissue has been measured to assess the amount of crosslinking. A stratigraphic

analysis of the shrinkage temperature of 25 μm layers of tissue cut sequentially parallel to the surface of the tissue has been made to investigate any variation due to penetration of the glutaraldehyde.

4.6 Chemistry of aqueous glutaraldehyde solutions

Commercial glutaraldehyde is normally supplied in 25 percent aqueous solution at acidic pH. Upon dilution the composition of the monomer is 4% free aldehyde, 16% monohydrate, 9% dihydrate, 74% cyclic hemi-acetal (194). In concentrated solutions the hemi-acetal forms dimers and trimers which readily revert back to the monomer upon dilution. Alpha and beta unsaturated polymers are also present in small amounts. The rate of formation of the alpha-beta unsaturates increases with pH, temperature and concentration (186). The monomer can be separated by distillation and/or multiple extraction with charcoal. The alpha-beta unsaturates absorb light strongly at 235 nm whereas the monomer absorbs light weakly at 280 nm, the extinction ratio of absorbance being 160:1. Hydrated aldehydes absorb UV very weakly. The ratio of the free monomer to the alpha-beta unsaturates can be monitored using UV spectroscopy. For purified glutaraldehyde a ratio of 2:1 in the absorbance peaks at 235 and 280 nm can be obtained. Several grades of commercial glutaraldehyde are available and the purity and effect of storage conditions for the 25% solutions has been reported by Gillet and Gull (187).

The purity of three different commercial solutions has been studied and the effects of distillation and filtration have been investigated. The rate of formation of the alpha-beta unsaturates has

been monitored after the solutions have been diluted and buffered to pH 7.4. In addition, the effect of adding pericardial tissue to glutaraldehyde has been monitored.

Three commercial solutions of glutaraldehyde were studied; technical glutaraldehyde (supplied by the University Chemistry Department), Agar Aids glutaraldehyde (vacuum distilled) and Sigma Chemical Co glutaraldehyde. All three were supplied as 25% solutions. In addition, technical glutaraldehyde was distilled and also filtered with activated charcoal. The commercial solutions were diluted to 0.25% with sodium phosphate buffer pH 7.4 assuming a stock concentration of 25%. The technical glutaraldehyde was purified by distillation and also by charcoal filtration and diluted so that the absorbance at 280 nm peaks was 0.24. The UV spectrum of all five solutions at 0.25% concentration was measured on a Beckman DU-7 spectrophotometer. The sodium phosphate buffer was used as a reference solution.

The two solutions, Sigma and distilled technical, were diluted to a concentration of 0.5, 0.25, 0.125, 0.06 percent, with the buffer. They were stored at room temperature and the UV spectrum measured at 1, 3, 7, 10, 17 and 32 days to assess the rate of formation of the alpha-beta unsaturates. Two solutions of Sigma and distilled technical were diluted to 0.25% and a piece of pericardial tissue (approximately 4 cm²) was added to 200 ml of each solution. The UV spectrum was measured after 2, 4, 7, 24 and 60 hours for solutions with and without tissue.

Examples of the UV spectrum for 0.25% solutions of Sigma and Agar Aids are shown in Figure 4.8. The peaks at 280 and 235 nm were

well-defined and a small peak at 200 nm was also detected. Table 4.4 shows the absorbance measured for five solutions at 235 and 280 nm. The Sigma, Agar Aids and the filtered and distilled technical were very pure whilst the technical was less pure. The absorbance at 280 nm for the diluted Sigma and distilled technical solutions is shown in Table 4.5 for concentrations of 0.5% to 0.06%. As expected, reduction in absorbance is directly proportional to concentration. In this range of concentration the absorbance can be used to monitor concentration of the monomer.

The rate of formation of the alpha-beta unsaturates is shown in Figure 4.9 for the Sigma and distilled solutions as a graph of absorbance at 235 nm against time. The rate of formation of alpha-beta unsaturates was greater for higher concentrations and slightly higher for Sigma than distilled technical. Figure 4.10 shows the effect of adding tissue to the 0.25 percent solutions. The rate of formation of alpha-beta unsaturates was greatly increased when tissue was added to the solutions (approximately ten times greater). This was not surprising as the formation of crosslinks in the tissue acted as a catalyst for polymerisation (190-192). Although the free monomer was used to form the alpha-beta unsaturates there was little reduction in the amount of free monomer in solution as monohydrate and dihydrate revert back to free monomer to maintain the balance.

There are various conditions which can affect the purity of aqueous glutaraldehyde solutions. Gillet and Gull (187) have shown storage of 25% solutions at acid pH of 4°C has little effect on the solutions. Our results showed that there were considerable differences in the commercial solutions and, more importantly, the

solutions changed rapidly when buffered and diluted to pH 7.4. Even more rapid polymerisation of the alpha-beta unsaturates was found when tissue was added to the glutaraldehyde.

The effects of increased amounts of alpha-beta unsaturates on the crosslinks formed in the tissue are not known. However, to standardise fixation conditions, a pure commercial solution has to be used, the solutions have to be freshly diluted and buffered, and solutions should only be used once for fixing tissue.

4.7 Thermal denaturation temperature of fixed pericardium

Measurement of the thermal denaturation temperature of fixed pericardium has been used as a simple physical test to assess the degree of crosslinking in fixed tissue. The rate of fixation and the structure of the crosslinks is dependent upon the pH, temperature and glutaraldehyde concentration (186-188). The variation in the thermal denaturation temperature (shrinkage temperature), with time and glutaraldehyde concentration, has been determined by heating tissue slowly in a water bath and determining the temperature at which the tissue contracts (185,196). A higher shrinkage temperature indicated a greater number of crosslinks. This did not indicate, however, whether the crosslinking was uniform throughout the tissue. In the leather industry shrinkage temperature measurements have been made on fresh skin using differential scanning calorimetry [DSC] (197). In DSC the heating rate of the specimen was controlled and the energy input to specimen monitored. A sharp increase in energy input was recorded at the transition temperature of the collagen, corresponding

to the collapse of the triple helical structure. This work used only very small samples of tissue. In this study this technique has been adapted to perform a stratographic analysis of the degree of glutaraldehyde tanning on the tissue by measuring individual shrinkage temperatures on a number of layers cut parallel to the surface of the pericardium. DSC has also been used to assess the effect of fixation time and glutaraldehyde concentration on shrinkage temperature.

Bovine pericardial sacs were collected and prepared as in Section 4.3. Fixation of the tissue was carried out with Agar Aids glutaraldehyde which was diluted and buffered (sodium phosphate) to pH 7.4. Tissue was placed in fixation baths of 0.25% and 0.5% glutaraldehyde and removed after 15 and 30 minutes; one and four hours; one, two, five, eight and 28 days. Samples were washed thoroughly in saline after fixation for 20 minutes and the shrinkage temperature measured on a Dupont (model 990/910) DSC. A heating rate of 1°C per minute was used and the energy scale was set to 400 uW per cm.

The penetration of the glutaraldehyde into the pericardium was assessed for fixation times of 28 days in 0.25% glutaraldehyde. Tissue was removed from the fixation baths, washed thoroughly, and cut into layers 25 μM thick using a cryogenic knife starting from the mesothelial surface. Frozen sections were referenced and stored in saline and shrinkage temperature was measured every fourth slice (100 μM).

The variation in shrinkage temperature with time and concentration is shown in Figure 4.11. There was no detectable difference in the rate of increase of shrinkage temperature at 0.5% or

0.25% concentration; in both cases the temperature appeared to reach a maximum after two hours fixation time. The tissue in the lower concentration showed a slightly higher value between two days and 28 days. This has also been shown by other workers (193,185).

The results of the shrinkage temperature measurements on the thin sections of tissue are shown in Figure 4.12. There was no significant difference between the layers in any pieces of tissue which suggests uniform penetration and fixation throughout the tissue.

Shrinkage temperature measurements are a simple physical method of monitoring the degree of crosslinking and the shrinkage temperature of small tissue samples can be determined accurately using DSC. It is not known however how sensitive the shrinkage temperature measurements are to variations in the different types of crosslinks proposed by Cheung (190-192). The results showed that the shrinkage temperature was stable beyond two days whilst it is known that the solution continued to polymerise after two days. Although the shrinkage temperature measurements indicated uniform penetration of the fixative, we cannot say whether crosslinking took place at the surface of the fibrils or whether it penetrated further into the molecular structure. Formation of glutaraldehyde polymers on the surface of fibrils may have restricted further penetration.

4.8 Discussion

Both the structure and material properties of bovine pericardium and the chemistry of glutaraldehyde fixation are complex and not fully understood. In this chapter I have described initial tests to

investigate the mechanical properties and structure of the tissue in one area of the sac and have described two simple studies in an attempt to produce standard uniform conditions for fixation of the tissue.

The ultraviolet spectroscopy showed that there were some differences in the purity of commercial glutaraldehyde solutions but, more importantly, the solutions polymerised rapidly when diluted and buffered to PH 7.4, and when tissue was added to the solution. The polymerisation of the glutaraldehyde will affect the types of crosslink forms and may also affect the penetration into the molecular structure of the tissue (192).

Thermal denaturation temperature measurements of fixed tissue indicated that the degree of crosslinking was constant after two days fixation time and uniform through different layers. We have shown that polymerisation of the glutaraldehyde solution increased with time and this may alter the chemical nature of the crosslinks for longer fixation times.

The standard method used for fixation in the rest of this study was to dilute Agar Aids (25% vacuum distilled glutaraldehyde) and buffer to 0.25% PH 7.4. The solution was used 24 hours after dilution and tissue was fixed in the same glutaraldehyde solution for a minimum of seven days and maximum of 30 days.

General investigation of the pericardial sacs showed that they were not homogeneous membranes and showed systematic variation in both tissue thickness and fibril orientation. Three areas with uniform properties were identified as possible areas for leaflet manufacture and initial mechanical tests have been completed in one of these

areas. Uniaxial tensile tests showed characteristic properties of non-linear visco-elastic force extension curves typical of most soft tissues. There did not appear to be any major differences between the properties of the tissue taken from cattle aged between 18 and 30 months and the properties of pericardium taken from calves aged 16 weeks in other studies (173). Our results showed some variation in the force extension curves between sacs and also between the two orientations of the same sac in the fresh tissue. Biaxial inflation tests showed that the fresh tissue was more extensible in the circumferential direction along the predominant direction of the fibrils than in the axial direction, but this was not confirmed in the uniaxial tests. There was, however, a large difference in the UTS of both the fixed and fresh tissue between the two orientations. Fixation increased the modulus of the initial soft incubation period causing a more gradual transition to the high modulus region of the force extension curve. This made the shape of the curve similar in both orientations. This increase in modulus will affect the flexibility of the fixed tissue at small extension ratios which could in turn affect the opening and closing action of the valve leaflets. The visco-elastic nature of the tissue was also important as the creep found in the first load points of the cycled fixed tissue of 1.02 and 1.07 determined the unloaded length to which the tissue returns during cycling. This extension may not be permanent (172) but will remain as long as the tissue is being cycled and this therefore has to be considered in the leaflet design.

The tissue in area 1 had an anisotropic structure which produced variation in some mechanical properties with orientation. The

uniaxial strips were cut parallel and normal to the optical pattern produced by the fibrils in an attempt to maximise these differences. It is not clear how to orientate the leaflets in the light of these initial results. Natural valve leaflets have strong fibres running circumferentially which would be consistent with making the circumferential direction of the leaflet the circumferential direction of the sac. However, the structure of the two materials are completely different and other factors have to be considered when selecting the orientation of the leaflet. These include the deformation of the fresh tissue, differential extension of the loaded leaflets, the flexibility of the tissue, and variations in tissue thickness.

The initial tests on the properties of the pericardium will be extended to other areas of the sac in further studies being carried out in the BioEngineering Unit at Strathclyde University.

The studies I have completed on the properties of the pericardial tissue and the fixation conditions allowed me to select one area of the sac for the manufacture of valve leaflets and establish a standard process for fixation of the tissue.

CHAPTER 5

VALVE DESIGN

5.1 Introduction

A major concern with the clinical performance of existing pericardial valves has been early tissue failure seen as tears in the leaflets adjacent to the cloth-covered stent. The laboratory tests described in Chapter 3 showed that these tears were primarily caused by abrasion and wear to the leaflets as they were pulled over the edge of the frame under tension in the closed position. Coaption stitches placed through the leaflet at the top of the posts may also have contributed to the tears in implanted valves. Two other valves under development (45,55) have used a different method of mounting the tissue in an attempt to improve valve durability. In one of these valves, however, the method of suturing the tissue to the frame has been modified following tears from sutures (55). The long-term durability of these valves is not known. Other areas of valve design investigated in Chapter 3 which affected valve function, and perhaps durability, were the method of fixation of leaflets, leaflet geometry and method of attaching the leaflet to the frames. In addition, all valves required considerable skill and precision to suture the leaflets to the frames, which can cause high rejection rates during manufacture.

The following design ideas were produced to give an improved pericardial heart valve.

Leaflets were mounted mechanically between two frames which were

clamped together. The leaflets and frames were precisely located to one another by radial pins and studs. This allowed a consistent method of manufacture and allowed leaflets to be interchanged and matched easily. It also allowed different covering materials to be used on the valve frames in order to reduce abrasion to the leaflets. One potential drawback of this more complex frame structure was the possibility of the frame becoming bulky, so restricting the orifice area of the valve.

This chapter describes five different design options for the frames and possible alternative covering materials. Different leaflet designs, geometries and methods of leaflet fixation are also described which were tested during the valve development.

5.2 Frame design

Five different options for the twin frame designs were produced. In the first two options leaflets were mounted over and outside a strong inner support frame. In the third option the tissue was mounted under the support frame and projected radially inwards. The fourth and fifth options were hybrids of these two configurations. Each option is illustrated with vertical sections through the frame at the base of a scallop and at a post. A radial view of the outside of the posts showing the frames without the leaflets and a horizontal section through a post. The diagrams are simplified by not showing the covering material for the frames.

i The leaflets were mounted over the outside of a strong inner acetate support frame with pins and studs projecting radially to

- locate the leaflets (Figure 5.1). A cloth-covered wire frame was placed over the inner frame to restrain the leaflets and an additional plastic ring clamped the leaflets in place in the base of the valve. The position of the wire frame could be adjusted to deflect the leaflets radially inwards.
- ii A similar inner support frame was used as above, but the outer sleeve was manufactured from a thin acetal cylinder profiled to the same shape as the inner frame (Figure 5.2). The outer sleeve was slotted at the base of each post to allow assembly over the inner frame and radial pins and studs. The outer frame projected about 1.5 mm above the top of the inner frame which allowed a thin rib to be incorporated along the top edge to deflect the leaflets radially inwards, if required. A locking ring was used in the base to secure the two frames together.
 - iii The leaflets were mounted underneath an inner support frame and located on the outside surface with securing pins. The inner frame had an inverted U shape at each post through which the leaflets passed, which allowed them to close completely together with no post in between (Figure 5.3). The inner frame was a complex shape profiled on both its upper and lower surfaces and an outer sleeve was similarly profiled to retain the leaflets in position. The leaflets projected radially inwards from the frame to take up a natural closed position.
 - iv The inner support frame had three slots located along the edge of each scallop through which the leaflets projected (Figure 5.4). At each post only a thin vertical rib separated the slots allowing adjacent leaflets to come together. A thin outer ring

was used to retain the leaflets in position in the base. The slot orientated the leaflets radially inwards so the natural unloaded position of the leaflets was closed.

v Both inner and outer frames were used to support the leaflets (Figure 5.5). The inner frame with truncated posts supported the leaflets in the base of the scallop whilst the outer frame supported the leaflets at the top of the posts. The leaflets passed through vertical slots in the outer frame which gave them a radial orientation and allowed them to seal together completely.

Options 1 and 2 had similar disadvantages to the conventional valve designs such as wear of the leaflets where they were pulled over the edge of the inner support frame. Both required a smooth covering material on the inner frame to reduce abrasion of the leaflet. In addition the posts projected between adjacent leaflets so an additional restraint or stitch was needed to seal the leaflets together at the top of the posts. However, fastening the leaflet in the base of the frame ensured that the stress concentration around the fastenings were away from areas of dynamic stress in the flexing portion of the leaflet, and away from the area of abrasion at the edge of the frame. In option 2, the more rigid outer sleeve gave a secure clamping action to locate the leaflets.

Options 3 and 4 allowed the leaflets to be mounted radially inwards, take a natural closed position and seal together at the posts. In option 3, however, the points of attachment to the frame were close to the flexing portion of the leaflets. The frame in option 4 was more difficult to manufacture and very difficult to

cover. Option 5 combined the advantage of the radial mounting at the posts with the fastenings in the base on the outside of the inner frame. Differential deflection between the two frames could cause distortion to the leaflets.

Frame configuration 2 was selected for the initial development work and particular attention was paid to the covering material used on the inner frame to reduce abrasion and the method used to seal the leaflets around the top of the posts. This configuration allowed the thin outer sleeve to project above the leaflets in the base of the scallops and at the posts which had the following advantages for valves in the mitral position. The leaflets were protected from the surgeons needle during implantation; rounded posts were less likely to cause damage to the myocardium, and the sewing ring was positioned away from the inflow edge of the valve so reducing the length projecting into the ventricle. In addition a protective thread could be placed around the top of the posts to prevent surgical sutures snaring around the posts during insertion.

5.3 Covering materials for the frames

The twin frame design allowed different materials to be used to cover the inner and outer support frames. The outer frame was covered with polyester cloth as in porcine and existing pericardial valves and the sewing ring was fabricated from the same cloth. The cloth was intended to act as a lattice or support framework for host tissue ingrowth and endothelialisation over the sewing ring and outside of the outer frame. This would allow the valve to be

incorporated readily into the natural orifice.

The requirements for the covering material for the internal frame were different. Primarily, it had to be smooth to eliminate abrasion to the leaflets at the edge of the frame. It also had to have good blood compatibility and preferably had to be fabricated over the frame without any seams on the internal surface, as this surface contacts the blood on the inflow aspect of the valve. The material had to be thin in order that the radial wall thickness of the assembled valve was kept to a minimum. It would also be an advantage if the material did not encourage host tissue ingrowth to avoid the valve orifice becoming restricted (Figure 1.6).

Several materials were considered suitable for covering the inner frame. These included bovine pericardium treated with glutaraldehyde, porcine pericardium treated with glutaraldehyde, expanded PTFE, and polyester cloth coated with polyurethane. These different materials were considered during the valve development.

5.4 Leaflet design and configurations

The studies of pericardial valves in Chapter 3 showed how the different leaflet designs affected valve function. It proved difficult to describe the leaflet geometries theoretically in either the open position, closed position under load, or natural unloaded position, due to the complexity of the geometries and non-linear extension of the fixed tissue. Indeed, no theoretical basis has been given for the leaflet design in any of the valves studied. Other workers have defined leaflet geometries in the closed position

(56,140). In only one case was the open position or method of opening described (55). Optimal leaflet geometries are more readily derived empirically in a function tester rather than by attempting to predict the complex extension and shape of the leaflets theoretically. In this section four basic leaflet designs and geometries that were studied in the function tester during valve development are described.

Two basic methods were considered for the fabrication of the leaflets. Firstly, the tissue was fixed with glutaraldehyde in its natural shape and, secondly, the leaflets were moulded during fixation into a complex shape with curvature in two planes into a geometry that closely related to the closed position of the leaflets. Fixation in a semi-open position was not considered feasible for pericardial leaflets (200) as any geometry which was not fully open or closed required complex reversals in the radii of curvature of the unloaded leaflets. It has been shown with porcine valve leaflets (126) and pericardium (172) that tissue extensibility was greatly reduced when stress or strain was placed on the tissue during fixation. Considerable emphasis has been placed on controlling the strain placed on the tissue during fixation. The frame configuration selected for development with the leaflets mounted over the outside of the inner support frame caused the leaflets to project upwards in a vertical cylinder when unloaded (open position). This was changed to the closed position by using the outer frame to deflect the tissue radially inwards at the top of the posts, by using coaption stitches at the top of the posts or by the shape formed in the leaflet during fixation.

The simplest geometry (A) for the tissue which was fixed in a flat sheet was a cylindrical or conical shell which was produced by bending the tissue in one plane. Leaflets formed into a cylindrical shell equal to the external radius r_0 of the stent allowed a full orifice for the open leaflet. Figure 5.6a shows a vertical section through the centre line of a leaflet with cylindrical geometries. CO¹B shows the open position for the leaf. The leaflet flexed into the unloaded closed position COB by reversing the curvature of the cylinder. The shape of the scallop in the stent CB defined the angle through which the leaflet flexed. In the example shown h the height of the post B equals r_0 and $\alpha = \text{TAN}^{-1} 0.5 = 26.5^\circ$, so the leaflet flexed through an angle $2\alpha = 53^\circ$. The scallop in the frame ACB was in a plane inclined at an angle α to the vertical defined by the intersection of two cylindrical surfaces. If the angle α was increased, the height of the frame h was increased. The vertical sections through the closed leaflets taken at 2.5 mm intervals from the centre line of the leaf are shown in Figure 5.6b. As the leaflets met in the plane OB there was a sharp change in the leaflet direction as the leaflets coapt. The area of coaption is shown in a projection of the leaflet in Figure 5.6d. The free edge of the leaf was defined 1 mm above the post B and the centre point O. Figure 5.6c shows the radial view on the post which had a triangular shape defined by the intersecting planes of the scallops.

Most of the coaption in this leaflet was above the line AEB joining the top of the posts (Figure 5.6d). The loaded closed position for the leaflet cannot be predicted but an extension of 20 percent under a load would cause a significant increase in the angle

2 α . The leaflet was not constrained in the vertical plane along its free edge whereas its position was precisely constrained by the edge of the scallop. These different boundary conditions will produce anisotropic strains and significant changes in leaflet geometries in the loaded position. The outer frame was used to deflect the leaflets radially inwards at the top of the posts so that it took up the closed position CEOB when unloaded. This geometry was used with different heights to the posts and angles α' , with small changes in the radius of curvature of the cylindrical shell and with a variable width in the leaflet at the top which produced a slightly conical shell.

An alternative geometry for the leaflet in the closed position was produced by changing the shape of the scallop in the frame. An example of this geometry is shown in Figure 5.7. The open position of the leaflet CO¹B remained unchanged as a cylindrical shell, but the scallop in the frame was defined by a plane at an angle $\alpha + \beta$ to the vertical with a short parallel vertical portion B¹B at the top of the post. The leaflet can be deflected by the outer frame at the top of the posts to take up an unloaded closed position defined by CEOBB¹ (OEC being the vertical section through the centre line of the leaflet) in Figure 5.7a. In the base of the leaflet the tissue was cylindrically shaped, inclined at an angle $2(\alpha + \beta)$ to the vertical. This shape changed towards the free edge of the leaflet where the vertical section CEO became curved. The position of point O remained unchanged from the previous geometry, but cutting away the scallop deeper in the frame at B¹ (Figure 5.7c) allowed the leaflets to come together in a deeper coaption (Figure 5.7b). Effectively, a wider portion of the leaflet was able to flex inwards. The increased

area of coaption on the leaflets (shown in Figure 5.7d) was below the line joining the top of the posts AEB. In the example shown, angle β was 3.5° and $2(\alpha + \beta)$ was 60° . The change in the unloaded closed position caused by the change in the scallop shape introduced greater anisotropic strains in the loaded closed position as the leaflet geometry deviated further from the cylindrical geometry. The angles α and β and radius r_0 and width of the leaflet were varied as in the previous example.

Figure 5.7b showed that radially the leaflet closed shape was curved producing a spherical shape. This curvature could be more easily produced and controlled by forming the spherical shape in the leaflet during the fixation. This was achieved simply by laying the tissue on a mould shaped to form the outside surface of the stent, the shape of the scallop and the geometry of the closed unloaded leaflet. In this method anisotropic strains were fixed in the tissue when forming the shape of the leaflet as opposed to them being induced by the loading of the leaflet in the closed position. Inducing this strain during fixation could affect the mechanical properties of the tissue and this had to be considered when forming the leaflets.

Two simple geometries were considered for the closed position, a spherical surface and a combination of cylindrical and spherical surfaces. Figure 5.8 shows an example of the spherical geometry. In Figure 5.8a the vertical section through the centre line of the leaflet OC shows radial curvature R_r moulded in the leaflet which was equal to $0.96r_0$. The open position O^1C was also spherical in shape having the reverse curvature of the closed surface. View b shows the vertical sections through the closed leaflet at 2.5 mm

intervals from the centre line and the line CB which was the line of intersection of the spherical shell with the cylindrical frame. This produced a narrower post as seen in view C. The radial curvature in the leaf allowed the leaflets to come together tangentially as two parallel surfaces in the area of coaption. This is illustrated in the horizontal section through the leaflet in view d. The radii of curvature for the spherical shell R_c was varied as was the position of the centre of the shell (D). The height of the leaf h (equal to r_0 in the example) was also varied. This geometry produced a small triangular hole in the centre of the valve between the three spherical leaflets. This was designed to close up as a small load was applied to the leaflets. The moulded shape also formed the cylindrical surface to the leaflet which was mounted around the outside of the frame. At the edge of the frame a small radii R_e was generated to give a smooth transition from the vertical cylinder to the spherical flexing portion of the leaflet (view a).

Figure 5.9 shows an example of the second moulded geometry. The closed shape of the leaflet shown as a vertical section CO (in view a) was a cylindrical surface in the base of the leaflet inclined at an angle δ to the horizontal, followed by a spherical surface in the centre of the leaflet with a small cylindrical surface at the top of the leaflet. As in the previous example $R_r = R_c = 0.96r_0$ and $h = 1.12r_0$. The vertical sections through the leaflet are shown in view b, the horizontal sections view d and the post in view c. This configuration differs from the previous geometry in the base of the leaflet where the leaflet had to flex through a smaller angle between the open and closed positions. As before, the open geometry was the

reverse curvature of the closed geometry. In the example shown γ equalled 30° . As before, a radius R_e was formed where the flexing portion of the leaflet intersects the cylindrical frame.

One possible disadvantage of the last two geometries was that fixation of the tissue in the spherical shape could alter its mechanical properties. A flat sheet of tissue formed into a cylindrical surface has little bending strain. For a radius r_0 and thickness t , bending strain $\epsilon_b = t/2r_0$. For the examples shown where $r_0 = 12.5$ mm and $t = 0.5$ mm $\epsilon_b = \pm 2\%$. However, to form the tissue into a spherical surface greater strains were induced which were more difficult to predict. A cylindrical piece of tissue (Figure 5.10) required an additional 9% extension in the length OC to form a spherical surface, if points O and C remained fixed. However, if tissue at O was displaced to O", approximately 1 mm, then the extension required radially was only a few percent. Similarly, the additional extension required circumferentially was also only a few percent. It did, however, introduce complex shear strains in the tissue. Ideally, the tissue should be positioned in the mould to minimise the strain placed on the tissue during fixation, so reducing the changes induced in the mechanical properties. At the edge of the mould a much smaller radius was fixed in the leaflet R_e (approximately 2 mm). This small portion of the leaflet was not expected to flex as the leaflet opened or closed, so the curvature fixed into the leaflet at the edge of the frame was effectively constraining it radially inwards.

5.5 Discussion

The unique design philosophy which uses twin cylindrical frames to support the leaflets, and radial pins to locate them, has been described in several forms. In each case the leaflets were mechanically mounted on pins and studs and could be interchanged easily to allow matching for synchronous movement. The frame design option selected for the valve development (option 2) allowed easier construction of the valve and more readily lent itself to the use of radial locating pins. The problem found in other commercial pericardial valves of abrasion of the leaflets against a cloth-covered inner frame, was reduced by selection of a smooth material to cover the inner frame. The abrasion and wear to the leaflets caused by different covering materials was assessed during the valve development. In addition, the problem of sealing the leaflets together around the top of the posts was also considered during the valve development described in the next chapter. The advantages of using an outer frame had to be offset against the overall increase in the radial width of the valve wall which reduced its potential orifice area. It was most important in the frame design that the leaflets opened up fully to utilize the internal diameter of the frame.

Although a valve construction using concentric frames has recently been described (202,203) for use in the operating theatre, it did not indicate the method of positioning or restraining the leaflets, or whether the leaflets could be readily interchanged.

The frame design described only the method of mounting and restraining the leaflets. Several different leaflet designs and

geometries have also been described. Previous work has only described a cylindrical or conical shaped leaflet for a bileaflet valve (55) and a spherical geometry for synthetic leaflet valves (140). I have attempted to describe a wider range of different leaflet geometries and methods of fixation combining both spherical and cylindrical geometries with fixation of the tissue both as a flat sheet and in curved shape. Function tests on other pericardial valves (Chapter 3) showed that the method of fixation and leaflet geometry significantly affected valve function, while methods of fixation also affect the material properties (Chapter 4). The leaflet designs proposed in this chapter were assessed by manufacturing a range of prototype valves with different leaflet geometries, and analysing the leaflet dynamics in the pulsatile flow test apparatus. These tests are described in Chapter 6.

CHAPTER 6

VALVE DEVELOPMENT: I

6.1 Introduction

An improved valve frame design and four different leaflet designs were described in Chapter 5. The frame design offered several advantages, such as precise location of the leaflets and interchangeability of the leaflets during manufacture, but potential problem areas, such as abrasion of the leaflets on the inner frame and the method of sealing the leaflets at the top of the posts, had to be investigated during the valve development. The frame design enabled easy assembly of the leaflets which allowed a wide range of prototype valves with the different leaflet geometries described in Chapter 5 to be manufactured and tested.

This chapter describes the development of the frames and fastenings, and the development of an optimal leaflet geometry. Four different leaflet geometries were tested in the pulsatile flow test apparatus. Different configurations were tested for each geometry corresponding to changes in the detailed sizes, and several prototype valves were tested for each configuration in order to reproduce any variations in function detected. This also helped to reduce the effect of any variations in the tissue properties.

The development work was carried out on size 27 mm mitral valves and the final design was scaled up and down for the other sizes of valves.

6.2 Frame development

A photograph of the two frames for a size 27 mm prototype valve is shown in Figure 6.1. The frames were machined out of solid acetal rod. The small pins and studs, which were injection-moulded, were pressed into the radial holes. The detailed shape and position of the pin and stud fastenings are described in Figure 6.2. Seven pins (3 to 9) were used to locate the leaflets in the base of each scallop and two studs were used to locate the tissue at each post. Each leaflet was manufactured with predetermined holes made with 0.5 mm tapercut needles which were located over the pins and studs. The outer sleeves were slotted at each post to allow the base of the sleeve to splay out and clip over the radial pins thus retaining the leaflet in position. These slots were wider at the top of the posts to allow the two studs to project through. Small washers were pressed over the ends of the studs to retain the leaflets in position (Figure 6.2). A thin locking ring was positioned over the base of the sleeve to clamp the two frames together. For the prototype valves made with tissue treated as a flat sheet (geometries A and B) the outer sleeve was manufactured with a deeper flange at the top of the posts so it projected over and around the inner frame, deflecting the leaflets towards the closed position when unloaded.

The four leaflet geometries were tested on frames without covering materials. To compensate for the covering materials, the internal and external diameter of the valve frame were increased. For the size 27 mm valve the outside diameter of the inner frame (the surface over which the leaflets flexed) was defined as 25 mm, while

the outside diameter of the outer sleeve was 26.5 mm. The internal diameter of the uncovered inner frame was 22.8 mm.

6.3 Leaflet geometries A and B

For leaflet geometries A and B the tissue was fixed with glutaraldehyde in the natural shape of the pericardial sac. This was achieved by placing tissue over 4" diameter perspex rings in a bath of glutaraldehyde, and placing a second ring over the tissue to restrain it at the edges. The tissue was allowed to take up its natural shape within the ring so it was relaxed, but as the fixation occurred the tissue appeared to tighten and shrink a little. Supporting the tissue on a ring avoided the wrinkles that could occur if the tissue was fixed as a flat sheet. The larger area of tissue covering the right ventricle (zones 1 and 3) was used and leaflets were cut from the centre of the mounting ring to avoid areas close to the edge where strain could have been placed on the tissue. Tissue thickness of 0.4 to 0.45 mm was selected with the epipericardial surface as the inflow surface of the leaflet. Typical uniaxial load extension curves for the tissue fixed in this manner are shown in Figure 6.3. The tissue showed similar characteristics to the tissue fixed as a flat sheet (Section 4.3). No specific orientation was taken when cutting these leaflets from the membrane. After fixation the tissue was floated on a flat template and five holes cut in the tissue corresponding to the mounting points, 1, 2, 6, 10, 11, in the frame. A second template was used to cut the edges of the leaflets (Figure 6.4). The key dimensions were the width of the leaflet between the fastening points

(1, 11) q , the height of the post supporting the flexing portion of the leaflet h_f , the height to the top fastenings h_g and the height to the centre of the free edge l . The approximate area of the flexing portion is also shown in Figure 6.4.

The basic cylindrical geometry of configuration A was described in Figure 5.6. The frame cut-outs or scallops were produced by the cylindrical surface of a 25 mm end mill inclined at an angle ($2\alpha = 53^\circ$) to the axis of the cylindrical frame. This produced a plane of intersection at an angle α (26.5°) to the axis of the frame. The detailed shape of the frame is shown in Figure 6.5 by a radial view of the post and a radial view on the centre of the scallop. The leaflet was cut with a width q of 26 mm, an overall height l of 17 mm and a height h of 13 mm. Two valve prototypes tested in the function tester showed this leaflet configuration was not stable in the closed position under a high back pressure. A photograph of one valve in the tester in the fully open position (test conditions: stroke volume 70 ml, rate 70 per minute - sine wave - peak flow 280 ml s^{-1}), and in the fully closed position (back pressure approximately 100 mmHg) is shown in Figure 6.6. In the fully open position the leaflets took up a full cylindrical shape providing a large orifice. However, in the closed position the valve was not competent as all three leaflets folded under themselves at the free edge creating a triangular orifice in the centre of the valve. The reason for this is explained in Figure 5.6. A significant portion of the leaflet above the line AEB was not in the area of coaption between adjacent leaflets. This triangular portion of the leaflet AOBE could not support the back pressure and folded along the line AEB creating the hole in the centre

of the valve.

The second geometry B was designed to overcome this problem. A greater portion of the stent frame was cut away to produce a deeper coaption between the leaflets when loaded (Figure 5.7), so a larger portion of the area AOB_E was supported by the other leaflets. Three different frames were manufactured for this configuration B1, B2 and B3 (Figure 6.5). In two frames, B1 and B2, the scallops in the frames were produced by a cylindrical cutter inclined at an angle $\alpha(\alpha + B) = 60^\circ$ to the axis of the cylindrical frame. The cut-out was restricted in depth to allow a short parallel post 2 mm wide. The overall height of the flexing portion of the leaflet h was 13 and 14 mm, with a leaflet width q of 26 mm and an overall length l of 17 and 18 mm for configurations B1 and B2, respectively. Several prototype valves of these configurations were tested. Figure 6.7 illustrates the function of a valve with configuration B1. In the unloaded position the leaflets were deflected inwards into the closed position by the outer frame, so they touched at their free edges but left small holes around the top of the posts and a small triangular hole in the centre. As in the previous configuration the leaflets opened to a full cylindrical orifice. In the closed position under pressure, the leaflets sealed together to form a competent valve. There was however a significant mismatch in the heights of the free edges of the leaflets with the least extensible leaflet sitting higher than the other two leaflets. The area of coaption under load shown in a side view on one leaflet was quite small. The maximum coaption depth h_c was approximately 3 mm and the reference point E, was not in coaption with the other leaflets. A small portion of the leaflet

above the line AEB was not in coaption with the other leaflets. A vertical section through the leaflet on the centre line OEC showed how the leaflet was displaced downwards as the pressure extended the tissue (Figure 6.8). The displacement was greatest towards the free edge of the leaflet where the leaflet was not restrained in the vertical direction. This explains why the less extensible leaflet was higher than the other two leaflets. If taken to an extreme this could allow the most extensible leaflet to prolapse below the other leaflets. The area of coaption between the leaflets not only sealed the leaflets together but prevented one leaflet prolapsing below the other two leaflets.

Configuration B2 was used to try and improve the depth of coaption between the leaflets and the stability of the closed position. The extra 1 mm in leaflet and post height improved the coaption depth slightly but mismatches in leaflet height occurred due to small variations in tissue extensibility. In Figures 6.8 and 5.7 the loaded closed leaflet took up a curved shape radially as well as circumferentially, which improved the coaption depth.

In the configuration B3 the frame scallop was cut away further by using a 25 mm spherical ball cutter (Figure 6.5). This effectively smoothed the profile of the scallop at the top of the post and allowed a greater portion of the leaflet to flex inwards. This was intended to provide a deeper coaption between the leaflets. Several prototypes were tested and their function is illustrated in Figure 6.9. Although the valve showed greater coaption than B2 and B1, h_c approximately 5 mm, there was still a mismatch in the heights of the three leaflets when closed under pressure. As before, the open

leaflets gave a large cylindrical orifice. At flow conditions of stroke volume 70 ml, rate 70 per minute (sine wave) the mean pressure difference across the valve was 1.6 mmHg at an RMS flow of 194 ml s⁻¹. This gave an effective orifice area of 3.0 cm². The closing regurgitant volume was 6.5 ml and the closed regurgitant volume 2.1 ml. In all these prototype valves made with tissue fixed flat, the leaflets transposed easily from the closed to the open positions with all leaflets opening up fully at low flows of under 50 ml s⁻¹.

The fundamental geometry of all these leaflet configurations meant that the area of coaption between the leaflets was not defined by the cylindrical surfaces which met at an acute angle. There was excess material in the coaption area of leaflets causing the free edges to twist and wrinkle and consequently the closed position of the leaflets was not the same on every cycle. The more stable spherical shape of the leaflet with a deeper coaption was only produced when the tissue was extended under load and was partially due to the geometry of the scallop in the frame. It was felt that if this spherical shape was produced in the tissue during fixation it would give a more stable closed position. In particular, as the leaflets came together they would meet as two parallel surfaces in the area of coaption.

6.4 Leaflet configurations C and D

The basic geometries of the moulded leaflets C and D were described in Figures 5.8 to 5.9. Leaflets were manufactured on single leaflet moulds so only a small area of uniform tissue was

required. A photograph of a size 27 mm mould is shown in Figure 6.10. The mould not only defined the shape of the flexing portion of the leaflet, but also the stationary cylindrical portion positioned around the support frame. The edge of the mould was rounded where the flexing portion of the leaflet intersected the cylindrical surface of the frame defined by radius R_e (Figure 5.7). The moulded shape formed the leaflet towards the closed position. Therefore, the outer sleeve was made a uniform thickness at the top of the posts as there was no need to deflect the tissue inwards. The mould was also used to position the array of holes 1 to 11 corresponding to the fastening points for the pins and struts (Figure 6.3).

The fresh tissue was placed on the moulds precisely, by initially floating it on a flat template as in Figure 6.4, and picking up five reference holes, 1, 2, 6, 10 and 11. As with the fixed tissue the critical dimensions were the width q and height h . The fresh tissue was placed on the mould and the five reference holes aligned to the appropriate holes on the mould. The mould and tissue were then submerged in a saline bath to allow the tissue to take up its position on the mould and the other six reference holes marked. The tissue and mould were placed in a glutaraldehyde bath for 24 hours and the tissue was removed from the mould and fixed for a minimum of six days in glutaraldehyde. The tissue on the mould extended beyond the free edge of the leaflet and this was cut using a further template once the shape of the leaflet was formed.

The fresh tissue was orientated so the radial direction of the leaflet OC was along the circumferential direction of the pericardial sac. Tissue was taken from zones 1 and 3 overlaying the right

ventricle. The orientation was selected so the most extensible axis of the fresh pericardium in the biaxial inflation tests (circumferentially) was in the radial axis of the leaflet OC, where the deformation was greatest. A fixed tissue thickness of 0.4 to 0.45 mm was used. The load extension curves for uni-axial tests of fixed tissue taken from the leaflets (Figure 6.11) showed that the loading part of the curves were similar in both directions and were also similar to the tissue fixed flat (Figure 6.3). As expected, strips taken radially in the leaflets had greater UTS. There was an increased variation in the extensibilities of the tissue taken from the moulds which suggested that the restraint placed on the tissue during fixation could have produced some change in the mechanical properties of the fixed tissue.

For the spherical geometry, two configurations, C1 and C2, corresponding to radii of curvature 11 and 12 mm were tested. The differences between the two geometries is shown in Figure 6.12. In the horizontal section C1, the smaller radii of curvature, allowed a wider post w , whilst in the vertical section the larger curvature, R_{12} , was inclined at less than 90° to the axis of the cylinder in the base of the cusp, due to the position of D_2 being outwith the cylindrical frame. The position of D and D_2 and hence the depth of the spherical surface d was calculated from the arc length S_{ab} where the spherical surface intersected the cylindrical shell of the frame. A depth d of 11 mm gave S_{ab} equal to 24.5 mm for both configurations. The width q for the fresh tissue template (26.5 mm) was calculated from $(S_{ab} + w)$ with a small correction for the radius R_e at each post. The height of the scallop h was 14 mm. Several

prototype valves of both configuration were tested. Non-synchronous opening of the leaflets was a major problem with both configurations. In particular, at low flows the pressure gradient was not sufficient to reverse the curvature of all the leaflets causing them to buckle into the fully open position. This was a particular problem in the base of the leaflet where the tissue had to flex through an angle of over 90 degrees. Figure 16.13 illustrates the function of one of the worst prototype valves tested at flow conditions B (stroke volume 70 ml, rate 70min^{-1}). The valve had a symmetrical unloaded position defined by the geometry of the mould, with a small triangular hole at each post and a small triangular hole in the centre. These closed up under a small back pressure (less 5 mmHg) to give a stable closed position with deep coaption between the leaflets. However, one leaflet in the open position did not reverse its curvature fully at a peak flow of 200 ml s^{-1} and a peak pressure difference of 2.8 mmHg. This was an effect seen in the other prototype valves at lower flows. It appeared that the best leaflet opening action was achieved if the leaflet reversed its curvature in the base first. If the free edge of the leaflet moved out towards the open position first, this could produce a tighter radius of curvature in the base of the leaflet, making it more difficult to reverse its curvature and open fully.

Leaflet geometry D (Figure 5.8) was used to obtain leaflets that transposed from the closed to the open position at lower flows and pressure differences. A cylindrical surface was used in the base of the leaflet inclined at an angle $(90 - \gamma)$ to the axis of the cylindrical stent. The angle γ was varied between 20 to 30 degrees for radii of curvature of 11 and 12 mm. Prototype valves were made

to configuration D1 with a radius of curvature R 12 mm and an angle $\gamma = 30^\circ$ and configuration D2, a radius of curvature R 11 and angle $\gamma = 25^\circ$. In all cases the leaflets opened up more readily at lower flows and pressures and also maintained a stable closed position.

The function of a prototype valve manufactured to configuration D1 is shown in Figure 6.14 for flow condition B. In the unloaded position the leaflets did not sit symmetrically, but this did not affect the leaflet function. The leaflets moved synchronously to the fully open position at 70 BPM, S.V.70, with a peak flow of 200 ml s^{-1} and had a stable open position with the leaflets taking a convex spherical shape as described in Figure 5.8. The portion of the leaflet fixed in a radius R_e at the edge of the frame moved very little. Consequently, a small portion of the leaflet around the edge of the frame formed an S shape when the leaflet reversed its curvature in the open position (Figure 3.6). The leaflets moved from the closed to the open position at low flows typically 80 ml s^{-1} corresponding to a pressure difference of 0.8 to 1 mmHg. The closed position of the valve was stable with an even height to the leaflets and a coaption depth h_c equal to 5 mm. The valve had an effective orifice area of 2.7 cm^2 with a mean pressure difference of 1.2 mmHg at an RMS flow of 150 ml s^{-1} , a closing regurgitant volume of 6 ml and a closed regurgitant volume of 0.5 ml.

The prototype valve manufactured to configuration D2 had similar function at flow conditions B (Figure 6.15). The unloaded position of the leaflets was more symmetrical. This was attributed to the slightly greater distance w at the top of the post, which allowed the tissue to bend uniformly around the top of the posts. As before the

leaflets opened at flows of approximately 80 ml s^{-1} corresponding to pressure differences of 0.8 to 1 mmHg and at a peak flow of 200 ml s^{-1} all leaflets opened up synchronously. As before the closed position was stable (coaption depth h_c equal to 5 mmHg). The valve had an effective orifice area of 3.0 cm^2 corresponding to a mean pressure gradient of 0.95 mmHg at an RMS flow of 149 ml s^{-1} , a closing regurgitant volume of 5.3 ml, and a closed regurgitant volume of 1.7 ml. Configuration D2 was considered the better option for the moulded leaflets due to the better unloaded position.

6.5 Discussion

The frames and fastenings developed, allowed the precise positioning of the leaflets on the frames, and when used with the flat tissue templates to locate the holes in the tissue, gave a highly reproducible method to producing the valves. Any variation in function seen between leaflets on the same prototype valve was more likely to be caused by variation in the tissue properties. It was estimated that critical dimensions on the leaflets could be reproduced to $\pm 0.5 \text{ mm}$ which was equivalent to changes in the leaflet extensibilities of $\pm 2\%$. Figure 6.3 showed that variation in the leaflet properties were greater than this.

Configurations A and B showed that the geometry of the closed leaflet under back pressure was an important factor in determining the stability of the closed valve. In particular, the area of coaption between the leaflets not only sealed the valve to prevent leakage, but gave mutual support to the leaflets. The shape of the cut-out or

scallop in the frames determined the geometry of the closed leaflet under pressure. The cylindrical geometry in configuration A was not stable as a portion of the leaflet close to the free edge was not fully supported. This was significantly improved in configuration B1 to B3 by cutting away more of the frame which allowed a greater portion of the leaflet to flex inwards giving a deeper coaption h_c .

This produced a more spherical shape to the closed loaded leaflet which was optimised when the frame cut-out was defined by a spherical surface in configuration B3. This spherical geometry and deeper coaption was only produced when the back pressure was applied on the leaflets. Consequently the geometry, position and height of the loaded leaflets was dependent on the extensibility of the tissue. This was illustrated by the mismatch in the heights of the closed leaflets. The coaption depth h_c was an important parameter in leaflet design, as it affected the stability of the closed position. This was a function of the closed leaflet geometry rather than the overall height h of the flexing portion of the leaflet. In all these prototype valves the leaflets were deflected towards the closed position when unloaded by the outer sleeve, but moved easily to the open position at low flows and pressure differences.

The leaflets moulded with a spherical geometry (configuration C and D) had a well-defined stable closed position under load. The spherical geometry gave a deeper coaption h_c and the leaflets met as parallel surfaces in the area of coaption. Consequently, any small variation in the tissue extensibility did not cause significant differences in the heights of the loaded leaflets. The main disadvantage of these moulded leaflets was that a significant pressure

difference was required to buckle or reverse the curvature of the leaflets from the closed to the open position. All the leaflets in configuration C did not open fully at low flows. Theoretical considerations for the least resistance to opening have given a minimum peak pressure difference of 0.4 to 0.95 mmHg for a natural aortic valve and 1 to 4 mmHg for synthetic leaflet valves (76). For bovine pericardial leaflets treated with glutaraldehyde the minimum pressure differences have been estimated as 1.3 to 2.2 mmHG (203). The minimum pressure difference required to open the valve leaflets increased with leaflet thickness and stiffness, and reduced with increased radius of curvature. These calculations made a number of approximations about the bending, compression and extension stresses, derived from uni-axial load extension curves (53). Leaflet flexibility may also be dependent on the microscopic structure of the tissue (173). In the worst prototype valve made from configuration C one leaflet did not open at a peak pressure difference of 2.8 mmHg. The leaflet was measured as being thicker in its base but its extensibility was not determined. Overall, the pure spherical geometry of configuration C did not give acceptable opening characteristics.

Geometry D with the cylindrical surface in the base of the leaflet gave better opening characteristics, with typical minimum opening pressure differences of 0.8 to 1 mmHg. The minimum opening pressures and flows were determined for both steady and pulsatile flows as the flow was being increased. The minimum opening pressure differences and flows (steady and peak) were measured just prior to the opening of the third leaflet, as when the leaflet opened the

pressure difference reduced due to the increase in the valve orifice. The minimum opening pressure differences 0.8 to 1 mmHg occurred at peak flows of 80 ml s^{-1} which are approximately 40% of the peak flows for a resting cardiac output in the mitral position, and 30% of the peak flows for a resting cardiac output in the aortic position. In addition, the time interval for the leaflet to move from the closed to the open position was also monitored using still frames on the video camera to ensure synchronous leaflet action at normal flow rates. To achieve uniform opening of the leaflets in configuration D the tissue thickness and extensibility had to be controlled during manufacture. The spherical shape of the open leaflet did not affect the hydrodynamic function of the valves as the effective orifice areas and regurgitation were similar to the valves with geometries A and B.

Configuration D2 was considered to give the best leaflet function with both a reproducible stable closed position and symmetrical unloaded position with acceptable opening characteristics. This leaflet configuration was used for further development of the valve.

CHAPTER 7

VALVE DEVELOPMENT II AND FINAL SPECIFICATION

7.1 Introduction

The development of a leaflet geometry which gave optimal function was described in the previous chapter. The leaflet was moulded in a geometry defined by cylindrical and spherical surfaces which closely approximated the closed position of the leaflet. Several areas of the valve design required further consideration. In particular, the materials used to cover the frames, and the abrasion caused to the leaflets at edge of the frames, the methods used to close the leaflets together at the top of the posts to prevent leakage, and whether the flexural durability of the tissue had been affected by forming the tissue in a spherical shape during fixation.

This chapter describes the evaluation of different materials to cover the frames and the accelerated fatigue tests carried out to assess the abrasion to the leaflets caused by the covering materials. In addition, several methods of closing the leaflets together at the top of the posts were investigated. The unloaded position of the leaflets shown in Figure 6.15 showed small triangular holes between the leaflets at the top of each post. These did not always seal up completely when the valve was fully closed. Several different prototype valves were manufactured with a different design at the top of each post. The function and leakage was assessed in the column tester and pulsatile flow test apparatus, and the durability assessed in the accelerated fatigue tester. The final specification for the

valve is also described for the range of aortic and mitral sizes and the importance of the valve manufacture discussed briefly.

7.2 Covering materials for the frames

Several knitted polyester cloths were considered for covering the outer sleeve and fabricating the sewing ring for the valve. These were manufactured by the School of Knitwear Technology at Leicester Polytechnic. The outer sleeve was covered by producing a cylindrical tube of cloth which was folded over the top of the frame. The excess material in each of the three scallops was pulled down so the cloth was stretched until it conformed to the profile of the upper edge of the sleeve. It was then sewn in a single seam along the base of the sleeve. The important characteristics for the cloth were:

- i Thickness - approximately 0.2 to 0.4 mm was required.
- ii Extensibility - sufficient stretch to conform to the shape of the frame.
- iii Coverage - adequate coverage of the acetal frame when stretched.
- iv Stability - to be sewn without running or snaring.

A 50 dtex/22 filament bulked polyester yarn was used on a warp knitting machine. For early development valves a Tricot structure was used which was very thin and extensible but did not give adequate coverage or stability for sewing. Other structures were assessed

and, finally, a locknit was selected as it gave greater stability and ease of sewing. It was slightly thicker (0.3 mm when stretched) due to its more complex structure. The extensibility was varied by adjusting the number of courses in the cloth, and the tension in the yarn, to allow the cloth to be stretched over the frame, but controlled to give an adequate coverage at the top of the posts. The coverage of the frames was monitored by photography at thirty times magnification. Figure 7.1 shows a photograph of the covered outer frame.

The covering materials for the inner frame were more critical as they had to eliminate abrasion to the leaflets at the edge of the frames. The important properties of this material were:

- i Smoothness - to reduce abrasion to the leaflets.
- ii Thickness - approximately 0.25 mm to minimise the overall bulk of the valve.
- iii Extensibility - to stretch and deform to the shape of the frames.
- iv Stability - to be able to suture the material without tearing.

The four materials considered were bovine and porcine pericardium, both treated with glutaraldehyde, PTFE (Gortex), and polyester cloth coated with polyurethane. The polyurethane coating on the cloth gave a smooth surface but was unacceptably thick adding over 1 mm to the overall thickness of the valve frame. The Gortex PTFE membrane was very thin, typically (0.1 mm), but was highly

extensible in only one direction, and so it would not conform to the frame. It was also very difficult to sew without tearing.

Both the porcine pericardium (thickness approximately 0.15 mm) and the bovine pericardium (thickness approximately 0.3 mm) were extensible enough to cover the frames. In both cases the tissue was stretched over the inner frame when fresh, and fixed with glutaraldehyde whilst in position. The porcine pericardium tended to wrinkle as it was stretched over the edge of the frame but this did not happen with the bovine pericardium which was slightly thicker. Bovine pericardium selected from an area 2 overlaying the left ventricle was used with a thickness of between 0.25 and 0.3 mm when fresh. A single piece of tissue was used to cover each frame with no seams on the inside surface of the frame (Figure 7.2). The tissue was overlapped in vertical seams down the outside of each post and sewn around the base of the valve. This cover added approximately 0.5 mm to the wall thickness of the inner frame. Consequently, for a size 27 mm valve the outside diameter of the inner frame, when covered, was 25 mm, and the internal diameter 21.8 mm. The width of the post when covered increased to approximately 2.5 mm.

The amount of abrasion to the leaflets at the edge of the frame was assessed by cycling two valves covered with bovine pericardium, two valves covered with Tricot knitted polyester cloth, and one valve with a naked acetal inner frame, in an accelerated fatigue tester. The bovine pericardium and acetal gave a relatively smooth surface for the leaflets to flex over at the edge of the frame while the open knit of the cloth gave a rough surface.

The results of the fatigue tests are shown in Figure 7.3.

Valves 27.1 and 27.2 with the cloth-covered frames failed after 42 and 78 million cycles (approximately equivalent to 1 and 2 years) with tears in the leaflets on the shoulder of the scallop at the edge of the frame caused by the abrasion of the leaflets on the cloth (Figure 7.4). The tear on the leaflet of valve 27.1 extended to the free edge causing the leaflet to prolapse while the test was stopped for valve 27.2 before the tear could extend to the free edge. All the leaflets showed the abrasion caused by the cloth on the edge of the inner frame. This is illustrated clearly in Figure 7.5a, the photograph of the inflow aspect of a leaflet taken from valve 27.1. In all leaflets the abrasion was greatest at the shoulder of the scallop, about 3 mm from the top of the post. Valve 27.3 with the uncovered inner frame was tested to 160 million cycles without failure while valves 27.4 and 27.5 with the pericardial-covered frames were tested to 430 million cycles without failure. A photograph of the inflow aspect of a leaflet from valve 27.4, after 430 million cycles, showed that there was some wear to the leaflet at the edge of the frame, but this was greatly reduced compared to the leaflets from valves 27.1 and 27.2 with cloth-covered frames.

Figure 7.6 shows photographs of valves 27.4 and 27.5 after 430 million cycles. There appeared little damage or fatigue to the flexing portion of the leaflet with only small marks in the centre of the free edge of the leaflet where there is a small radius of curvature in the closed leaflets as they come together. This extensive cycling indicated that moulding the leaflets in a spherical configuration during fixation had not significantly affected the flexural durability of the tissue. There was a slight tendency for

the free edges of the leaflets to remain apart at the top of the posts, both when unloaded and loaded. This gave an increase in the closed regurgitant volume when the valves were cycled in the function tester at the end of the fatigue test. Otherwise the hydrodynamic function of these valves was unchanged.

These tests showed conclusively that the bovine pericardial covering caused the least abrasion to the leaflets and significantly improved the valve durability. This is illustrated in a vertical section through the frames in the base of the scallop at point C (Figure 7.7).

7.3 Closure of the leaflets at the posts

In the prototype valves described previously, the leaflets had not been brought together in apposition at the top of the posts. This is seen in the unloaded valves and some closed valves where the leaflets did not seal together fully allowing a small closed regurgitation of 1 to 3 ml per stroke in the mitral position. After valves 27.4 and 27.5 were cycled in the fatigue tester this leakage increased. The leakage was variable from valve to valve and may have been dependent on how the leaflets were positioned on the fastening at the back of the post. The pericardial cover on the frame may also have affected the leakage as it increased the effective width of the post w . Other commercial valves have coaption stitches to close the leaflets together at the posts (Chapter 3) but they have been indicated as possible sources for tears in the leaflet. Any suture placed through the tissue in the flexing position of the leaflet, or

at the edge of the frame, will produce a stress concentration. Therefore, any method of closing the leaflets together has to be assessed in the fatigue tester as well as the function tester.

Four options were considered for sealing the leaflets together, two of which involved the use of sutures. The leakage occurred due to the small gap between the leaflets on the inside of the post (Figure 7.8). The gap closed up as the leaflets moved together under back pressure but did not seal completely. In the prototype valves manufactured previously, the leaflets projected 1 mm above the top of the posts in an attempt to prevent leakage. As an alternative to this, valves were made where the top of the post projected inwards to fill the space between the leaflets, and the leaflets were cut level with the top of the posts. Two stitch configurations were also used to seal the leaflets together (Figure 7.9). In both cases the leaflet was extended 2 mm above the top of the post ($h=16\text{mm}$) and a small stitch hole made 1 mm from the free edge of the leaflets. The leaflets were brought into apposition with a stitch above the post, but were not stitched to the post. When the valve was closed under pressure the stitch did not restrain the inward movement of the leaflets, so a stress concentration was avoided. In stitch A the suture looped over the free edge of the leaflets, around the back of the leaflets, and knotted at the back of the post. In stitch B the suture was looped around the back of the post twice and knotted at the back of the post. In both cases, the ends of the suture were sewn into the cloth-covered outer sleeve.

Prototype valves manufactured to the four different options were assessed in the function tester and column tester. In valves without

the stitch, but with the leaflets above the posts, a small variable leakage was measured in the column tester (3 to 5 ml s⁻¹) and a closed regurgitant volume of 1 to 2 ml. In valves without the stitch, with the inward projecting posts and the leaflets cut at the top of the posts, the leakage was greater (6 to 10 ml s⁻¹ in the column tester and 2.5 to 4 ml closed regurgitant volume). In this second case the gap at each post in the closed valve under pressure could be seen in the function tester (Figure 7.10a). In the previous prototypes the leaflets were probably sealed together above the top of the posts. Both stitch configurations sealed the valves completely at the top of the posts which reduced the leakage to 1 to 2 ml s⁻¹ in the column tester and less than 1 ml closed regurgitant volume (Figure 7.10b). However, the stitches did restrict the fully open position of the free edge of the leaflet (Figure 7.11) which slightly reduced the effective orifice area of the valve. For stitch configuration A, flow conditions B, this gave an effective orifice area of 2.7 cm² compared to 3.0 cm² for the valves without the stitch. The stitches constrained the leaflets in the fully open position causing a sharp bend in the leaflet close to the stitch which could cause increased stress levels. These would be greater at high flows and in smaller valves when the pressure difference across the open valves was larger.

The durability of the valves which were stitched at the top of the posts was assessed in the accelerated fatigue testers (Figure 7.12). Four size 27 mm valves, 27.6 to 27.9, with stitch A, were cycled and compared to 27.4 and 27.5 without stitches. In addition, six size 31 mm valves, 31.1 to 31.6, with stitch B, were cycled.

Valves 27.6 to 27.9 were tested to 440 million cycles without failure or damage to the leaflets around the stitch, which confirmed similar durability to valves 27.4 and 27.5 without the stitch. These valves are shown in Figure 7.13 after 440 million cycles. The performance of valves 31.1 to 31.6, with stitch B, was not as good. One stitch hole elongated after 150 million cycles in valve 31.1, and after 200 to 300 million cycles in other valves. The elongations occurred towards the back or outside of the leaflets (Figure 7.14). This was caused by the leaflet moving against the suture as it opened fully which gradually eroded a slot in the tissue. It probably occurred more rapidly in sutures that were not as tight. The elongated stitch holes eventually tore to the free edge of the leaflet. At this stage the damaged leaflets had good hydrodynamic function but tended to be displaced lower down under pressure than the leaflet with intact stitches. They also had abnormal opening and closing action. This seemed to contribute to the ultimate failure of the valves which will be discussed later.

These tests showed that stitch A did not cause tissue failure and gave an adequate seal between the leaflets at the top of the posts. It also gave a more symmetrical unloaded valve.

7.4 Final specification

The development work allowed a final specification for the size 27 mm mitral valves to be reached which was scaled up for the larger mitral valves and down for the smaller aortic valves. The final specification incorporated leaflet configuration D2, a pericardial

covering for the frame, and stitch configuration A.

The leaflet geometry D2 was defined by two cylindrical surfaces which intersected in the centre of the leaflet in a spherical surface. This was shown in Figure 5.9 and is illustrated in three dimensions in Figure 7.15. The cylindrical surface in the base of the leaflet formed the lower third of the leaflet, and was inclined at angle $\gamma = 25^\circ$. For the size 27 mm valves the radii of curvature of the cylindrical and spherical surfaces, R_C , R_S , were each 11 mm while the depth of cut d was 11 mm. The height of the frame scallop h_f was 14 mm, the height of the flexing portion of the valve leaflet was 16 mm which gave an overall height for the valve H of 20 mm. The arc length S_{ab} was 24.5 mm and the uncovered post width W was 2 mm. The critical dimensions for implantation are shown in Figure 7.16. The outside diameter of the covered outer frame D_{out} was 27.5 mm and the internal diameter of the covered inner frame was 21.8 mm. The implant height in the mitral position H_{imp} was 15 mm while the implant height in the aortic position was 19 mm. The implant diameter for the mitral position D_{out} was 27.5 mm, while the implant diameter for the aortic supra-annular position was taken as a nominal 27.5 mm, which is the outside diameter of the outflow aspect of the valve.

The valve was developed in sizes 19 to 27 mm for the aortic position and sizes 25 to 31 mm for the mitral position. The valves were similar in both positions except for the design of sewing ring and the shape of the base of the valve. In the mitral position the sewing ring was placed away from the inflow aspect of the valve so reducing the implantation height H_{imp} , and the outside diameter of the sewing ring D_s was larger. In the aortic position the base of

the valve was scalloped and a smaller sewing ring was positioned towards the inflow edge of the valve to give a supra-annular configuration with no projection into the aortic orifice. The diameter of the aortic sewing ring D_3 was smaller. The sizes of the key dimensions are given in Table 7.1. All the dimensions are scaled up or down in accordance with the diameter of the valve. In the aortic position overall height H was reduced by 0.5 mm in the base, and a scallop depth of 1.5 mm used to shape the base. Average leaflet thicknesses of 0.45 mm and 0.4 mm were used for the mitral and aortic valves, respectively. A photograph of the inflow and outflow aspect of a size 27 mm mitral valve and size 25 mm aortic valve are shown in Figures 17.17 and 17.18. These illustrate the differences in the sewing ring configurations.

7.5 Manufacture

The frames, sleeves and locking rings were manufactured out of solid acetal bars with general tolerances of ± 0.025 mm and ± 0.01 mm on critical dimensions. The injection moulded pins and studs were pressed into the frames with interference fits (± 0.05 mm). The inner frame was covered with a single piece of bovine pericardium (Figure 7.1) which was sutured around the base of the valve. A tube of polyester cloth was sewn to the tails of the pericardium projecting from the base of the valve. The outer sleeve was covered in polyester cloth as shown in Figure 7.2. Leaflets were formed on the moulds as described in Section 6.4 and fixed in glutaraldehyde for a minimum of seven days. The leaflets were selected and matched for

thickness and uniformity. A variation of 0.03 mm in thickness of the leaflets (t) in one valve was acceptable. Variation in thickness of up to .03 mm was accepted in any one leaflet but, if a gradient was measured, it had to be thinner in the base than the top of the leaflet. The leaflets were placed on an inner frame jig whose dimensions matched the covered inner frame and were retained in place with an outer jig. The function of the three leaflets was tested under a range of pulsatile and steady flow conditions for synchronous and uniform leaflet action. Any malfunctioning leaflets were replaced until a matched set was obtained.

The three leaflets were taken off the test jig and assembled onto a covered inner frame for the final assembly of the valve. The washers were pressed over the studs to secure the leaflets to the posts, a single stitch placed through the leaflets above the top of each post, the outer frame clipped over the projecting pins, and a locking ring slid into position in the base of the valve. At this stage in the valve assembly the functional parts of the valve had been secured in position and only the tails of cloth and pericardium extending from the base of the valve required to be sewn into place and a sewing ring fabricated from the cloth. The details of these final sewing procedures differed for the aortic and mitral sewing ring configurations. Essentially, each tail of cloth or pericardium was turned onto the outside of the cloth-covered sleeve and sewn in place, and two cloth tails were rolled together to form the sewing ring or cuff which was held in place with a final circumferential seam. This sewing added additional security to the valve construction as the pericardium from the cover of the inner frame was sewn to the cloth

covering of the outer frame. After the final assembly each valve was tested under pulsatile flow and steady flow conditions, before being placed in its final sterilisation and storage solution of 4% buffered formaldehyde.

7.6 Discussion

Fatigue test results for the prototype valves, with different covering materials on the inner frame, showed that the pericardial covering on valves 27.4 and 27.5 reduced the abrasion to the leaflets caused by the cloth on valves 27.1 and 27.2. The failure mode in valves 27.1 and 27.2 was similar to that described for commercial valves with cloth-covered frames in Chapter 3. The lifetime of 430 million cycles (the equivalent of 11 years) without failure confirmed that, with a smooth covering material such as pericardium, it was not necessary to rely on biological processes such as tissue ingrowth to maintain the integrity of the tissue at the edge of the frame (149,150). There was some wear to the leaflets along the edge of the pericardial-covered frames which may have been caused by the leaflets being compressed against the edge of the frame when the leaflets were in the closed position.

The tests also confirmed that the pericardial leaflets had good flexural fatigue properties and that fixation of the leaflets in the spherical shape did not affect the flexural durability of the tissue (55). The only sign of wear or damage was in the centre of some leaflets close to the free edge where the three leaflets met at a point. In this area striation and markings were found on the smooth

outflow mesothelial surface of some leaflets. The closed leaflets had high bending strains at this point particularly in the circumferential direction. It may well be that markings were the start of tissue disruption due to compressive bending stresses on the outflow surface of the tissue (53). Membrane stresses in this area were quite small (135,136).

The leaflets were sealed together at the top of the posts to prevent leakage. This was achieved with stitch configuration A which closed the leaflets together but did not restrain them to the post, so avoiding stress concentrations around the stitch when the valve was closed under pressure. The stitch did constrain the leaflet movement in the fully open position and this could induce stress in the tissue around the stitch. The fatigue tests on valves 27.6 to 27.9 tested to 400 million cycles showed that the stitch did not cause tissue damage. It was important to control precisely the position of the stitch holes and the tension in the suture. It was not easy to measure the flow through the valve or the forward flow pressure difference in the fatigue testers but, in the test conditions used, the peak flow through the valve was calculated at between 330 and 460 ml s⁻¹ for an amplitude of 3 to 4 mm at 12 Hz. Stitch configuration B in size 31 mm valves was not as good and movement of the leaflet against the thread elongated the hole in the tissue and eventually caused a small tear in some leaflets. This may have contributed to the eventual failure of some leaflets which will be discussed fully in the next chapter.

The final specification reached for the size 27 mm valve was scaled up or down to manufacture the other sizes of mitral and aortic

valves. Quality control was an important factor in the manufacture of all the valves. The unique design of mounting the leaflets on pins and studs allowed the leaflets to be matched and function-tested on a jig prior to final assembly. To a great extent this eliminated the need to reject valves for poor leaflet function after final assembly. The quality control function tests allowed the leaflets to be matched for symmetrical opening and closing, even coaption between the leaflets when closed, and a symmetrical open position. These tests often revealed small variations in leaflet properties which were not detected prior to the test. Synchronous opening was assessed under steady and pulsatile flows and a minimum opening flow of 5 l min^{-1} , 80 ml s^{-1} , was taken as an acceptable limit. This corresponded to minimal opening pressure difference of less than 1 mmHg for the size 27 to 31 mm valves, increasing to approximately 2 mmHg for the 19 mm valves. This increase was due to the smaller radii of curvature in the smaller valves (141).

The development work described in the last two chapters has produced a valve with optimal leaflet function and good durability in initial accelerated fatigue tests for the size 27 mm valve. Prototype valves were manufactured in all sizes to this final specification and evaluated in the laboratory and in animal trials.

CHAPTER 8

LABORATORY EVALUATION

8.1 Introduction

Prototype valves have been manufactured to the final specification given in Chapter 7 for sizes 25 to 31 mm in the mitral position, and sizes 19 to 27 mm in the aortic position. Photographs of a size 27 mm mitral and 21 mm aortic valve were shown in Figures 7.17 and 7.18. A number of prototype valves have been made in each size. One valve of each size has undergone a full evaluation in the pulsatile flow test rig and ten size 25 mm mitral valves have undergone limited tests to assess the reproducibility of the manufacturing process. Size 27, 29 and 31 mm valves were manufactured for fatigue tests and size 25 and 21 mm valves were manufactured for animal trials.

The sizes of valves are usually taken as a nominal implant diameter (Figure 17.16) but this can vary between different manufacturers. Table 8.1 shows how the key dimensions and implant sizes of the Glasgow Valve compare with other pericardial valves for size 29 mm mitral and size 23 mm aortic valves.

In this chapter the results of the laboratory function and fatigue tests on the prototype valves are described and the results compared with similar studies on commercial pericardial valves described in Chapter 3.

8.2 Hydrodynamic function tests

The function of the prototype valves was assessed under steady and pulsatile flows as described in Chapter 2, and leaflet motion studied by video camera and synchronised still frame photography. The leaflet function of the prototype valves was similar in all sizes with little variation due to the scaling of the leaflet geometries. Figure 8.1 shows sequential photographs at 10 ms intervals of the opening and closing of a size 27 mm valve in the mitral position with the test apparatus under flow conditions B (rate 70 min^{-1} , stroke 70 ml, cardiac output approximately 4 l min^{-1}). The leaflets took approximately 70 ms to move from the open to the closed position and approximately 40 ms to move from the closed to the open position. The time to open was dependent on the shape of the flow waveform whilst the time to close was dependent on the size of the valve and the volume of fluid swept back by the leaflets. The leaflets moved synchronously and uniformly under these flow conditions (the peak flow was 200 ml s^{-1}). The leaflets opened in the base or belly of the leaflets first with the free edges moving outwards after the curvature on the base of the leaflet had been reversed. This was similar to the action described for the MM and HP valves in Chapter 3, and proposed for natural aortic valves (124). During closure the leaflet tended to move inwards at the edge of the frame and the base first with the area of the leaflet at the free edge and in the centre being the last to reverse its curvature.

At much lower flows and pressure differences it was always possible to detect slight differences between the opening

characteristics of the leaflets due to the inherent variation in their mechanical properties. The most sensitive test to detect this was to slowly increase a steady flow through the valve and view the sequential opening of the leaflets as the flow and differential pressure across the valve increased. Figure 8.2 showed two size 25 mm mitral valves at a steady flow of 40 ml s^{-1} (2.4 l min^{-1}). In Figure 8.2a one leaflet had not transposed from the open to the closed position, while in Figure 8.2b the free edge of one leaflet had opened but the belly remained in the closed position producing a shelf. In the first case the leaflet was less extensible so required a larger gradient to transpose it to the open position, while in the second valve the leaflet material was slightly thicker in the base. In both these valves the leaflets opened up fully at steady flows of less than 80 ml s^{-1} (4.8 l min^{-1}) and functioned normally under minimal pulsatile flow conditions specified in the quality control tests for manufacture.

The precise positioning of the leaflets on the radial pins and studs and the precise manufacture of the leaflets allowed the dimensions of the flexing portion of the leaflets to be defined precisely. This gave uniform open and closed positions for the leaflets. Variations in the opening and closing actions described above was attributed to inherent variation in the mechanical properties of the tissue (extensibility and thickness). Figure 8.3 shows a size 25 mm mitral valve in the function tester (flow conditions B) showing the valve unloaded, closed under pressure and fully open. In each case the position and geometry of all three leaflets was uniform. There was deep coaption between the closed

leaflets hc 4 to 5 mm which gives a stable closed position. This is an improvement over some low profile valves described in Chapter 3 which had less coaption between the closed leaflets.

Figure 8.4 shows the mean pressure difference across the valves plotted against RMS forward flow for sizes 25 to 31 mm in the mitral position, and sizes 19 to 27 in the aortic position. The pressure difference was measured 25 mm upstream and 50 mm downstream of the mitral valve and 50 mm upstream and 50 mm downstream of the aortic valve (see Chapter 3). At the upstream pressure measurement point the diameter of the test sections was 57 mm so the fluid had negligible kinetic energy. The downstream measurements were made 50 mm from the valve sewing ring in the area where the jet of fluid passing through the open valve had contracted to a minimum. Consequently the maximum pressure difference across the valve was measured. The pressure recovery in the aortic position was not measured. The mean pressure difference plotted in Figure 8.4 is for the time interval defined by the zero pressure point at the start of forward flow and the zero flow point at the end.

As expected the mean pressure difference increased with reducing valve size. For the mitral position at flow conditions B (RMS flow 150 ml s^{-1}) pressure differences varied from 1.0 to 2.5 mmHg for the size 31 to 25 mm valves, whilst at the highest flows (corresponding to a cardiac output of approximately 8.5 l min^{-1}) the mean pressure difference varied from 3.5 to 8 mmHg. In the aortic positions, the RMS flows were greater than the mitral position due to the shorter systolic time period. However, the graph of mean pressure difference against RMS flow was similar in both positions for the size 25 mm

valve. The size 27 mm valve had a greater pressure difference in the aortic position due to the aortic diameter (28mm) affecting the full opening of the leaflets. At flow conditions B (RMS flow 250 ml s⁻¹) the mean pressure gradient varied from 3 to 14 mmHg for the size 27 to 19 mm valves. At the highest flows (Cardiac output 8.5 l min⁻¹) the mean pressure difference varied from 7 to 22 mmHg for the size 27 to 21 mm valves. The size 19 mm valve was not tested at the highest flow.

In both the mitral and aortic positions the effective orifice area EOA of the valves increased with flow as shown in Table 8.2. At higher flows the larger pressure difference opened the leaflets wider. Table 8.3 compares the calculated EOA for the valve at the highest flows with the actual maximum orifice area defined by the internal diameter of the frame. The EOA is the calculated area of contraction of the jet downstream of the valve (assuming no viscous losses). This is less than the actual area of the orifice by the discharge coefficient ratio. A discharge coefficient of 0.8 is not unreasonable for an orifice which suggests that free edges of the valve leaflets opened up approximately to the full orifice of the valve.

The mean pressure difference measured across ten size 25 mm mitral valves, at flow condition C, to assess the repeatability of the valves manufactured are given in Table 8.4. The variation $\pm 2SD \pm 0.62$ mmHg was greater than the variation found on a single valve, and was attributed to variations in the properties of the leaflets in different valves. This variation would not be detected clinically.

The mean pressure differences of the size 29 mm mitral and size

23 mm aortic valves was compared to the pressure differences found with other pericardial valves in Figure 8.5. The size 29 mm Glasgow Valve (GHV) had the same pressure difference as the MM valve. The other valves had higher gradients which were caused by restriction to the opening of the leaflets at their free edges (Chapter 3). The Glasgow Valve had the smallest frame internal diameter D_i (Table 8.1) so it made the greatest use of the orifice available. In the aortic position the size 23 mm Glasgow Valve had a slightly greater pressure difference than the HP and MM valves and similar pressure difference to the ISU and ISLP valves. The latter two used flared stents which gave a comparatively larger orifice at the top of the stent posts (Table 8.1). The HP valve also increased its overall diameter D_{out} from the nominal 23 mm size, which gave it similar characteristics to the MM valve. The slightly increased gradient in the Glasgow valve compared to the HP and MM valves was basically due to the bulkier frame and smaller internal diameter D_i . In comparison with other bioprosthetic valves, the size 25 mm mitral Glasgow Valve had a lower pressure difference than the 29 mm porcine valves (118) while the size 23 mm aortic valve had a similar pressure difference to the size 25 mm Carpentier-Edwards porcine valve.

The regurgitant volumes passing back through the valves are plotted in Figure 8.6. The regurgitation was measured while the valve was closing and while it was closed, and each volume was averaged over the five waveforms tested. The closing regurgitation was greatest in the size 31 mm valve and lowest in the size 19 mm valve. This was due to the larger volume of fluid swept back by the leaflets and the longer time period to close in the larger valves.

There was also additional displacement of fluid due to the extension of the leaflets under the back pressure as the leaflets moved to the closed position. The closing regurgitation was similar in both the mitral and aortic positions for the size 25 and 27 mm valves. The closed regurgitation was similar in all sizes of mitral valves and all sizes of aortic valve, but was greater in the aortic valves. The closed regurgitation (leakage) mainly occurred through the cloth-covering on the outer frame and the sewing ring. The sewing rings were sealed to the valve mounting ring with silicon rubber, but the sewing ring and cloth-covering were not coated with silicone rubber to simulate tissue ingrowth. The construction of the sewing ring in the aortic position may have allowed a greater leakage through the closed valve. In addition, the longer diastolic time period when the aortic valve was closed also increased the closed volume.

Figure 8.7 shows the regurgitation of the Glasgow Valve with other pericardial valves for the size 29 mm mitral and size 23 mm aortic. The regurgitant volumes were similar for all the size 29 mm mitral valves. In the aortic valves (size 23 mm) the closing volumes were similar but the closed volumes were slightly higher in the ISU and ISLP, due to the slightly different construction of the sewing ring. In clinical use we would expect that the closed leakage would reduce as the host tissue grew into the sewing ring and cloth.

The energy losses across the Glasgow Valve during forward flow, closing, and closed regurgitation are compared to other size 29 mm mitral and size 23 mm aortic valves in Figure 8.8. These results confirmed that the overall hydrodynamic function of the Glasgow Valve was similar to existing commercial pericardial valves. For all the

valves in the mitral position the energy losses during regurgitation were greater than the energy losses during forward flow, even at the highest flow rates (waveform E). The ISU 29 mm valve which was the most obstructive valve (Figure 8.4) also had the greatest total energy loss. In the aortic valves, the forward flow pressure differences and consequently the forward flow energy losses are greater. The MM 23 and HP 23 had slightly lower forward flow energy losses than the Glasgow valves, while the regurgitant energy losses were similar in all valves.

8.3 Fatigue test results

Accelerated fatigue tests have already been described in Chapter 7 in which valves of different specifications were cycled to over 400 million cycles at 12 Hz. This took approximately one year. Before these tests to determine the final specification were completed additional tests were started. The results of all the fatigue tests completed are summarised in Figure 8.9. In total, nine valves manufactured to the final specification have been tested (four size 27 mm and five size 29 mm). In addition, seven valves with the different stitch configuration were also tested (six size 31 mm and one size 29 mm). The results of these extra seven valves were discussed as they gave additional explanations of failure modes. Each valve was tested in the function analyser before and after the fatigue tests.

The four size 27 mm valves completed 440 million cycles (equivalent of 11 years) without failure and have already been

illustrated in Figure 7.13. On some of the leaflets there were markings on the mesothelial surface at the centre of the leaflet close to the free edge. Table 8.5 shows that there was little change in the hydrodynamic function of the valves before and after the test. There was slight reduction in the mean pressure difference across the valves and a slight increase in the closing regurgitant volume. This may have been caused by the leaflets being stretched a little by the repeated cycling in the fatigue tests.

Four of the size 29 mm valves were tested to 400 million cycles without failure while one valve 29.1 failed after 156 million cycles with a hole in the centre of the free edge of the leaflet (Figure 8.10). This failure was probably caused by bending stresses in the closed leaflet at the point where the three leaflets come together in the centre of the valve. The valve had a large regurgitation 23.8 ml per stroke when tested after the fatigue test, due to the leakage through the tear. When valves with large regurgitant volumes were tested the mean aortic pressure was set to 70 mmHg instead of 95 mmHg in an attempt to simulate the loss of pressure that would occur clinically.

In the other four size 29 mm valves, valve 29.2 showed a small tear in the tissue above the stitch above the top of one post after 330 million cycles while valve 29.5 showed a similar tear in one leaflet after 380 million cycles. Valves 29.3 and 29.4 were cycled to 400 million cycles without damage (Figure 8.11). Some leaflets however showed marks in the centre close to the free edge in the same position as the hole in the failed 29.1 valve. Both valves 29.2 and 29.4 were cycled to 400 million cycles without further damage after a

small tear was detected above the stitches. Function tests after completion of the fatigue test showed that these small tears did not affect the hydrodynamic function of the valves which remained unchanged. Similarly, there was little change in the hydrodynamic function of valves 29.3 and 29.5 after the fatigue test (Table 8.5).

In valves 31.1 to 31.6, and valve 29.6, with stitch configuration B, small tears were detected in leaflets of all valves at the stitch between 160 and 400 million cycles. In all cases the stitch hole elongated as described in Section 7.4. The test was continued after the damage was detected and in four valves further damage and ultimate failure was found in the same leaflets. In two of the valves 31.2 and 31.5, elongation of the stitch hole was also associated with lamination of the tissue at the top of the same post. The failure time for these valves is shown in Figure 8.9 and photograph of the damaged leaflet shown in Figure 8.12. In two of the valves, 31.1 and 31.3, the leaflet with the tear dropped lower than the other two leaflets when closed under pressure. In both cases a small hole appeared in the leaflet at the edge of the frame on the shoulder of the scallop. This occurred at 210 and 290 million cycles, 50 and 20 million cycles after the initial tear was detected. At this point the tests were stopped. One possible reason for the holes occurring was that as the leaflet dropped the tissue was deformed over the inside edge of the frame producing excessive bending stresses at this point. Function tests of the two valves after the failure, showed that there was little difference in the regurgitant volumes going back through the closed valves (Table 8.5). However, both failed leaflets had an abnormal opening and closing action on the side where the hole

occurred.

In valves 31.2 lamination of the leaflet, close to the torn stitch hole, increased as the test was continued until eventually at 300 million cycles a small hole appeared in the leaflet 3 mm away from the top of the post. The lamination of the tissue appeared to give permanent extension to the tissue and this caused an abnormal opening action to the leaflet. The leaflet appeared to open and close by bending at the point where the hole occurred. It is likely that bending stresses caused the hole in the tissue. This small hole did give a small increase in the closed regurgitant volume (4.9 ml) in the function test (Table 8.5).

In valves 31.5 and 29.6 the leaflets with the torn stitch hole eventually tore at the top of the posts at the edge of the frame (Figure 8.11). This was most severe in valve 31.5 which failed after 318 million cycles with a large regurgitation while in valve 29.6 the valve was still competent after 400 million cycles. Function tests on these two valves after the fatigue test, showed a large regurgitant volume for valve 31.5 as the tear allowed the leaflet to prolapse below the other two leaflets, but only a small increase in the regurgitation in valve 29.6 (2.6 ml) where the tear did not extend very far down the post. In the other two valves, the leaflets with the tear at the stitch hole were tested to 400 million cycles without further damage.

These valves, although not to the final specification, showed that small holes can occur in the leaflets either at the edge of the frame or in the moving position of the leaflet. These appeared to occur if the leaflet motion was abnormal and may have been caused by

excessive kinking or bending. The tears occurring at the top of the posts in valves 31.5 and 29.6 were probably due to high tensile stresses in an area of the leaflet which was weakened by some wear.

Comparison with the lifetimes for the commercial valves in Figure 3.9 confirm the improved durability of all the Glasgow valves with a significant reduction in wear and abrasion at the edge of the frames.

8.4 Discussion

Extensive function tests carried out on the full range of prototype valves have shown that the hydrodynamic function of the valve developed was very similar to existing commercial pericardial valves. Small variations in pressure differences compared to the commercial valves tested were due to the differing restrictions placed on the opening of the free edges of the leaflets and the overall orifice area of the valve frames. Closing regurgitation was similar in all valves while closed regurgitation was dependent on the construction of the cloth covers and sewing rings. The opening characteristics of the Glasgow Valve were similar to the HP and MM valves, the leaflets of which were also moulded in the closed position.

There was some variation in the mechanical properties of the leaflets which affected both the leaflet dynamics at low flows and to a lesser degree the pressure difference across the valve. It is important to reduce this variation to a minimum during the manufacture of the valve. Although inspection of, and thickness measurements of, the leaflets were made before assembly, testing the leaflets on a jig

under pulsatile and steady flows proved to be the most sensitive test to detect variation in the leaflet properties. The extensibility of the leaflet proved to be the most critical parameter as a stiff leaflet gave a slow or lazy opening action while a very extensible leaflet dropped below the heights of the other two leaflets when closed under pressure. The provision to test the leaflets on a jig prior to final assembly proved an important design feature, and should improve the overall consistency of manufacture and reduce the percentage of valves rejected after final test. The variation found in this type of valve makes it imperative to test every valve manufactured.

Fatigue test results on the Glasgow Valve confirm its superior durability and the elimination of premature failure of other commercial valves due to abrasion of the leaflets on the edge of the cloth-covered frames (Figure 3). Only one major failure (valve 29.1) was found in the fatigue tests on the nine valves manufactured to the final specification which were cycled to over 400 million cycles. Slight damage was seen at the commissure stitch on two valves after 330 and 380 million cycles, but this did not affect the valve function. These tests confirmed the resilient nature of fixed pericardial tissue.

The failure of valve 29.1 and some of the size 31 mm valves occurred where the bending stresses in the leaflets were very high, at the centre of the free edge, when abnormal leaflet action and kinking occurred or where the leaflet stretched and kinked over the inside edge of the support frame (Figure 8.12). In these areas the radii of curvature were typically 1 to 2 mm, which gave much greater bending

strains than the normal curvature found in the leaflet. All the leaflets were cut with the fibrils in the pericardium predominantly running in the radial direction. The effect of rotating the axis by 90°, so that the fibrils ran circumferentially, was not investigated. However, further studies of the durability of pericardial valves will be made to investigate the effect of the orientation of the leaflets in the sac on valve durability. This rotation would have made the leaflets similar to the natural leaflets with the direction of highest ultimate tensile strength in the direction of maximum tensile stress (circumferentially). Bending stresses were also greatest in the circumferential direction and it is not known whether the tissue is more resistant to bending along or across the fibrils.

Some damage was detected at one of the stitches above the posts in two size 29 mm valves. This was seen as a tear in the tissue above the stitch hole, approximately 1 mm long to the free edge, adjacent to the loop of thread which passed over the free edge. This was caused by the bending stresses which occurred at this point when the leaflet was fully open. The stitch was important in sealing the free edges of the leaflets above the post and the stitch configuration used was clearly superior to the configuration used in the size 31 mm valves.

It is difficult to assess the significance of defects found in the valves after long periods in the fatigue tests as, clinically, biological affects such as tissue ingrowth and calcification are likely to have a greater effect on valve function and durability. Indeed, experience of function testing explanted clinical valves after

two to four years implantation time shows that leaflet mechanics are dramatically changed after implantation due to tissue overgrowth, calcification and blood deposits on the leaflets. Although accelerated fatigue tests gave quite accurate prediction of the mechanics of early failure in commercial pericardial valves they will be a less accurate indication of failure modes after eight to ten years when biological effects will be more dominant. Nevertheless, these fatigue tests provided a very harsh test on the mechanical durability of the valves.

CHAPTER 9

ANIMAL TESTS

9.1 Introduction

Although the valve has undergone extensive laboratory tests for both function and durability, these tests did not give information about biological effects such as calcification, thrombogenicity or tissue ingrowth. Our experience with explanted clinical valves described in Chapter 1 showed that these biological effects can cause significant changes in the valve appearance and function. A Hancock pericardial valve (size 23 mm), which was considered to be functioning normally in vivo, was explanted after 20 months. The appearance of the valve tissue was good although there was excessive host tissue ingrowth over the sewing ring and edge of the leaflets. Assessment of the explanted valve function in the pulsatile flow test apparatus gave a mean pressure difference of 6 mmHg (EOA 1.4 cm²) at an RMS forward flow of 185 ml s⁻¹, compared to 3.2 mmHg (EOA 2.0 cm²) at the same flow for an identical valve prior to implant. The restricted opening of the leaflets and pressure drop was caused by adherence of the leaflets to the cloth-covered frames and tissue ingrowth over the edge of the outflow surface of the leaflets. Calcification has also caused dramatic changes to the function of tissue valves. An Ionescu-Shiley size 31 mm pericardial valve explanted after four years with severe calcification had a mean pressure difference of 26 mmHg compared to 2.0 mmHg for an identical valve prior to implant for an RMS flow of 150 ml s⁻¹. The only way

to assess the effect of these biological processes prior to clinical implantation is to carry out implants in animals.

No ideal animal model is available for bioprosthetic valves. Mitral valve replacements have been carried out in dogs (36), but this requires small sizes of valves (21 to 25 mm). Young calves have also been used but they grow very rapidly and are not suitable for longer term studies. Sheep have also been used successfully for mitral valve replacement (203) but they have been reported to cause accelerated calcification (204).

Sheep aged approximately 18 months have been selected for initial animal studies with this valve. They are readily available and are relatively easy to operate on and manage postoperatively. Their size, although smaller than humans, is generally larger than dogs, and a 25 mm mitral valve can easily be implanted in the mitral position. The range of cardiac outputs in sheep is typically 2 to 4 lmin^{-1} . At 18 months they are almost fully developed and they do not outgrow the prosthesis.

9.2 Methods

Valves were implanted in the mitral position of 10 'grey-faced' sheep aged 18 to 21 months. The operative procedure involved left thoracotomy through the fifth intercostal space, and cardiopulmonary bypass by cannulation of the descending aorta and the right ventricle through the pulmonary artery. The heart was maintained in fibrillation throughout the procedure and bypass carried out at normal temperatures. Bypass times were between 40 to 70 minutes and pump

flows between 2 to 3.5 l min⁻¹. The left atrium was opened through a vertical incision in its appendage and the native mitral valve was not removed. Size 25 mm valves were implanted using 12 2/0 Tycron sutures with pledgets. The sheep were given a five day course of Penicillin and Streptomycin as prophylaxis against infection. No anticoagulants were given. Seven sheep survived the planned implant period of three months and valves were explanted at between 13 and 16 weeks. Two other sheep died within 24 hours of the operation with respiratory failure. These deaths were not valve-related. One sheep died after eighteen days with infective endocarditis around the valve annulus and vegetation and thrombus on the inflow aspect of the valve. The animal had been infected since the operation and *Streptococcus faecalis* was isolated in the blood tests.

Cardiac output and pressure difference measurements were attempted in six of the seven survivors prior to sacrifice. After sacrifice, the heart and valves were examined in situ and the lungs examined for macroscopic abnormalities. Other major organs were removed for histological examination. The valve was removed from the heart and a macroscopic examination carried out in the laboratory. The valves were then washed in sterile saline and their function assessed in the pulsatile flow test apparatus. The valve was then fixed in glutaraldehyde and x-ray films taken in an attempt to identify areas of calcification on the leaflets. The valve was then taken apart and an x-ray film taken of the individual leaflets. The leaflets and frame were then sent for histological studies.

Two of the valves implanted (1 and 2) were not manufactured to the final specification and configuration B (Chapter 7) was used for

the suture above the posts. The other five valves (3 to 7) were manufactured to the final specification.

9.3 General description and testing of the explanted valves

The explanted valves are shown in Figures 9.1 to 9.7 and the x-ray films are shown in Figures 9.8 and 9.9. All the explanted valves showed good tissue ingrowth over the sewing rings and outer cloth-covered frames, and this extended about 1 mm over the edge of the outflow surface of the leaflets. Tissue ingrowth stopped at the edge of the pericardial covering on the inflow aspect of the valve. All the valves were free from thrombus and the pericardial tissue was in good condition. There were small deposits of calcium visible on some leaflets in some of the valves and these were also detected on x-ray films.

Valve 1 shown in Figure 9.1 had a surgical suture looped over the post between leaflets 3 and 1 which caused some distortion to the leaflets and prevented them from closing together when unloaded. There was also some calcification and stiffening of the leaflets at this commissure (Figures 9.8 and 9.9). The gap between the unloaded leaflets sealed under back pressure in the function test to give a competent valve with normal regurgitation as shown in Table 9.1. The forward flow pressure differences listed in Table 9.1 was increased by approximately 30 percent in the explanted valve due to the restricted leaflet opening caused by the calcification. The minimal opening flow for leaflet 3 was increased from less than 80 ml s^{-1} before implant to 110 ml s^{-1} after explant due to the stiffening caused by

the calcification at the left hand commissure. This valve had suture configuration B at the commissure.

Valve 2 shown in Figure 9.2 also had a small gap between leaflets 3 and 1 in the unloaded valve. As with valve 1 these leaflets had suture configuration B at the top of the posts. Leaflet 1 was stiffened with calcification on the right hand commissure (Figures 9.8 and 9.9). A pledget and surgical suture was looped over the post between leaflets 2 and 3 but this did not affect the leaflet function. The function tests showed that the gap between leaflets 3 and 1 closed under pressure to give a competent valve with little difference in the regurgitation before implant and after explant. The mean pressure difference across the explanted valves was increased by approximately 30% (Table 9.1) and the in vivo peak pressure gradient was 4 mmHg for a cardiac output of 2.4 l min just prior to sacrifice.

Valve 3 shown in Figure 9.3 was manufactured to the final specification (as were valves 4 to 7) and had a better unloaded position for the leaflets. A surgical suture was looped over one post but this did not appear to affect the leaflets. Small calcium deposits were detected on the inflow aspect in the base of leaflet 1, which distorted the unloaded leaflets, and also at the right hand commissure of leaflet 1, and both commissures of leaflet 2 (Figures 9.8 and 9.9). There was extensive tissue ingrowth over the base of leaflet 3. The calcification greatly increased the pressure difference across the explanted valve (Table 9.1). Leaflet 1 opened at a minimal flow of 120 ml s^{-1} , while the calcification at the commissure of leaflet 2 restricted its opening at the free edge. In

vivo measurements prior to explant showed a peak pressure drop of 4 mmHg.

Valve 4 shown in Figure 9.4 also had some visible calcium deposits on the outflow surface at the edge of leaflets 2 and 3 about one third of the way up the right hand posts. This was confirmed on the x-ray films. The calcium deposits stiffened the leaflets and the mean pressure difference across the explanted valve was doubled due to the restricted opening of the leaflets. However, all leaflets opened at a minimal flow of 80 ml s^{-1} . Peak pressure gradient in vivo was 3 mmHg at 2.2 l min^{-1} cardiac output.

Valve 5 in Figure 9.5 appeared good with no visible calcification or wrinkling of the leaflets. The inflow view showed a small dimple in the base of leaflet 3 which was also slightly higher than the other two leaflets at the free edge. Tissue ingrowth was also quite extensive on the outflow aspect in the base of leaflet 2. The function test results (Table 9.1) showed that the mean pressure difference was increased by 20% in the explanted valve due to tissue ingrowth and the regurgitation was unchanged. In vivo pressure measurements showed a peak pressure difference of 3 mmHg.

The leaflet of valve 6 shown in Figure 9.6 also appeared good with no visible calcification or distortion in the unloaded leaflets. The x-ray films confirmed that the valve was free from calcification. Tissue ingrowth was quite extensive in the base of leaflet 1. The function tests showed that the pressure difference across the explanted valve increased by between 25 to 30%. This was probably due to the tissue ingrowth restricting the opening of the leaflets. In vivo pressure measurements were not completed in this animal.

Valve 7 also appeared free from calcification and distortion of the leaflets (Figure 9.7). X-ray films detected a small deposit of calcium on the right hand commissure of leaflet 2 (Figures 9.8 and 9.9). In the function test, leaflet 3 did not open fully in the base even at the highest flows tested, and the leaflet appeared to be stiffened in this area. This may have been associated with tissue ingrowth. As a consequence the mean pressure difference of the explanted valve was increased by over 50%.

9.4 Pathology of explanted valves

The explanted sheep valves are currently being studied in the Pathology Department at Glasgow Royal Infirmary, using optical microscopy, scanning and transmission electron microscopy, and x-ray element analysis. Initial results show little change in the structure of the tissue before implant and after explant shown in sections of the leaflets in Figure 9.10. The areas of calcification seen visually and on x-ray film were confirmed with electron microscopy element analysis. Extensive studies are planned for the leaflets and the results will be compared with specimens of other explanted clinical pericardial valves such as ISLP.

Initial results have confirmed the macroscopic findings that the valves have performed satisfactorily in vivo.

9.5 Discussion

The function of the valves implanted for three months in the

mitral position in sheep, without anticoagulation therapy, has been satisfactory. Explanted valves were free from thrombus and showed good tissue ingrowth over the sewing ring and outer frame-covering with the valve being well-incorporated into the native orifice. Although some valves showed some calcification which stiffened the leaflets and affected valve function, it has been recognised that sheep do provide an accelerated model for calcification of bioprosthetic valves (204). The calcification appeared at varying places on the leaflets although it always tended to be towards the edge of the support frame where bending stresses were greatest. This is consistent with findings from other workers (205). In our case the calcification appeared on both the inflow and outflow surfaces of the leaflets. There is no clear explanation for the varying amounts of calcification between valves or between leaflets on the same valves. The looped surgical suture on valve 1 which distorted the leaflet probably also caused the calcification at the top of the post in this valve. It is likely that calcification will be dependent on the variable structural and mechanical properties inherent in the leaflets and this should be investigated further.

The pulsatile flow tests showed that there were changes in the valve function caused by tissue ingrowth over the edge of the leaflets as well as calcification. The tissue ingrowth restricted the portion of the leaflet that could flex to the open position which caused a significant increase in the pressure difference measured in the in vitro tests. This was consistent with our limited experience of function testing explanted clinical pericardial valves. It is clear that biological processes in vivo do affect leaflet dynamics and the

pressure differences, and it is important to be able to study the function of explanted valves in the laboratory and compare valve function at explant to the function prior to implant. At present, valve designs and improvements are based primarily on valve function prior to implant. In vivo pressure measurements confirmed the satisfactory function of the valves, but the accuracy of these measurements was limited and it is inappropriate to base a detailed analysis of valve function on these measurements.

The sheep implants have shown satisfactory function over a period of three months and, currently, further tests are being carried out with five size 21 mm mitral valves implanted in dogs without anticoagulation therapy. A randomised clinical trial is planned comparing a standard porcine valve with the Glasgow pericardial valve.

CHAPTER 10

DISCUSSION AND FURTHER WORK

The overall long-term clinical performance of the Ionescu-Shiley Standard pericardial valve has been good. However, a significant number of valves have been explanted due to leaflet prolapse and regurgitation caused by leaflet tears (up to 4% per patient year). Limited clinical experience in Glasgow with the more recently developed low profile pericardial valves has shown similar tissue failure in some of these valves. In some follow-up studies, rates of primary tissue failure are higher than valve failures due to calcification or thromboembolic events. A characteristic failure mode has been described in most of the explanted pericardial valves with tears in the leaflets occurring close to the edge of the cloth-covered frames. A number of different causes have been suggested for these failures but it is not clear from the clinical studies which is the major factor contributing to these tissue failures. Although there have been large numbers of follow-up studies of valve implants, including multi-centre trials, the number of detailed studies of explanted valves is few (206).

My experience of explanted porcine and pericardial valves in Glasgow has shown significant changes in valve function and leaflet dynamics after explant compared to valve function for comparable valves prior to implant. As well as tears in the leaflets and calcification which have been widely reported, tissue ingrowth also affected leaflet function and caused an increase in the pressure difference across some valves of between 25 to 50%. In the

pericardial valves tissue ingrowth was found up to 2 mm over the edge of the leaflet which changed the geometry of the open leaflet and in some cases caused leaflet flutter. In one porcine valve the tissue ingrowth restricted the valve orifice but did not grow over the flexing portion of the leaflets. The advantage of lower pressure differences across pericardial valves compared to porcine valves, found in hydrodynamic tests, may not be fully realised clinically due to tissue ingrowth affecting valve function in vivo. This could explain the similar pressure difference measurements found for porcine and pericardial valves using Doppler ultrasound measurements in vivo (118). More detailed analysis of both the function and pathology of explanted prosthetic valves is required to assess how biological processes affect long-term valve function.

Hydrodynamic studies on four pericardial valves showed that different leaflet designs and construction methods affected valve and leaflet function. In particular, leaflet geometry, method of fixation, and position of coaption stitches, affected leaflet dynamics and transvalvular pressure differences. Our studies of bovine pericardium have confirmed that it is a complex material with variation in the mechanical properties between sacs, between different sites on the same sac and before and after fixation. They have also shown anisotropic properties at one site. Both differing material properties and valve designs can have an effect on long-term valve durability. However, accelerated fatigue tests completed on four different types of valves have shown that in all valves, abrasion of the leaflets against the edge of the cloth-covered frames caused leaflet tears and premature valve failure. These accelerated fatigue

tests are artificially harsh for pericardial valves as biological effects, such as blood deposits on the cloth and tissue ingrowth which can reduce abrasion and reinforce the leaflets at the edge of the frame, are not simulated. Care must be taken when extrapolating failure rates from fatigue tests to the clinical situation. Nevertheless, the fatigue tests did predict the mechanism of failure which caused the tissue tears in the explanted valves I have studied. In both the laboratory tests and with explanted valves, abrasion of the leaflets on the cloth-covered frame was the major cause of leaflet tears. In the fatigue tests the tears started lower down the posts at the shoulder of the scallop as opposed to the top of the post in the clinical valves. This may be due to an abnormal closing action of the leaflets seen in the fatigue tester or due to greater tissue ingrowth lower down the posts in the clinical valves. In the ISU valve the coaption stitches pulled through the tissue producing small tears in both the fatigue tests and in explanted valves, but they did not appear to cause the major tears. If the abrasion to the leaflets is eliminated, greatly improved durability is expected, and the influence of other factors such as leaflet geometry and material properties can be determined.

In this improved valve design which utilises twin frames, the pericardial covering on the inner frame greatly reduced wear and abrasion of the leaflet in accelerated fatigue tests when compared to other valves made with cloth-covered frames. Valves were cycled to over 400 million cycles without failure, the equivalent of ten years. One valve failed with a hole in the centre of the leaflet at the free edge which was probably caused by bending stresses. All the leaflets

were cut so that the fibrils in the tissue were predominantly orientated radially, so at the point of failure the bending strains were across the fibrils. It is not known if the tissue has better flexural durability across or along the fibrils. This will be assessed in the future by manufacturing leaflets with alternative orientations but this can only be carried out once the mechanical properties of the tissue at other areas of the sac have been determined, and the anisotropic nature of the tissue is more fully understood. Although the leaflets were orientated with the direction of lowest ultimate tensile strength (determined in the uniaxial tests) in the circumferential direction, none of the leaflets showed excessive extension or failure in tension circumferentially. These tests showed that fixed pericardium is a highly durable material and can support repeated flexion and high tensile stresses. Lower values of ultimate tensile strength found in one direction in uniaxial tests may be a consequence of cutting the tissue in thin 3 mm strips across the direction of the fibrils.

Coaption stitches caused a small tear in a leaflet in two valves in the fatigue testers after 320 million cycles, and these were probably caused by the restriction and bending strain placed on the leaflets in the fully open position. Closure of the leaflets at the posts is essential to prevent leakage and also to prevent the separation of the leaflets at the free edge as seen in animal valves 1 and 2 which had stitch configuration B. The stitch configuration used brings the two leaflets together, without constraining the leaflets in the closed position and having a minimum of restraint in the fully open position.

The fatigue tests and animal tests have confirmed the stability of the closed leaflet geometry. This is achieved with fixation of the leaflet on a mould in the closed position with a geometry which gives deep coaption between the leaflets. Although in other low profile pericardial valves the coaption between the leaflets has been reduced, experience with explanted valves of this type shows mismatch in the heights between the closed leaflets under pressure, which can easily lead to prolapsed leaflets, and central regurgitation. Fixation of the leaflets in the closed position can cause problems with synchronous leaflet opening. The geometry of the leaflets that I have described, the ability to mould the shape in the leaflet without introducing large changes in its mechanical properties, and being able to match, test and replace leaflets on a jig prior to final assembly, allow the valve to be manufactured with synchronous leaflet action. The precise location of the leaflets on the pins and studs also helps to achieve synchronous leaflet action. The inherent variations in the properties of biological materials make it essential to test the function of every valve manufactured.

The valves explanted from sheep showed some small calcium deposits which were expected as it had been reported by other workers. More significant was the variation in leaflet function caused by tissue ingrowth over the edge of the leaflets. Tissue ingrowth over the sewing ring and cloth covering of the outer frame is desirable but ideally this should stop at the edge of the flexing portion of the leaflets. Tissue ingrowth over the leaflet at the edge of the frame, typically between one and two millimetres, restricted the portion of the leaflet that could flex to the open

position and influenced the synchronous opening, uniformity of the open position of the leaflets, and the transvalvular pressure difference. This was seen in other explanted clinical valves where tissue ingrowth over the outflow surface of the leaflet and adherence of the inflow surface of the leaflet to the cloth-covered frames, restricted the opening portion of the leaflet, increased the pressure difference, and produced abnormal leaflet dynamics and flutter. These changes in leaflet function are clearly undesirable and should be studied further and related to the detailed design of each valve. It is essential to test the hydrodynamic function of explanted valves to compare this to the function prior to implant and relate the changes to valve histology and pathology.

This improved design of the Glasgow valve has shown good function and durability in the laboratory tests and satisfactory results in initial animal trials. Material properties of pericardium and valve durability will be studied further, and further implant studies in animals are planned. A randomised clinical trial is planned to compare a porcine valve to the Glasgow pericardial valve.

APPENDIX I

STANDARD CONDITIONS FOR VALVE FUNCTION TESTS

The following tests have been carried out to assess the effect of a number of conditions and parameters on the results of the function test.

i Forward flow time intervals

Four reference points were defined during the forward flow time interval (Figure A1.1). Point 1: start of forward flow, Point 2: the start of positive differential pressure; Point 3: end of positive differential pressure; and Point 4: end of forward flow. For mechanical valves, Points 1 and 2 coincide, whereas for tissue valves a small forward flow was detected before a positive differential pressure. This was due to relaxation of the valve and leaflets as the negative back pressure reduced. The differential pressure was always negative (Point 3) before the end of forward flow due to deceleration of the fluid. Four time intervals were used to average the differential pressure and flow signals. These were: Points 1 to 4: flow to flow, FF; Points 1 to 3: flow to pressure FP; Points 2 to 4: pressure to flow PF; and Points 2 to 3: pressure to pressure PP. The effect of the different time intervals on the mean differential pressure, RMS flow graphs is shown in Figure A1.2 for the Bjork-Shiley spherical disc valve BSS and the Ionescu-Shiley Low Profile (ISLP) valve. For the BSS valve, Points 1 and 2 coincide so the intervals shown, PF and PP, were equivalent to

intervals FF and FP. In both valves the PP interval gave slightly higher pressure readings than the PF interval. In the tissue valves the FF and FP intervals were much lower. The start of the interval includes a short period of time when the differential pressure has a high negative value which produces an artificially low result. The signals should be averaged between the zero flow points FF to eliminate the inertia term from equation 4. In practice the start of forward flow was difficult to define due to relaxation of the valve so the pressure flow PF interval was used as the standard measurement. The results of the pressure interval were also recorded as it has been used by other centres and is used clinically.

ii Position of pressure measurements

The upstream measurement was made 25 mm from the mitral valve and 50 mm from the aortic valve where the test sections had maximal cross-sectional area. The downstream measurements were taken 25, 50 and 75 mm from the mitral valve and 25, 50, 100 and 150 mm from the aortic valve. The variation in the mean pressure difference graphs with the position of the pressure measurements is shown in Figure A1.3 for the BSS 23 mm aortic valve and BSS 29 mm mitral valve. The mitral position showed a slight reduction in the pressure difference 75 mm downstream of the valve whilst in the aortic position there was between 20 and 25% pressure recovery 150 mm downstream of the valve. Close to the valve the differential pressure signal was quite noisy due to turbulence and recirculation, so Point B, 50 mm downstream of either valve,

was selected as the standard measurement point. Further away from the valve it is not known how a physiological geometry, i.e., ventricular cavity or curved aorta would affect the pressure recovery.

iii Valve position

Valves were tested in different positions in both the mitral and aortic positions. The mean pressure difference was reduced by about ten percent when the pressure was measured in the major orifice of the BSS 29 mm mitral valve. This was due to the downstream jet impinging on the pressure tapping. The minor orifice was taken as the standard position for the pressure measurement. In all other valves no significant variation was found in pressure measurement with valve position.

iv Reverse flow time interval

The reverse flow period was defined by Points 4 and 1 (Figure A1.4). Point 5 determined the end of dynamic or closing regurgitation and the beginning of static or closed regurgitation. It was defined as the lowest negative value for reverse flow prior to the constant leakage. Position of this point affects the ratio of the two regurgitant volumes but not the total regurgitation. The energy loss calculations were more sensitive to the position of this point as the pressure difference is changing very rapidly at this point in the cycle.

Valve orientation

The dynamic (closing) regurgitation was dependent on the orientation of tilting disc valves. When valves opened in the vertical plane with gravity assisting closure, regurgitation was lower than when the valve opened on the horizontal plane. This is shown in Figure A1.5 for the BSS 29 mm mitral valve. All mechanical valves were positioned so the leaflets or discs opened in the horizontal plane.

vi Shape of the ventricular pressure waveform

The dynamic (closing) regurgitation of the mitral valve was dependent on the shape of the ventricular pressure waveform. In the rigid test section the rate of rise of ventricular pressure was high (dp/dt). This was reduced by introducing a compliance into the pump chamber. This in turn reduced the dynamic regurgitation by 0.5 ml (Figure A1.6). It also produced variable lower frequency oscillation in the pressure waveform which were difficult to control. For this reason rigid chambers without compliance were used as standard conditions.

APPENDIX II

LIST OF PUBLISHED WORK

1. Fisher J, Jack GR, Wheatley DJ. Design of a function test apparatus for prosthetic heart valves. Initial results in the mitral position. Clinical Physics and Physiological Measurement 1986; 7: 63-73.
2. Fisher J, Reece IJ, Wheatley DJ. The in vitro evaluation of six mechanical and six bioprosthetic heart valves. Thoracic Cardiovasc Surgeon 1986; 34: 157-162.
3. Simpson IA, Fisher J, Reece IJ, Houston AB, Wheatley DJ. In vitro comparison of bioprosthetic valve function using Doppler ultrasound. Cardiovascular Research, 1986; 29: 317-321.
4. Reece IJ, Fisher J, Sethia B, MacArthur KJD, Wheatley DJ. A comparison of experience with the Hancock and Ionescu-Shiley Low Profile pericardial bioprostheses. Z Kardiol 1986; 75: 232-236.
5. Fisher J, Wheatley DJ. A heart valve prosthesis. European Patent Application EP853065549, 1986 (In Press).
6. Fisher J, Wheatley DJ, Jack GR, Cathcart L, Spyt T. Design and development of an improved pericardial heart valve. Proc ESAO, Life Support Systems 1986 (In Press).
7. Wheatley DJ, Fisher J, Reece IJ, Spyt TJ, Breeze P. Primary tissue failure in pericardial heart valves. J Thorac Cardiovasc Surg (In Press).

8. Fisher J, Reece IJ, Wheatley DJ. Laboratory evaluation of the design, function and durability of four pericardial heart valves. Proc I MechE Seminar in Heart Valve Engineering, 1986 (In Press).
9. Barbenel JC, Zioupos P, Fisher J. The mechanical properties of bovine pericardium. Proc I MechE Seminar in Heart Valve Engineering, 1986 (In Press).
10. Macdonald I, Fisher J, Evans AL, Wheatley DJ. A microcomputer-based data acquisition system for a prosthetic heart valve test apparatus. J Med Eng Technol (In Press)

(Papers 1 - 4 enclosed)

ABSTRACTS PRESENTED OR TO BE PRESENTED AT SCIENTIFIC MEETINGS

1. Fisher J, Wheatley DJ. In vitro evaluation of seven prosthetic heart valves in the aortic position.
IPSM Meeting, Measurement of Cardiac Function, Hull, 1986.
2. Wheatley DJ, Fisher J. An improved pericardial bioprosthetic valve.
European Society for Cardiovascular Surgery, Brighton, 1986.
3. Fisher J, Reece IJ, Wheatley DJ. In vitro study of the function of four size 19 mm prosthetic heart valves in the aortic position.
BES Meeting, Blood Flow, Glasgow, 1986.
4. Fisher J, Wheatley DJ, Jack GR, Cathcart L. Leaflet design and manufacture in pericardial heart valves.
BES Meeting, Blood Flow, Glasgow, 1986.

5. Barbenel JC, Zioupos P, Fisher J. Mechanical and structural properties of bovine pericardium.
BES Meeting, Blood Flow, Glasgow, 1986.
6. Simpson IA, Fisher J, Reece IJ, Houston AB, Wheatley DJ. In vitro assessment of bioprosthetic valve function using Doppler ultrasound.
BES Meeting, Blood Flow, Glasgow, 1986.
7. Barbenel JC, Fisher J, Zioupos P. Mechanical properties of bovine pericardium.
Society of Biomaterials, Bologna, 1986.
8. Wheatley DJ, Fisher J. Design and development of an improved pericardial heart valve.
Society of Thoracic and Cardiovascular Surgeons, Edinburgh, 1986.

Design of a function test apparatus for prosthetic heart valves. Initial results in the mitral position

J Fisher^{†‡}, G R Jack[†] and D J Wheatley[†]

[†] Department of Cardiac Surgery, Royal Infirmary, Glasgow G31 2ER, Scotland

[‡] Department of Clinical Physics and Bioengineering, West of Scotland Health Board, Glasgow, Scotland

Received 27 June 1985, in final form 2 September 1985

Abstract. A test rig has been developed to investigate the function of prosthetic heart valves under pulsatile flow conditions. The rig uses a servo-controlled pump to produce a physiological flow waveform through the valve. The pressure difference across the valve and flow through the valves are measured to assess the valve function. The mean pressure difference, root mean square (RMS) forward flow and regurgitant volumes are calculated on a computer. In the initial study, seven popular mechanical prostheses (sizes 29 and 27 mm) were evaluated in the mitral position under five different flow conditions. The mean pressure difference was dependent on the position of the downstream pressure tapping, the orientation of the valve and the time interval used to average the signals. The orientation of some valves also affected the regurgitant volumes. These variations (10-25%) were similar in size to the differences measured between individual valves. Test conditions have to be specified very carefully for accurate comparison of valve function to be made.

1. Introduction

The methods used to test the function of prosthetic heart valves under pulsatile flow conditions have become increasingly sophisticated since the work described by Weiting (1969) and Wright and Temple (1971). The complex function of the left heart and arterial system have been simulated in several ways, producing varying test conditions for the valves. Most test rigs that have been developed can be divided into four discrete sections:

- (i) the pump used to generate pulsatile flows;
- (ii) the chambers for testing the valves;
- (iii) the afterload and peripheral circulation; and
- (iv) the measuring instruments and data analysis.

Two types of pumps have been used. A pneumatic actuator controls the ventricular pressure precisely but the flows produced vary with load (Yoganathan *et al* 1979). A servo-controlled positive displacement pump can reproduce the complex physiological flow waveforms precisely (Martin *et al* 1981), but may also produce abrupt changes in the ventricular pressure waveform at the beginning and end of systole when the valves are opening and closing (Scotten *et al* 1983).

Two different configurations have been used for the valve test chambers. Straight test sections have been used to produce uniform flow patterns upstream of the valve (Martin *et al* 1981). Alternatively, the complex geometry of the left ventricle has been simulated (Kohler *et al* 1981, Scotten *et al* 1983, Reul 1984) in an attempt to produce

more realistic flow patterns. A standard afterload has been used in most rigs (Westerhoff *et al* 1971).

The measuring techniques and data analysis have improved with the introduction of mini- and microcomputers (Walker *et al* 1984). The measurements most commonly used to assess valve function are the mean pressure difference across the valve as a function of root mean square (RMS) forward flow and the reverse flow through the valve. The flow has been measured directly with an electromagnetic flowmeter (Yoganathan *et al* 1979) or can be derived from the velocity signal of the pump (Tindale and Trowbridge 1983). It has already been shown that the pressure difference is dependent on the position of the downstream pressure tapping in the aortic position (Tindale *et al* 1982) but it may also be dependent on the orientation of the valve and the time interval used to average the signal. In some studies an orifice area equation has been used to express the ratio of the RMS flow to the square root of the pressure difference. This can be misleading if the ratio is dependent on the flow (Tindale *et al* 1982) or if different empirical constants are used (Gabbay *et al* 1978). The reverse flow through the valve is usually expressed as two regurgitant volumes per cycle, during the period that the valve is closing and during the period that it is closed.

The difficulties involved in modelling the left ventricle and arterial system are reflected in the variety of systems which have been used to test valves. Particular problems occur when trying to match the inertia, compliance and geometry of the system whilst trying to measure accurately the instantaneous flow through the valve under test. An electromagnetic flow meter has to be used in a cylindrical tube several diameters long to ensure uniform flow patterns through the transducer and should be connected by rigid chambers to the valve under test (Gabbay *et al* 1978, Yoganathan *et al* 1979). This column of fluid introduces significant inertia into the system which can cause distortion of the flow and/or pressure waveforms. When the flow meter is used in a much shorter tube (Scotten *et al* 1983) with a non-compliant ventricle, the pressure in the ventricle is still distorted during the closure of the mitral valve. Systems have been described with a flexible ventricle, with variable source impedance (Reul 1983) and with a rigid ventricular chamber and flexible aorta (Tindale and Trowbridge 1983) but in neither case was the flow through the valve measured. A modular test system has been developed using rigid chambers which allow the flow through, and pressure across, the valves under test to be measured directly in both positions. The modular construction will allow the addition of different test sections at a later stage. Seven popular mechanical prostheses have been tested under varying flow conditions in the mitral position. The effects of varying the position of the pressure tapplings, the orientation of the valve, and the time interval for averaging the signal have been investigated and the results compared with data from other centres.

2. Description of the test apparatus

A positive displacement pump (Super Pump model SP3891, Cardiac Development Laboratories) is used to produce the pulsatile flow. The lead screw of this piston pump is driven by a velocity servo system which is controlled by a specially adapted programmable waveform generator. The shapes of the pump velocity waveforms, derived from data described by Walker *et al* (1984), are shown in figure 1 for the five different flow conditions used.

The waveforms reproduce the main characteristics of the cardiac cycle, such as a systolic period of approximately 300 ms, a reducing diastolic period with increasing

Function test apparatus for prosthetic heart valves

65

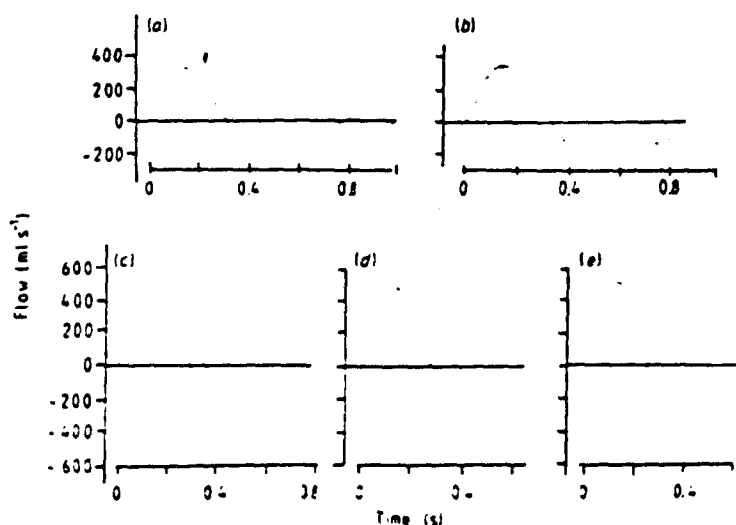


Figure 1. The pump velocity waveforms shown as flow in ml s^{-1} (positive flow is systole) for the five test conditions. Waveforms: (a) rate 60 min^{-1} , stroke volume (SV) 60 ml, (b) rate 70 min^{-1} , SV 70 ml, (c) rate 80 min^{-1} , SV 80 ml, (d) rate 100 min^{-1} , SV 80 ml, (e) rate 120 min^{-1} , SV 80 ml

heart rate, an asymmetric systolic flow wave, and an end-diastolic flow peak at low heart rates due to atrial contraction.

The layout of the test rig is shown in figure 2 for testing valves in either the mitral or aortic position. The shape of the mitral test sections conforms to the specification given by Weiting (1969) (figure 3). The downstream pressure tapings A, B and C are 25, 50 and 75 mm respectively from the valve.

The ventricular chamber used is a straight cylindrical pipe (Weiting 1969, Yoganathan *et al* 1979) and does not simulate the boundary conditions for flow produced in the ventricular cavity (Köhler 1975, 1978).

All the test sections were machined from acrylic blocks and the internal surfaces polished to give maximum visibility of the valve under test. Flow straighteners (a lattice of 2 mm diameter polypropylene drinking straws) are used 150 mm upstream of each valve to produce a uniform flow pattern. The valves are mounted in acetel flanges which are clamped between O-ring seals in the ends of the test sections. A standard

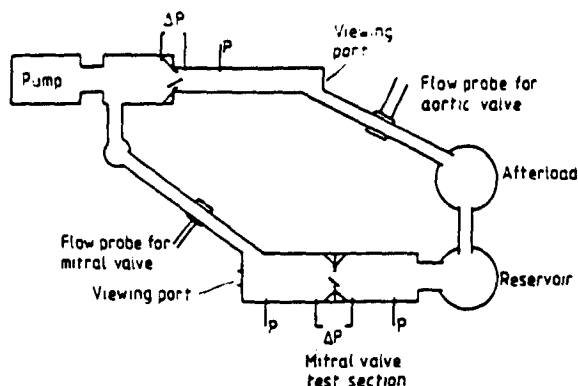


Figure 2. Layout of the test rig (ΔP shows the differential pressure taps and P the direct pressure taps).

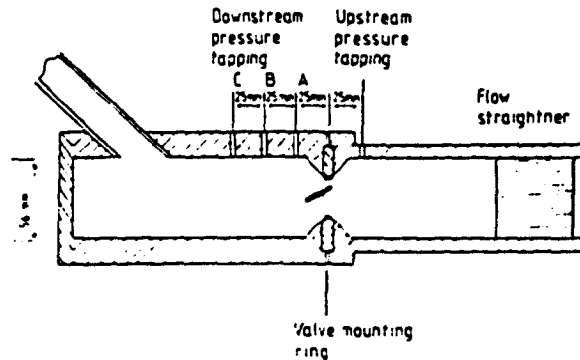


Figure 3. Mitral valve test section showing the position of the down-stream pressure tappings.

peripheral circulation and afterload is used. Normal saline (0.9% sodium chloride solution) is used for testing mechanical valves in order that the results can be compared with similar tests on tissue valves.

An electromagnetic flow meter (Gould Statham SP 2201) with a 26 mm diameter probe is used to measure the flow through the valve under test. It is positioned in a straight tube a distance of eight diameters downstream of the valve. Its accuracy is given as $\pm 6 \text{ ml s}^{-1}$ for uniform flow patterns and has a frequency response of -6 db at 50 Hz. The pressure in three sections of the test rig, the atrium, the ventricle and the aorta, are measured using Elcomatic (EM 721) transducers. A differential transducer (Gaeltec 3CT special) is used to measure the small forward flow pressure difference across the valve. The transducer is used in the -5 to $+20 \text{ mm Hg}$ range to give maximum sensitivity. It has a specified accuracy of $\pm 0.3 \text{ mm Hg}$. The transducer is connected to the test rig with 2 mm diameter rigid tubing. Under these conditions the transducer has a measured resonant frequency of 110 Hz which agrees closely with the theoretical value derived from the volume displacement. The four transducers are driven by Elcomatic (EM 722) amplifiers. The four pressure signals, the flow signal and the position and velocity signals from the piston pump, are fed into an Apple II microcomputer through an analogue to digital (A-D) converter (Interactive Structures Inc, AI 02). The A-D converter reads each signal every 5 ms and has a resolution of 256 increments for the signal amplitude. This resolves the differential pressure signal into 0.1 mm Hg increments and the flow signal into 2 ml s^{-1} increments. A software package has been developed for the data acquisition and processing which will be described in detail elsewhere. Basically, the package consists of four programs, a calibration mode, a real-time display mode for setting up the conditions in the rig, a data acquisition and processing mode, and a calculations and analysis mode.

3. Test procedures

The pressure transducers are calibrated statically and calibration factors stored in the computer. The displacement and velocity of the pump are calibrated by oscillating a column of fluid in a calibrated cylinder. The pump is then used to calibrate the electromagnetic flowmeter for each of the flow waveforms used. The zero position of the flow and pressure signals are set immediately prior to the measurements being taken to minimise drifts.

The computer is used in the real-time mode to set the conditions in the rig. Three signals, the pump rate, stroke volume and mean aortic pressure, are displayed on a colour monitor. The pump velocity waveform, stroke volume and rate are set by adjusting the programmable waveform generator and the mean aortic pressure set to 95 mm Hg by adjusting the afterload. Each mitral valve is tested under the flow conditions shown in figure 1. When the rig conditions are stable, the acquisition programme is run and the six signals are stored over a period of 20 s. The average waveform is then calculated for each signal, stored on floppy discs and plotted on an Annadex printer. The flow and differential pressure signals are analysed by defining five reference points on the cycle: point 1, the start of forward flow; point 2, the start of positive pressure difference; point 3, the end of positive pressure difference; point 4, the end of forward flow, and point 5, the end of the large reverse flow due to the valve closing (figure 4). For a mechanical valve, points 1 and 2 coincide and the mean pressure and RMS forward flow are calculated between points 1 to 3 and 1 to 4. The regurgitant volumes are measured between points 4 to 5 whilst the valve is closing and points 5 to 1 whilst it is closed.

In this initial study, the function of seven popular mechanical valves (table 1) has been investigated in the mitral position. The mean pressure difference during forward

Table 1. Function of seven popular mechanical valves.

Valve manufacturer	Type	Size	Abbreviation
Bjork-Shiley	Spherical disc	27	BSS 27
Bjork-Shiley	Convexo-Concavo Disc 60°	27	BSC 27
Bjork-Shiley	Spherical disc	29	BSS 29
Bjork-Shiley	Convexo-Concavo Disc 60°	29	BSC 29
Omniscience	Tilting disc	29	Ox 29
Duromedics	Bileaflet	29	DM 29
St Jude	Bileaflet	29	SJ 29

flow was measured at pressure tapings A, B and C for the BSS 29 and DM 29 valves. All the valves were tested in different orientations. The disc valves were tested with the disc opening in the horizontal plane and the pressure tapping in the major and minor orifice and also with the disc opening in the vertical plane with the major orifice lowest. The bileaflet valves were tested in the horizontal and vertical planes.

4. Results

The pressure and flow signals for the BSS 29 valve are shown in figure 4 for test conditions C. Pressure oscillations occur when the valves are opening and closing due to them being tested in rigid chambers. The ventricular pressure increases rapidly at the start of systole as there is no compliance in the ventricular or pump chambers. The pressure oscillation (frequency about 20 Hz) decays over two cycles. It is primarily caused by the inertia of the column of fluid in the flow meter; the fluid decelerates rapidly when the mitral valve closes. The inertia of the fluid in the rigid aorta also contributes to the aortic pressure oscillation which has a smaller amplitude. A small oscillation is also shown in the aortic pressure at the end of systole as the aortic valve closes. Figure 5 shows the mean pressure difference for the three different pressure tapings measured in the minor orifice of the BSS 29 valve. The pressure at tapping

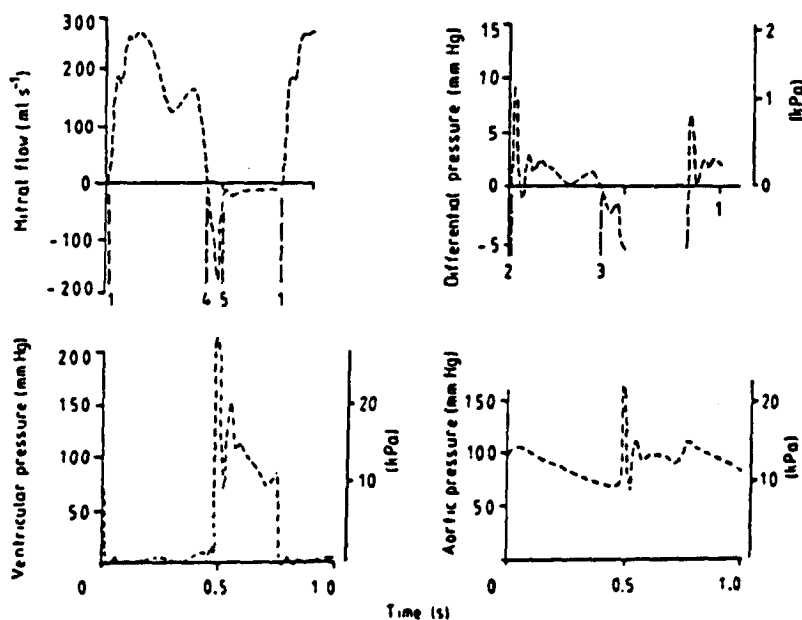


Figure 4. The flow and pressure signals for the BSS size 29 valve under test conditions C. Points 1 to 5 on the differential pressure and flow signals define the time intervals used for analysing the data.

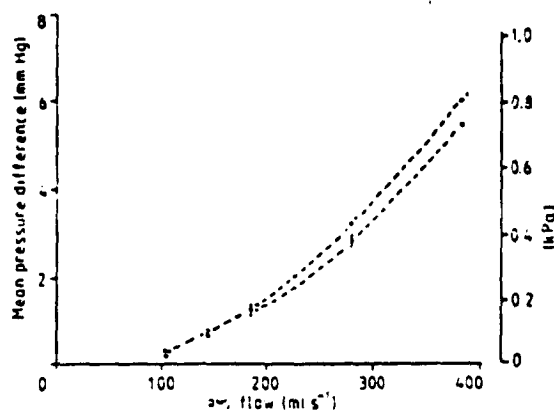


Figure 5. The mean pressure difference plotted against RMS forward flow for the BSS 29 valve. ●, Pressure tapping C; ■, tapping B; ▲, tapping A. The error bars show ± 2 SD ± 0.15 mm Hg.

C was less than at the other two tappings. The reduction of approximately 10% is significant at the two highest flows. The error bars (± 2 SD ± 0.15 mm Hg) show the repeatability of 10 measurements at each flow taken over a period of four weeks. Similar results were found for the DM 29 valve. Pressure tapping B was used as the standard position for all other tests.

The mean pressure difference measured in the major orifice of the Bjork-Shiley tilting disc valves was lower than in the other two orientations (figure 6). The difference, approximately 15%, is significant above 200 ml s^{-1} for the BSS 29 valve. The Os 29 and bileaflet valves showed no significant change in pressure difference with valve orientation. For all the tilting disc valves, the closing volume was less in the vertical plane with gravity assisting the valve closure. This is shown in figure 7 for the BSS 29

Function test apparatus for prosthetic heart valves

69

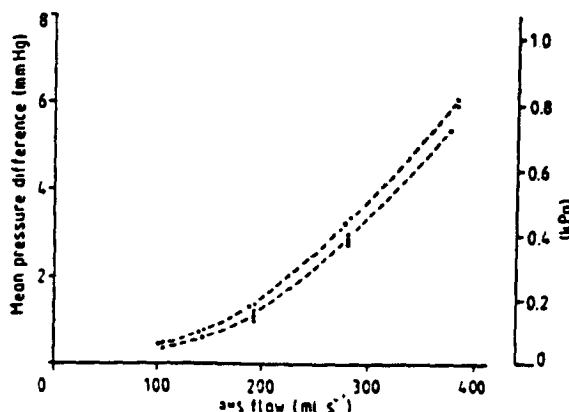


Figure 6. The mean pressure difference plotted against RMS flow for different orientations of the BSS 29 valve. ●, horizontal plane, major orifice; ▲, horizontal plane, minor orifice; ■, vertical plane. The error bars show ± 2 SD.

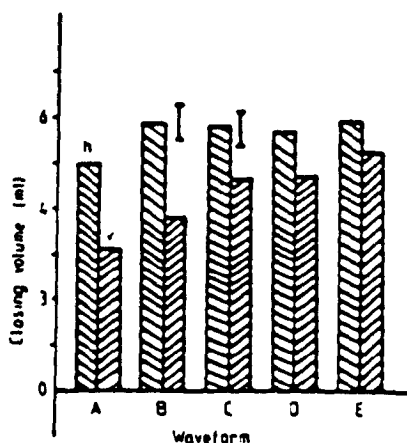


Figure 7. The closing volume of the BSS 29 valve in the horizontal (h) and vertical (v) planes. The error bars show ± 2 SD ± 0.6 ml.

valve. The error bars ± 0.6 ml show the repeatability taken over 10 measurements. The closing volume also varied slightly with the flow conditions. No significant variation with valve orientation was found in the closing volume of the bileaflet valves.

The pressure flow graphs are shown in figure 8 for all the valves opening in the horizontal plane, with the pressure measured in the minor orifice of the tilting disc valves. The mean pressure difference is increased by approximately 10% if the average is taken between the zero pressure points (1 and 3) as opposed to the zero flow points (1 and 4). Figure 9 shows the average regurgitant volumes (closing and closed) for the valves in the horizontal plane.

5. Discussion

The test rig allows prosthetic heart valves to be tested under standard pulsatile flow conditions. The repeatability of the flow and pressure measurements is very good and

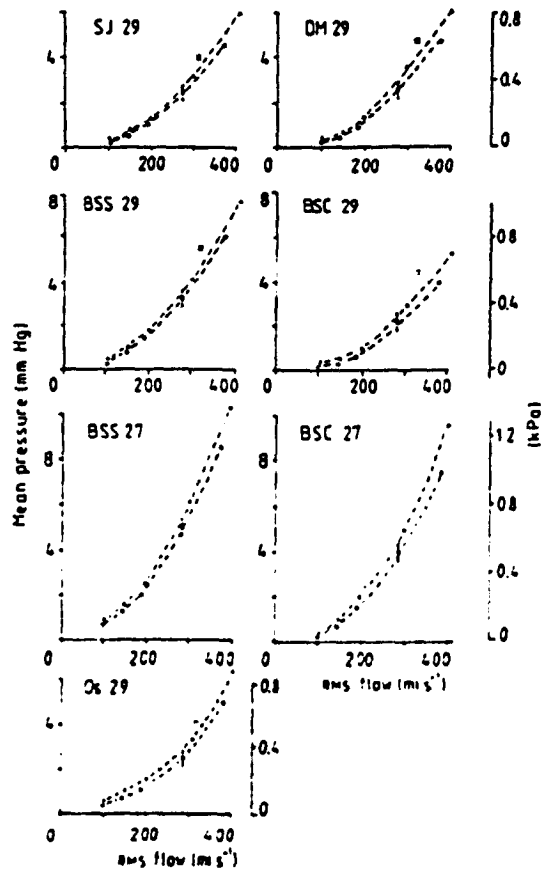


Figure 8. The mean pressure difference plotted against RMS flow for all the valves. Δ , averages taken between the zero pressure points, \bullet , averages taken between the zero flow points. \square , shows data by Scotten *et al* (1983, 1984), \circ , shows data from Stevenson *et al* (1982), \square , shows data by Gabbay *et al* (1978). Error bars ± 2 SD.

the overall accuracy is limited by the systematic errors due to non-linearity and hysteresis in the flow and pressure signals. These errors have been estimated at ≈ 0.3 mm Hg and ≈ 6 ml s^{-1} .

The pressure waveforms measured in the ventricle and aorta are not ideal and are a consequence of measuring the flow through the valve in rigid chambers. The largest oscillation in the ventricular pressure occurs when the mitral valve is almost closed, and does not affect the forward flow measurement. The oscillation is similar to waveforms described by Scotten *et al* (1983) and its amplitude and frequency are dependent on the type, size and closing characteristics of the mitral valve under test.

This initial study shows that the position of the pressure tapping, the valve orientation and the time interval selected for averaging the signals all have a significant effect on the mean pressure difference. The reduced pressure difference measured at tapping C is probably caused by a small fraction of the kinetic energy from the jet being recovered as potential energy (Kohler 1975) as previously described in the aortic position (Tindale *et al* 1982). Inside a physiologically shaped ventricle the flow patterns will be significantly different, and static pressure measurements will consequently vary. For this reason, tapping B closer to the valve has been selected as a standard measure-

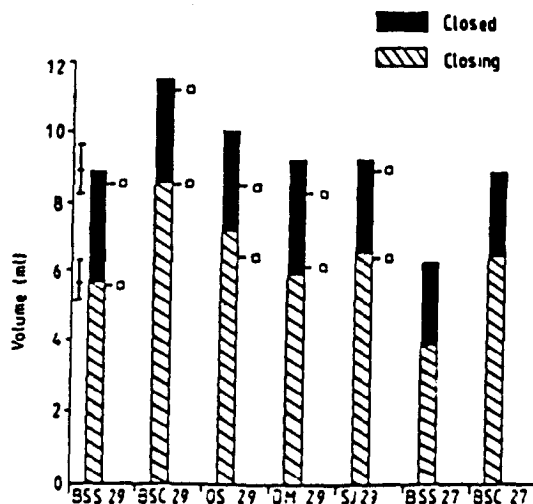


Figure 9. The average regurgitant volumes for all seven valves opening in the horizontal plane. \square shows the values obtained by Scotten *et al* (1983, 1984). Error bars ± 2 SD.

ment point. In this position, valve orientation also affects the measurement. The reduced pressure measurements found in the major orifice of the Bjork-Shiley valves are caused by the jet impinging on the downstream pressure tapping. This effect is not detected in the other valves where the discs and leaflets have larger opening angles. The mean pressure difference is approximately 10% higher if the averages are taken between the zero pressure points (1 and 3) instead of the zero flow points (1 and 4). This is not surprising as during the short period of time between points 3 and 4 when the flow is decelerating, the differential pressure is significantly negative (figure 4). The graphs of pressure and RMS flow (figure 8) show that valves of the same size have similar characteristics. At an RMS flow of 300 ml s^{-1} , the most obstructive valve, BSS 29, has a mean pressure difference of 4 mm Hg whilst the least obstructive, BSC 29, has a mean pressure difference of 3 mm Hg (zero pressure measurements). The size 27 valves have an increased pressure difference of 1 mm Hg at 300 ml s^{-1} over the size 29 valve due to their smaller orifices. The results from other test centres are shown in figure 8. Good agreement is found with the results of Stevenson *et al* (1982) and Gabbay *et al* (1978) but the results of Scotten *et al* (1983, 1984) are systematically higher. This could be caused by the different geometries used in the test apparatus or the different test fluids used. Figure 7 shows that when gravity assists the valve closure in the vertical plane, the closing volume is reduced by between 20 and 30%. In the bileaflet valves, no net difference is found in the closing volume as one leaflet is assisted by gravity and the second leaflet has to work against gravity. However, synchronised photography shows that the lower leaflet closes 30 ms earlier than the upper leaflet. This may be an explanation for asynchronous closing described elsewhere (Yoganathan *et al* 1984). The comparison of the regurgitant volumes in figure 9 for the different valves shows that the volumes are less for the smaller valves and also less for the more obstructive valves (BSS 29 compared with BSC 29). The closing volumes agree closely with the results of Scotten *et al* (1983, 1984). The slightly higher leakage when the valve is closed can be explained by a higher ventricular pressure. The effect of the shape of the ventricular pressure signal on the closing volume of the mitral valve has not been investigated in this study, but the rapid increase in ventricular pressure (figure

4) at the start of systole may force additional fluid through the mitral valve before it is fully closed. This may explain why results for the closing volume of valves measured in an elastic system are lower (Kohler *et al* 1981, Kohler and Schroder 1982).

The results in this study show that variation in the test conditions can have a significant effect on valve function. It is imperative that all the test conditions are defined precisely so that the variation between different types of valves can be correctly assessed. The variation found between valves of the same size was quite small and it is unlikely that differences in pressure measurements of less than 1 mm Hg or differences in regurgitant volumes of less than 1 ml would be noticed clinically.

Acknowledgments

We would like to acknowledge the assistance of Mr R Marshall in testing the valves and Ms L Cathcart in preparation of the diagrams.

Résumé

Mise au point d'un appareil permettant l'étude des prothèses cardiaques. Résultats initiaux en position mitrale.

Les auteurs ont développé un appareil permettant d'étudier le fonctionnement des prothèses cardiaques dans des conditions de débit variable. Ce dispositif utilise une pompe servo-contrôlée pour simuler une variation 'physiologique' de débit à travers la valve. La différence de pression de part et d'autre de la valve, ainsi que le débit à travers la valve, sont mesurés pour évaluer son fonctionnement. La différence de pression moyenne, le débit direct efficace et les volumes de régurgitation sont calculés à l'aide d'un ordinateur. Au cours d'une étude initiale, sept prothèses mécaniques courantes (dimensions 29 et 27 mm) ont été évaluées en position mitrale pour cinq conditions différentes de débit. La différence de pression moyenne est fonction de la pression de courant inverse, de l'orientation de la valve et de l'intervalle de temps d'échantillonnage nécessaire pour les signaux. Avec certaines valves, leur orientation affecte les volumes de régurgitation. Ces variations (10-25%) sont comparables aux différences mesurées entre les valves individuelles. Les conditions de test doivent donc être spécifiées avec beaucoup de soin afin de permettre une comparaison précise du fonctionnement des valves.

Zusammenfassung

Entwicklung eines Funktionstestgerätes für Herzventil-Prothesen. Erste Ergebnisse bei mitraler Lage.

Eine behelfsmäßige Vorrichtung zur Untersuchung der Funktion von Herzventil-Prothesen unter pulsierenden Strömungsbedingungen wurde entwickelt. Bei der Vorrichtung wird eine Pumpe mit Servoregelung verwendet, um eine physiologische Wellenform der Strömung durch das Ventil zu erzeugen. Die Druckdifferenz quer zum Ventil und die Strömung durch die Ventile wurde zur Bestimmung der Funktion des Ventils gemessen. Die mittlere Druckdifferenz, der mittlere quadratische Fehler bei der Vorwärtsströmung und die zurückfließenden Volumina wurden mit Hilfe eines Computers berechnet. In der Anfangsphase wurden sieben bekannte mechanische Prothesen (Größe 29 und 27 mm) in mitraler Lage unter fünf verschiedenen Strömungsbedingungen ausgewertet. Die mittlere Druckdifferenz war dabei abhängig von der Stelle, an der hinterher der Druck gemessen wurde, sowie von der Ausrichtung des Ventils und dem Zeitintervall, das für die Mittelwertbildung der Signale verwendet wird. Die Ausrichtung einiger Ventile beeinflusste sogar die zurückfließenden Volumina. Diese Schwankungen (10-25%) waren von ähnlicher Größenordnung wie die zwischen einzelnen Ventilen gemessenen Unterschiede. Um die Funktion der Ventile genau vergleichen zu können, müssen die Testbedingungen sehr sorgfältig gewählt werden.

References

- Gabbay S, McQueen D M, Yellin E L and Frater R 1978 *In vitro* hydrodynamic comparison of mitral valve prostheses at high flow rates *J. Thorac. Cardiovasc. Surg.* 76 771-83

- Kohler J 1975 Opening angle and torque of the Bjork-Shiley and Lillehei-Kaster heart valve prostheses *Proc. Eur. Soc. Artificial Organs* 2 33-5
- Dynamick kunstlicher herzkappen *Dissertation RWTH, Aachen*
- Kohler J, Ehrentraut G and Stormer B 1981 Haemodynamics of four new prosthetic heart valves *Proc. Eur. Soc. Artificial Organs* 8 361-8
- Kohler J and Schroder W 1982 Closing volume and leakage of four new prosthetic heart valves *Proc. Eur. Soc. Artificial Organs* 9 115
- Martin T R P, Tindale W B, Van Noort R and Black N M 1981 *In vitro* heart valve evaluation: Fact or fantasy *Trans. Am. Soc. Artificial Organs XXVII* 475-79
- Reul H 1983 *In vitro* evaluation of artificial heart valves *Advances in Cardiovascular Physics* vol 5, part IV ed D N Ghista (Basel: Karger) pp16-30
- 1986 Cardiovascular simulation models *Life Support Systems* 2 77-89
- Scotten L N, Walker D K and Brownlee R T 1983 The Bjork-Shiley and Ionescu-Shiley heart valve prostheses. *In vitro* comparison of their hydrodynamic performance in the mitral position *Scand. J. Thorac. Cardiovasc. Surg.* 17 201-9
- 1984 Prosthetic mitral valve orientation—its effect on valve function *in vitro* *Life Support Systems suppl.* 2 86-8
- Stevenson D M, Yoganathan A P and Franck R H 1982 The Bjork-Shiley heart valve prosthesis. Flow characteristics of the new 70° model *Scand. J. Thorac. Cardiovasc. Surg.* 16 1-7
- Tindale W B, Black M M and Martin T R P 1982 *In vitro* evaluation of prosthetic heart valves, anomalies and limitations *Clin. Phys. Physiol. Meas.* 3 115-30
- Tindale W B and Trowbridge E A 1983 Evaluation *in vitro* of prosthetic heart valves. Pulsatile flow through a compliant aorta *Life Support Systems* 1 173-88
- Walker D K, Scotten L N and Brownlee R T 1984 New generation tissue valves. Their *in vitro* function in the mitral position *J. Thorac. Cardiovasc. Surg.* 88 573-82
- Weiting D 1969 Dynamic flow characteristics of heart valves. *PhD Thesis* University of Texas in Austin
- Westerhof N, Elzinga G and Sibbema P 1971 An artificial arterial system for pumping hearts *J. Appl. Physiol.* 31 776-81
- Wright J T M and Temple L J 1971 An improved method of determining the flow characteristics of prosthetic mitral heart valves *Thorax* 26 81-8
- Yoganathan A P, Chauv A, Gray R J, Woo Y N, De Roberts M and Williams F P 1984 Bileaflet tilting disc and porcine aortic valve substitutes: *In vitro* hydrodynamic characteristics *J. Am. College Radiol.* 3 313-20
- Yoganathan A P, Harrison E C and Corcoran W H 1979 Pressure drops across prosthetic aortic heart valves under steady and pulsatile flow—*in vitro* measurements *J. Biomech.* 12 153-8

In Vitro Evaluation of Six Mechanical and Six Bioprosthetic Valves

J. Fisher¹, I.J. Reece², and D.J. Wheatley²

¹ West of Scotland Department of Clinical Physics and Bioengineering, and

² Department of Cardiac Surgery, Royal Infirmary, Glasgow, Scotland

Summary

The in vitro function of 6 tissue valves and 6 mechanical valves (all size 29) was assessed in a purpose-built pulse duplicator under different pulsatile flow conditions. Valve function was analyzed by measuring the mean pressure difference across each valve during forward flow, and the reverse flow through each valve during valve closure (dynamic regurgitation) and in the fully closed position (static regurgitation). Although valves of the same type showed similar characteristics, there were significant differences in function between different types of valves. Porcine valves showed much higher forward flow pressure gradients than pericardial, tilting disc, or bileaflet mechanical valves. However, the porcine valves showed least regurgitation, with pericardial valves having less regurgitation than mechanical valves.

Key words: Mitral valve - Bioprosthetic - Mechanical evaluation

turers. The newer valves were compared to those which are in widespread use throughout the world in order to produce a clear insight into their possible functional advantages.

Methods

The function of 6 tissue valves and 6 mechanical valves (11 size 29 mm and one size 30 mm) was assessed under pulsatile flow conditions in the mitral position of a purpose built pulse duplicator. Details of the valve tested are given in Table 1. Valve function was assessed by measuring the differential pressure across each valve during forward flow and by measuring the reverse flow through each valve. The reverse flow was measured in 2 parts, dynamic regurgitation during valve closure and static regurgitation when the valve was closed. The function test apparatus (1) is shown schematically in Fig. 1. The essential features of the apparatus were as follows:

The pulsatile flow was produced by a purpose built servo controlled piston pump¹ (6). The flow through the valve was measured with an electromagnetic flowmeter². The mean pressure difference across the test valve was measured with a differential transducer³ with the upstream pressure measurement taken 25 mm from the valve and the downstream pressure measurement taken 50 mm from the valve. Direct measurements were made of the pressure in the ventricular, aortic and atrial test sections to establish the correct test conditions.

The mechanical valves were positioned so that opening and closure occurred in the horizontal plane in order to eliminate the effects of gravity. The downstream pressure measurements were made in the minor orifice of the tilting disc, a major orifice of the bileaflet valves adjacent to the strut in the ball and cage valve and adjacent to a post in the tissue valves (Fig. 2). The measured pressure and flow signals and the displacement and velocity signals from the pump were collected for a period of 20 seconds on an Apple II microcomputer and stored for subsequent analysis. Each valve was tested under 5 different pulsatile flow conditions (Fig. 3) corresponding to cardiac outputs of between 3 and 9 L min⁻¹. The fluid medium used for all tests was 0.9% sodium chloride solution. A video camera (Panasonic WVP A1) was used to analyze the opening and closing action of each valve during the test cycle allowing still frame assessment at intervals of 20 ms. The pressure difference and flow signals were analyzed by calculating the average waveform from the data collected and by defining 5 points on these waveforms during each cycle (Fig. 4). Point 1 defines the start of forward flow and Point 2 the start of positive differential pressure. For a mechanical valve these points coincide but for the tissue valves a small positive forward flow is observed before a positive differential pressure could be measured. This is due to forward displacement of the fluid as the valve leaflets relax when the pressure in the ventricle is reduced. Point 3 defines the end of the positive pressure signal and Point 4 the end of forward flow. The differential pressure becomes negative for a short period at the end

¹Cardiac Development Laboratories,

²Gould SP 2201,

³Gaeltec 3CT special,

In vitro testing of heart valves remains the only way of ensuring satisfactory function prior to production for animal and human implantation. The established methods of in vitro evaluation involve function testing at steady and pulsatile flows with assessment of pressure drop and regurgitation, and also durability studies in fatigue testers.

The literature abounds with data on individual valves at various sizes (2, 6, 9), but it is often difficult to compare this data due to variations in the apparatus and methods used to test the valves. Furthermore, the rapid progress made in heart valve designs, with a greater number of valves available for use, has led to further difficulty in correlating the profusion of data available.

The recent introduction of low profile pericardial valves (6), modified orifice porcine valves (7) and bileaflet mechanical valves (5) illustrates the various design options available to valve manufacturers in order to enhance valve performance.

This study was undertaken in order to consolidate knowledge concerning the in vitro performance of these newer designs by comparing 6 mechanical and 6 bioprosthetic designs in the same function test system. The 29 mm mitral valve was selected as being representative of a useful valve size which is often selected clinically and which falls in the middle of the size range available from the manufac-

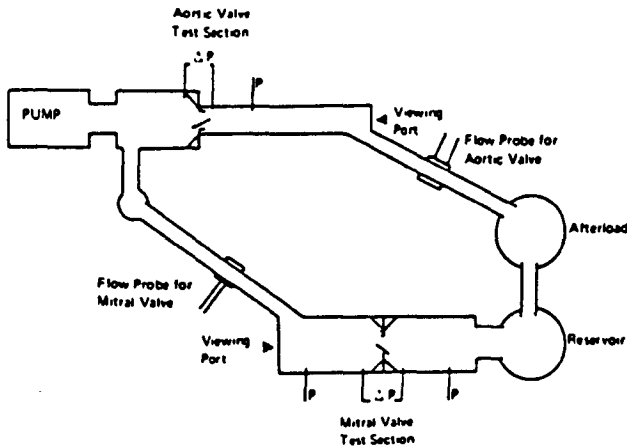


Fig. 1 Diagram of the function test apparatus

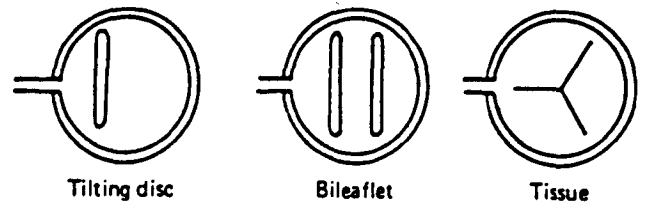


Fig. 2 Orientation of the valves and position of the pressure measurements for the tilting disc, bileaflet and tissue valves

of forward flow as the flow is decelerating. In this study the mean pressure difference and root mean square (RMS) forward flow were calculated between points 2 and 3 and points 2 and 4. Point 5 defines the end of the reverse flow through the valve during closure. The dynamic regurgitant during valve closure was calculated between Points 4 and 5 and the static regurgitation, when the valve was closed, was calculated between points 5 and 1.

The effective orifice area for each valve was calculated for each flow condition from the formula given by Gahhavi (2)

$$EOA = \frac{QRMS}{51.6 AP}$$

Where QRMS is the root mean square forward flow, AP is the mean pressure difference, and EOA is the effective orifice area.

Results

The mean pressure difference across each valve was plotted as a function of RMS forward flow and given for the mechanical valves in Fig. 5 and for the tissue valves in Fig. 6. The repeatability of the measurement was found to be $\pm 2SD = 0.15$ mmHg. The pressure measurements were systematically lower during the longer interval between points 2 and 4. The measurement included the short period of time that the flow was decelerating when there was a small negative differential pressure. This negative pressure starts the closure of the valves while there is still some forward flow. Four of the mechanical valves, BSM, OS, ST and OM, had almost identical forward flow pressure differences while the BSS valve, which is no longer manufactured, had a marginally higher pressure drop (Fig. 5).

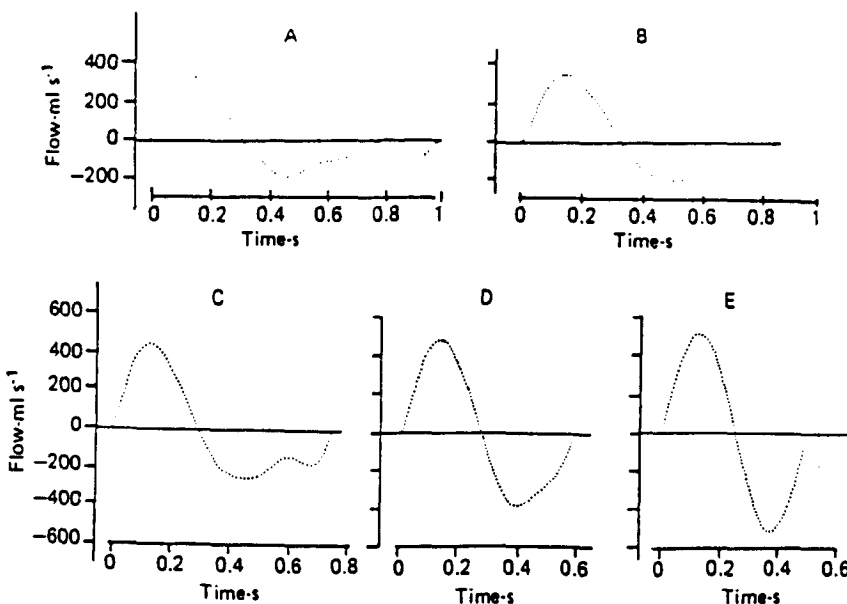


Fig. 3 Five flow waveforms used for testing valves (negative flow shows flow through the mitral valve). Waveform A - 60 beats per min (BP Min), stroke volume (SV) 60 ml
Waveform B - 70 BP Min, SV 70 ml
Waveform C - 80 BP Min, SV 80 ml
Waveform D - 100 BP Min, SV 80 ml
Waveform E : 120 BP Min, SV 80 ml

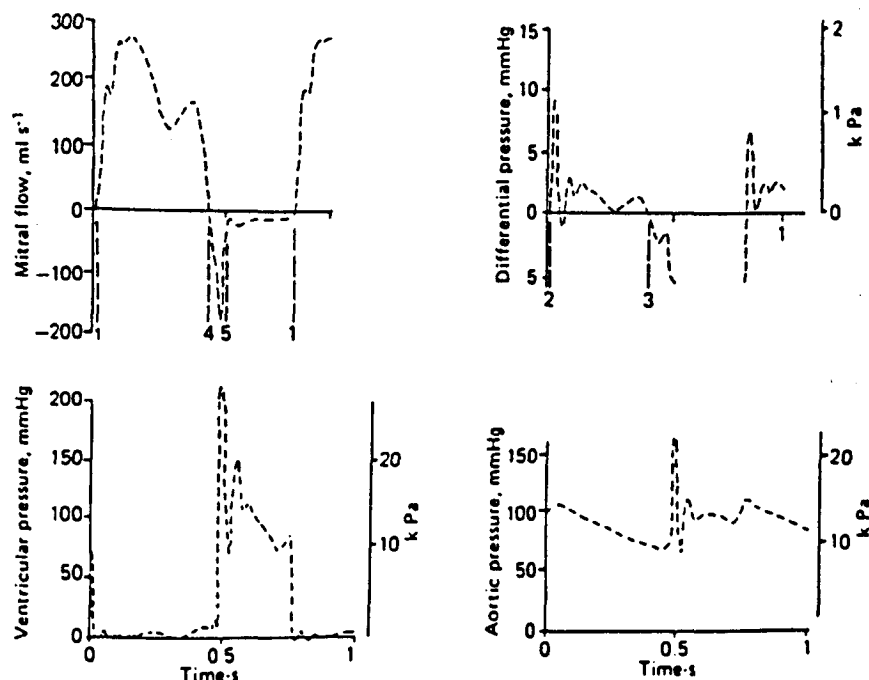


Fig. 4 Pressure and flow signals for BSS29 valve (test conditions - waveform C) showing the time intervals used for analyzing the signals

Table 1 Test valves evaluated

Valve manufacturer	Type	Name	Size	Abbreviation
Shiley Co	Tilting disc	Björk-Shiley Disc	29	BSS 29
		Björk-Shiley Monostrut	29	BSM 29
Ommiscience	Tilting disc	Ommiscience	29	OS 29
St. Jude Medical	Bileaflet	St. Jude	29	SJ 29
Duromedics	Bileaflet	Duromedics*	29	DM 29
Edwards Laboratories	Ball and cage	Starr Edwards	30	SE 30
<i>Tissue</i>				
Shiley Co	Pericardial	Ionescu Shiley low profile	29	ISLP 29
Hancock	Pericardial	Hancock pericardial	29	HP 29
Mitral Medical	Pericardial	Mitral Medical	29	MM 29
Edwards Laboratories	Porcine	Carpentier-Edwards	29	CE 29
Hancock	Porcine	Hancock	29	H 29
Wessex Medical	Porcine	Wessex	29	W 29

*Hemex in USA

Table 2 Variation in effective orifice areas with flow for tissue valves

Flow waveform	RMS forward flow ml.s ⁻¹	ISLP	HP	MM	CE	H	W
A	100	2.3	2.3	2.1	1.5	1.3	1.2
B	140	2.7	2.3	2.3	1.7	1.5	1.4
C	185	2.9	2.6	2.7	1.9	1.6	1.5
D	280	3.1	2.8	3.2	2.0	1.7	1.7
E	385	3.2	3.0	3.5	2.0	1.8	1.9

The SE ball and cage valve had a much larger forward flow pressure drop, confirming that the ball causes a significant obstruction to forward flow. All 3 pericardial valves had similar pressure differences with a variation of less than

1 mm at the highest flows. The 3 porcine valves all showed much higher pressure differences with the CE valve marginally lower than the H or W valves. At the lower flows, the leaflets of the tissue valves did not open fully. This gave a

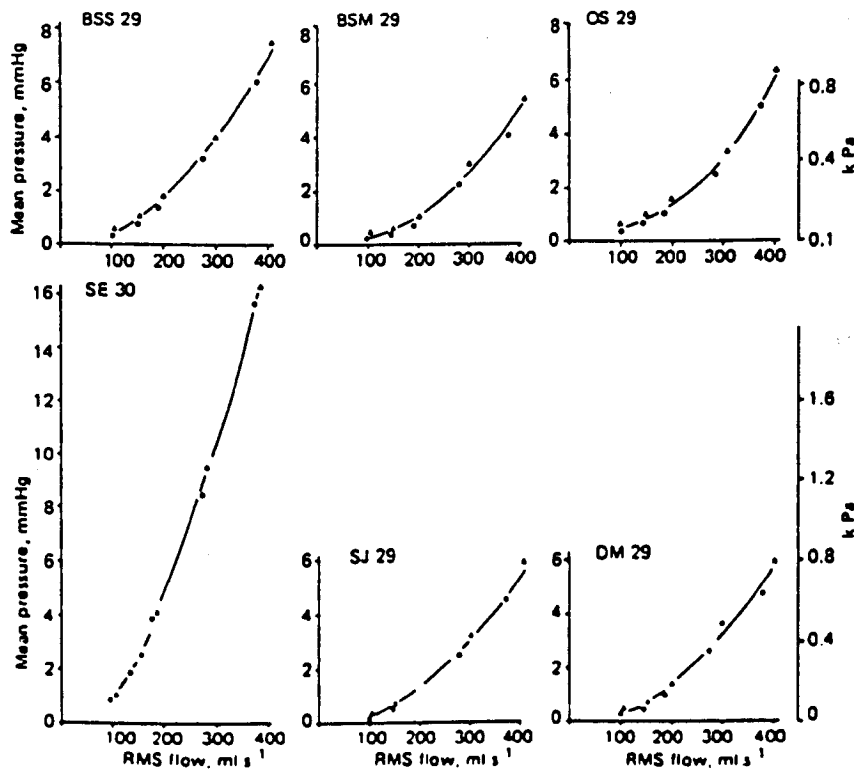


Fig. 5 Mean pressure difference plotted against RMS forward flow for 6 mechanical valves. ▲ mean pressure measured between points 2 and 3, ● mean pressure measured between points 2 and 4

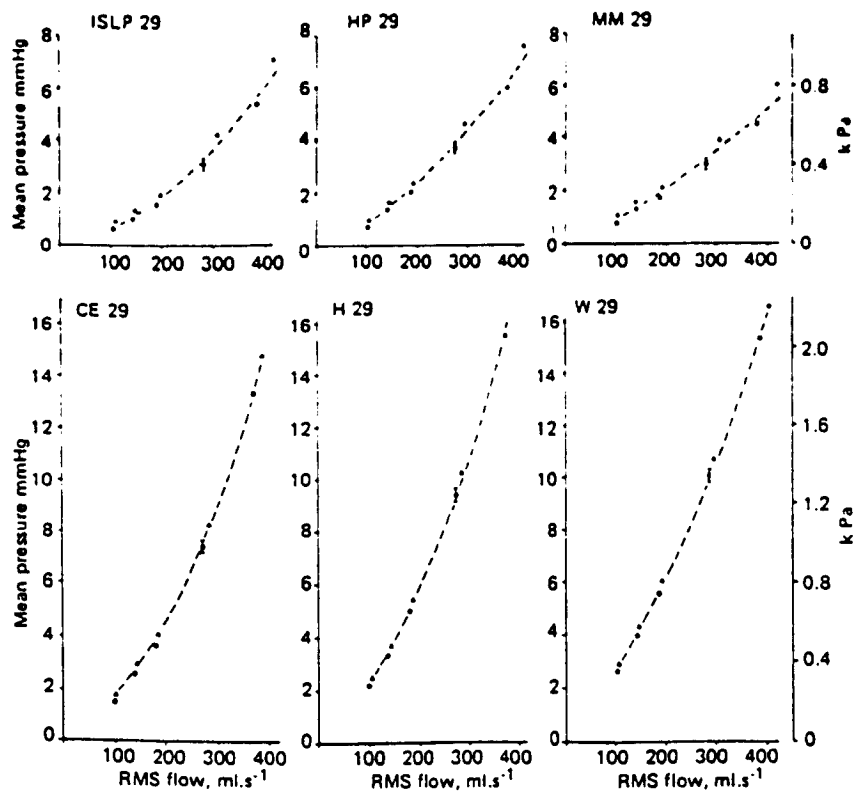


Fig. 6 Mean pressure difference plotted against RMS forward flow for 6 tissue valves. ▲ mean pressure measured between points 2 and 3, ● mean pressure measured between points 2 and 4

reduced effective orifice area (Table 2). The marked differences in the pressure drops between the 3 types of valves is shown for all flow conditions in Fig. 7. Four mechanical valves (excluding the BSS valve and SE ball and cage valve) have slightly lower pressure differences than the pericardial

valves (between 0.5 and 1.5 mmHg lower). Porcine valves have consistently greater pressure differences.

Average regurgitant volumes measured for the 5 flow conditions are shown in Fig. 8. The repeatability of the meas-

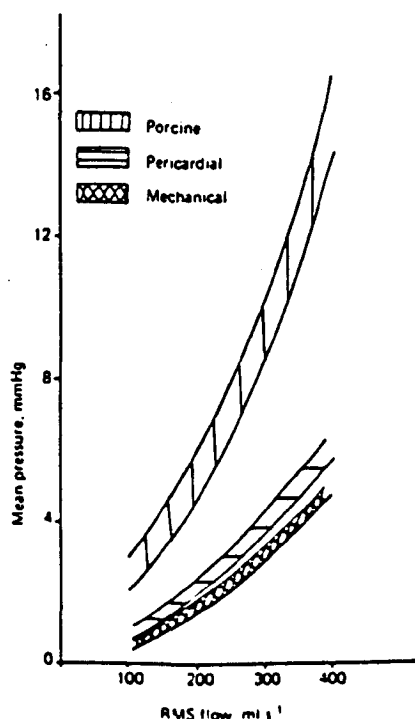


Fig. 7 Mean pressure difference plotted against RMS forward flow for the 3 groups of valves mechanical (excluding SE30 and BSS29) pericardial and porcine

urements was ± 2 SD ± 0.7 ml. Reverse flow through the closed mechanical valves occurred between the rigid occluder and the annular ring. In the closed porcine valve, reverse flow occurred between the tissue and the cloth on the inside of the stent. There was negligible leakage through the closed pericardial valves (Fig. 8). Dynamic regurgitation, while the valve was closing, was similar in the mechanical and pericardial valves, between 6 and 8.5 ml, whilst in the porcine valves it was much less. The total regurgitation was lowest in the porcine valves, 5 to 7.2 ml, slightly higher in the pericardial valves, 7 to 7.8 ml, and largest in the mechanical valves, 7 to 11.2 ml.

Discussion

It is difficult to simulate the complex physiological conditions that occur in the left heart and arterial system whilst

making accurate measurements of the pressure across, and flow through, the valves under test. This is reflected in the different types of test apparatus that have been used to assess valve function (1, 2, 3, 6, 8). Both positive displacement pumps which control flow (1, 2, 6) and pneumatic actuators which control pressure (3, 8) have been used. In some test rigs left ventricular geometry has been modelled (3, 6) while in others rigid cylindrical test sections have been used (1, 2, 8). The rigid cylindrical chambers used in our test apparatus allowed the instantaneous flow through the mitral valve under test to be measured with an electromagnetic flow probe positioned in a tube several centimeters downstream of the valve under test. The boundary conditions for flow in the left ventricle were not simulated and the inertia of the fluid in the rigid test sections caused pressure peaks and oscillations when the flow was accelerated and decelerated as the valves opened and closed (Fig. 4). The oscillations do not occur clinically or in a test rig with an elastic ventricle which is pressure controlled (3). In particular, the rapid rise in ventricular pressure found in our test rig at the start of systole may have had an effect on the closing characteristics of the mitral valves. The results obtained from these studies demonstrate a clear stratification in in-vitro performance between the 3 major valve types.

The mechanical valves (excluding the Starr Edwards valve) showed a consistently lower pressure drop than the biological valves at each flow studied. The porcine valves were associated with the highest pressure drop and the pericardial valves fell between these 2 but pressure drops were closer to those observed with mechanical valves. The close banding of the pressure drop results for each valve group (typically less than 2 mmHg at high flows) suggests that valves in the same group would not be differentiated clinically. The variation of the orifice area with flow for the tissue valves is caused by the larger pressure differences forcing the leaflets further open at high flows. This confirms that flows should be specified when using derived orifice areas as a parameter of valve function (8).

Studies of the dynamic regurgitation during closure again produced stratification of the results of the 3 valve types

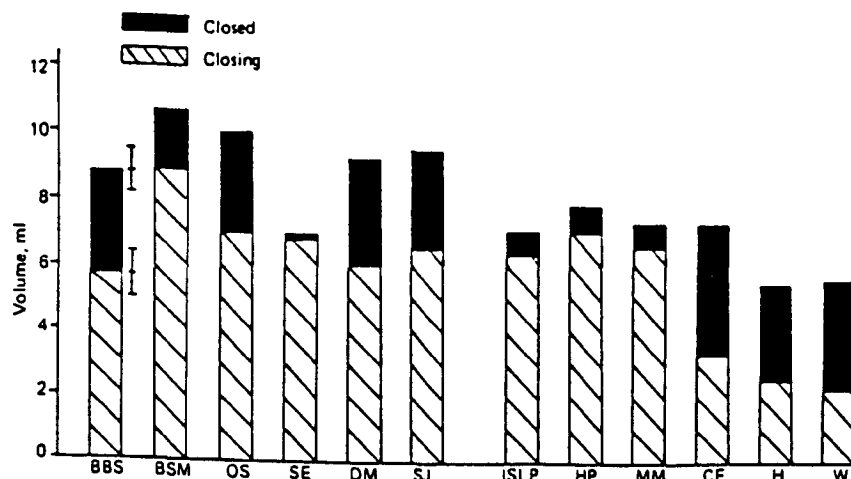


Fig. 8 The average regurgitant volumes for the valves. The dynamic regurgitant volume is shown as the valve is closing and the static regurgitant volume while the valve is closed

with no major difference within each valve group. The porcine group had a significantly lower dynamic regurgitation than the other 2 types but this is not surprising as the leaflets did not open as wide.

While some regurgitation during valve closure is characteristic of all valves, this is influenced by the rate of closure and showed some variation with the different flow-time waveforms used. The measurements of dynamic regurgitation during closure are similar to the results of Walker and co-workers (6, 7) but were higher than those found in a test rig with an elastic pressure-controlled ventricle (3, 4). In our test rig the rapid rise in ventricular pressure and the pressure peak at the start of systole may have forced more fluid back through the valves during closure than would normally occur clinically. It is very likely that the dynamic regurgitation during mitral valve closure is dependent on the rate of rise of ventricular pressure. Other factors, such as orientation (1, 5) of the valve, will also affect measurement of dynamic regurgitation.

Static regurgitation was lowest in the pericardial valves. When completely closed, fluid leakage occurred through the porous material of the frame-covering of the bioprosthetic valves and was greater in the porcine valves where there is continuity between the porous material below and above the attachments of the porcine aortic leaflets. This phenomenon would be present early after implantation but should rapidly diminish with the build-up of fibrin deposits on and within the frame and as the process of endothelialization of the frame-covering progresses. The pericardial valves have almost no continuity of the frame-covering on each side of the closed leaflets and the leaflets form a continuous surface over the outside of the frame which seals the valve closed. In addition, they have a suture placed so as to bring the pericardium of the leaflets into apposition at the top of the posts, thus eliminating static regurgitation to a great extent.

With the mechanical valves, static regurgitation occurs between the occluder and the annular ring and is considered to be an essential feature of the design, allowing "washing" of the sealing area. Static regurgitation with mechanical valves remains constant after implantation.

In this study, we have used 2 parameters to analyze valve function, forward flow pressure drop and total regurgitation. For pressure drop, the order of merit for the valve is mechanical, pericardial and porcine (lowest to highest), whilst for total regurgitant volume, the order is reversed, i.e., porcine,

pericardial and mechanical (lowest to highest). In recent studies, a single parameter has been used to analyze valve function by combining energy losses during forward and reverse flow (6). In vivo, the heart may tolerate energy losses across the mitral valve, due to relatively small regurgitation, better than energy losses due to pressure drops during forward flow. This is because a normal left ventricle is able to compensate for energy losses due to regurgitation by increased work, whereas the consequences of energy loss associated with forward flow pressure drop are reflected in raised left atrial and pulmonary venous pressures. When considering the in-vivo function of these valves in the mitral position, we believe that forward flow pressure drop is the more important determinant of satisfactory function and cardiovascular hemostasis.

We have studied the mechanical function of these valves in vitro. The overall clinical function of the newer valves must await the results of clinical implantation studies currently underway.

References

- 1 Fisher, J., G.R. Jack, and D.J. Wheatley: Design of a Function Test Apparatus for Prosthetic Heart Valves. *Clin. Phys. Physiol. Meas.*: 1986 (in press)
- 2 Gubbay, S., D.M. McQueen, E.L. Yellin, R.M. Becker, and R. W.M. Frater: In Vitro Hydrodynamic Comparison of Mitral Valve Prostheses at High Flow Rates. *J. Thorac. Cardiovasc. Surg.* 76 (1978) 771-783
- 3 Kohler, J., G. Ehrentraut, and B. Stormer: Hemodynamics of Four New Prosthetic Heart Valves. *Proceed. ESAO VII* (1981) 361-368
- 4 Kohler, J.: In Vitro Hemodynamics of 33 Technical and Biological Heart Valve Prostheses. *Proceed. ESAO XII* (1985) (in press)
- 5 Scotten, L.N., D.K. Walker, and R.T. Brownlee: Prosthetic Mitral Valve Orientation - Its Effect on Valve Function In Vitro. *Life Support Systems* 2 (1984) 86-88
- 6 Walker, D.K., L.N. Scotten, and R.T. Brownlee: New Generation Tissue Valves - Their In Vitro Performance in the Mitral Position. *J. Thorac. Cardiovasc. Surg.* 88 (1984) 573-581
- 7 Wright, J.T.M., C.E. Eberhardt, M.L. Gibbs, T. Saul, and C.B. Gilpin: Hancock II - An Improved Bioprosthesis. Pp. 425-444 in: Cohn, L.N., and V. Gallucci, eds.: *Cardiac Bioprosthesis*. New York, Yorke Medical Books 1982
- 8 Yoganathan, A.P., A. Chaux, R.J. Gray, Y.N. Woo, M. DeRobertis, F.P. Williams, and J.M. Matloff: Bileaflet, Tilting Disc and Porcine Aortic Valve Substitutes: In Vitro Hydrodynamic Characteristics. *JACC* 3 (1984) 313-320
- 9 Yoganathan, A.P., Y.N. Wood, F.P. Williams, D.M. Stevenson, R.H. Franck, and E.C. Harrison: In Vitro Fluid Dynamic Characteristics of Ionescu-Shiley and Carpentier-Edwards Tissue Bioprostheses. *Artif. Organs* 7 (1983) 459-469

Comparison of Doppler ultrasound velocity measurements with pressure differences across bioprosthetic valves in a pulsatile flow model

I A SIMPSON,* J FISHER,† I J REECE,† A B HOUSTON,* I HUTTON,* D J WHEATLEY†

*From the University Departments of *Medical Cardiology and †Cardiac Surgery, Royal Infirmary, Glasgow*

SUMMARY Continuous wave Doppler ultrasound was used *in vitro* to assess the pressure differences across four different cardiac bioprosthetic valves in a pulsatile flow test apparatus. Valves were tested under four different flow conditions. Pressure differences were calculated from the maximum flow velocity measured by Doppler ultrasound and correlated well with the pressure differences measured directly in the flow model ($r=0.98$). Thus Doppler ultrasound can accurately measure pressure differences across bioprosthetic valves *in vitro*.

There has been much interest in assessing bioprosthetic valve function *in vitro* by determining flow profiles and pressure gradients across the valve prostheses in order to assess forward flow characteristics and degree of mechanical obstruction.¹ The valuable information gained from these studies is, however, limited, since they cannot easily be extrapolated to the clinical situation, and few *in vivo* haemodynamic data are available. Doppler ultrasound has been used accurately to measure blood flow velocities both *in vivo* and *in vitro*² and has potential therefore in measuring the velocity of the flow jet across prosthetic valves. This has been successfully used in the clinical situation in a small number of patients to assess prosthetic valve gradients³⁻⁵ and compare them with results obtained at cardiac catheterisation. No *in vitro* data are, however, currently available to support the correlation of Doppler ultrasound flow velocity measurements with pressure differences across these prostheses. Appreciable differences in valve function and design exist between the traditional porcine bioprostheses and the new pericardial bioprostheses,⁶ and it is therefore of considerable importance to establish the validity of the Doppler technique for different bioprosthetic valves under a variety of pulsatile flow conditions.

Address for correspondence and reprints: Dr I A Simpson, University Department of Medical Cardiology, Royal Infirmary, Glasgow G31 2ER, Scotland.

Key words: Doppler ultrasound; velocity measurements; pressure differences; bioprostheses; flow model.

Material and methods

A pulsatile flow apparatus had been designed to assess the forward flow pressure drops and regurgitant volumes through prosthetic valves in the mitral position. The layout of the test model is shown in fig 1. The pulsatile flows are produced by a purpose built servo controlled piston pump (Superpump Cardiac Development Laboratory, Victoria, Canada). The pressure difference across the valve is measured with a differential transducer (Gaeltec JCT special, Dunvegan, Scotland) with the upstream pressure tapping 25 mm from the valve and the downstream pressure tapping 50 mm from the valve mounting ring. The flow through the valve is measured with an electromagnetic flowmeter (Gould SP2201) with a 24 mm probe. The pressure and flow signals are digitised and stored on an Apple microcomputer for subsequent analysis. Data are collected over a period of 20 cycles, and a mean waveform calculated for each signal.

In this study the valves were tested under four different flow conditions (fig 2) corresponding to cardiac outputs of between 4.5 and 9 litre·min⁻¹. The peak flow and peak pressure differences were measured for all four waveforms, and in addition the end diastolic flow and pressure were measured for waveforms A and B. The Doppler ultrasound transducer was positioned in a Perspex plate aligned along the axis of the test section parallel to the through valve flow and the transducer sealed in position throughout the study (fig 3). The valves were tested in 0.9% saline that was repeatedly aerated during the

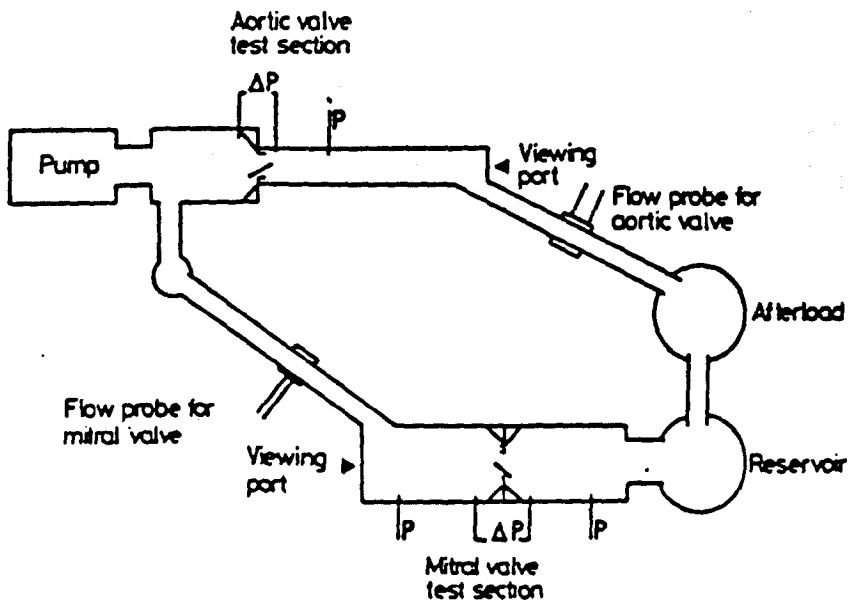


FIG 1 Diagram of the layout of the pulsatile flow test apparatus showing the position of the differential pressure measurement (ΔP) and the flow probe.

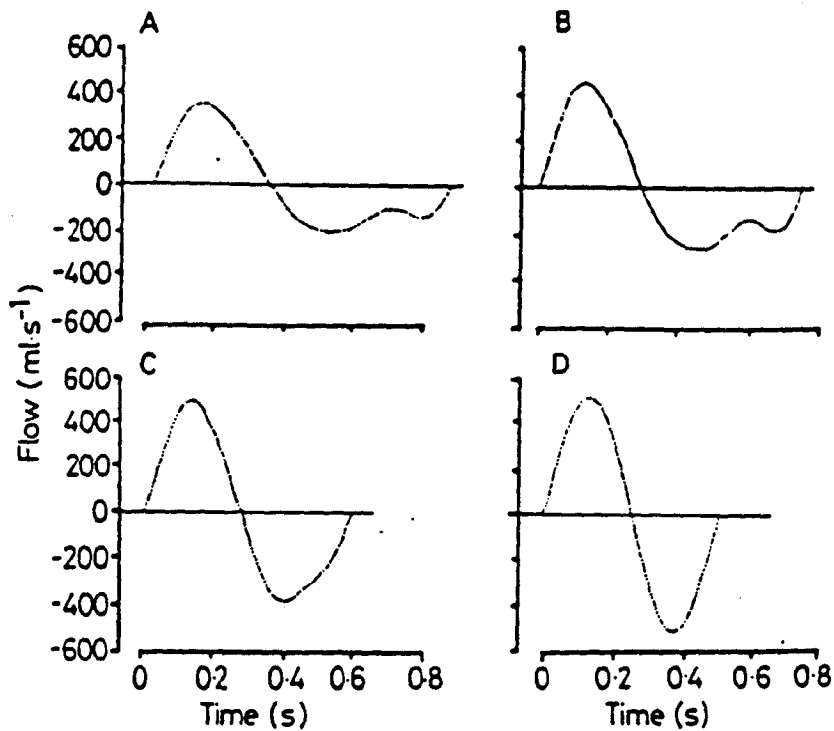


FIG 2 Flow waveforms in the test apparatus. Negative flow indicates the flow through the mitral valve. Waveform A — heart rate (HR) 70 beats·min⁻¹, stroke volume (SV) 70 ml; waveform B — HR 88 beats·min⁻¹, SV 80 ml; waveform C — HR 100 beats·min⁻¹, SV 80 ml; waveform D — HR 100 beats·min⁻¹, SV 80 ml.

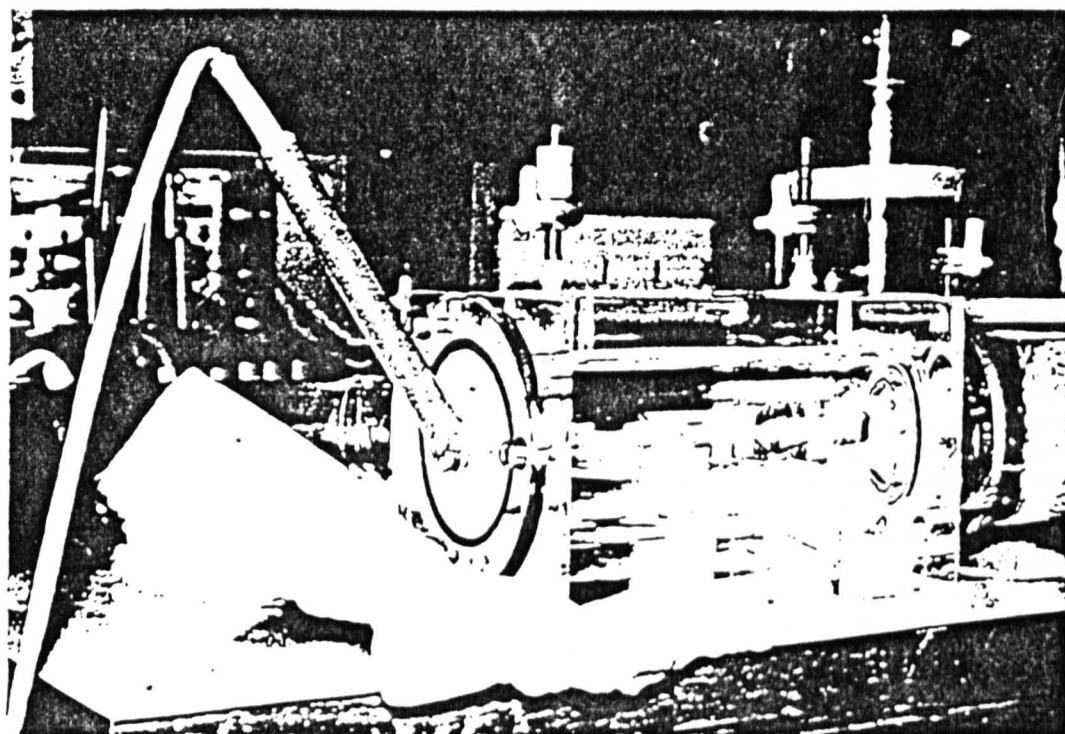


FIG 3 2 MHz Doppler transducer fixed in test apparatus in direct line of through valve flow.

study in order to provide satisfactory ultrasound reflection for the Doppler recordings. The Doppler transducer used was a 2 MHz continuous and pulsed wave double piezoelectric crystal probe (Vingmed, Norway) used in the continuous wave mode, where ultrasound is continuously transmitted from one crystal and the reflected ultrasound continuously received by the other. The Doppler unit used was a Vingmed Alfred velocimeter, which incorporates a quadrature demodulator enabling analysis of both the direction and magnitude of the Doppler velocity shift. The Doppler velocimeter was interfaced to a Doptek spectrum analyser, which includes a flow separation outphaser allowing acceptance of the quadrature Doppler signal for subsequent analysis. For more accurate real time analysis of the Doppler signal the spectrum analyser provides a visual display of the whole range of frequency shifts throughout the simulated cardiac cycle. The spectrum analyser incorporates a conversion of frequency shift to velocity for the 2 MHz transducer used, and from the spectral display therefore the peak flow velocity could be directly measured using a real time movable cursor. From the measured peak flow velocity the pressure difference across the prosthetic valve was then calculated from the peak flow velocity measured by Doppler using the modified Bernoulli equation.^{7,8} To

allow for the lower mass density of 0.9% saline compared with blood, the equation used was $P = 3.75V^2$ where P = pressure drop in mmHg and V = peak velocity in $m \cdot s^{-1}$ rather than $P = 4V^2$ as would be used in vivo. These results were compared with those obtained from direct pressure measurement within the pulsatile flow model.

Four bioprosthetic valves (size 29 mm) were studied in the test apparatus. They included two new pericardial bioprostheses, Hancock pericardial and low profile Ionescu-Shiley, and two porcine bioprostheses, the new Wessex bioprosthesis and the more traditional Carpentier-Edwards.

Results

Satisfactory Doppler signals were obtained from all four valve prostheses, and the Doppler recording (fig 4a) reproduced similar flow waveforms to those obtained from the electromagnetic flow meter (fig 4b). Measured Doppler velocities ranged from $76 \text{ cm} \cdot \text{s}^{-1}$ to $264 \text{ cm} \cdot \text{s}^{-1}$ with a mean of $152 \text{ cm} \cdot \text{s}^{-1}$ for the porcine bioprostheses and from $50 \text{ cm} \cdot \text{s}^{-1}$ to $184 \text{ cm} \cdot \text{s}^{-1}$ with a mean of $105 \text{ cm} \cdot \text{s}^{-1}$ for the pericardial bioprostheses. These correspond to the measured pressure differences of 2.5-27 (mean 10.4) mmHg for the porcine bioprostheses and 1.0-11.3 (mean 4.15) mmHg for the

320

I A Simpson, J Fisher, I J Reece, A B Houston, I Hutton, D J Wheatley

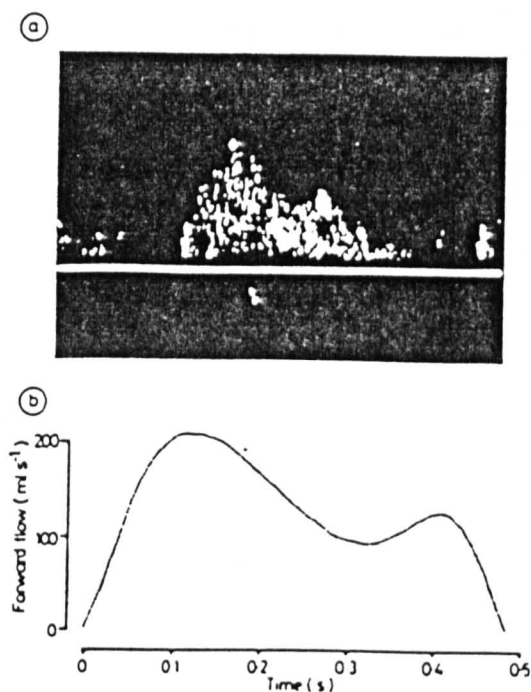


FIG 4 (a) Doppler spectral signal of flow waveform A and (b) flow waveform A measured by electromagnetic flow probe.

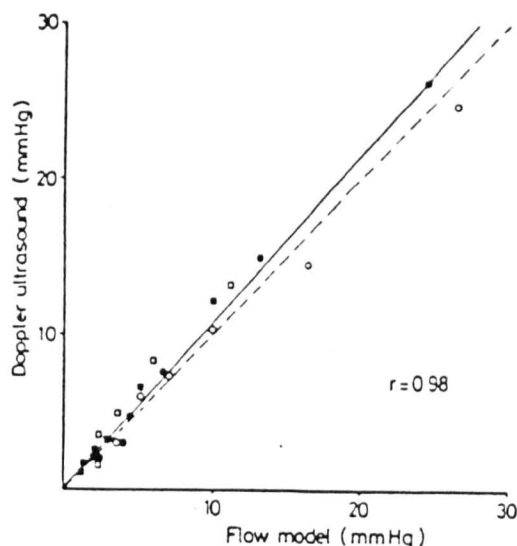


FIG 5 Comparison of the pressure differences at each flow waveform measured by Doppler ultrasound and directly in the flow model. (●) Carpentier-Edwards; (□) Hancock pericardial; (■) low profile Ionescu-Shiley; (○) Wesssex bioprostheses.

pericardial bioprostheses. As expected, using both Doppler and direct *in vitro* measurements significantly higher velocities and pressure differences were obtained with the porcine bioprostheses than with the pericardial prostheses. The relation between the measured pressure difference and that derived from the Doppler flow velocity for all valves is shown in fig 5. The correlation between the two methods was 0.98 with a gradient close to unity.

Discussion

Doppler ultrasound has major potential in the non-invasive haemodynamic assessment of bioprosthetic valve function, and its accuracy in assessing transvalvar flow velocities and pressure gradients in these valves must be clearly established.

In order to derive the pressure difference from the Doppler flow velocity using the modified Bernoulli equation several assumptions have to be made. The equation fails to account for viscous losses due to friction, non-streamlined through valve flow, losses due to turbulence, contraction of the velocity jet, and velocity of fluid proximal to the valve. Despite these assumptions, however, our results were within 3 mmHg of the measured pressure difference in all cases. Doppler ultrasound tended to slightly overestimate the measured pressure difference in three of the valves studied, which may be explained by the velocity profile of the jet.⁶ This was not found with the Wesssex bioprosthesis, which has a prominent muscle shelf and may slightly affect the orientation or velocity profile of the jet.

Though we found a good correlation *in vitro* the potential for greater variation exists *in vivo* particularly with the orientation of the ultrasound beam in the direction of maximum through valve flow. Examination of mitral bioprostheses from the apical position and aortic bioprostheses from the suprasternal, right parasternal, and apical positions should, however, allow the Doppler ultrasound beam to be oriented sufficiently close to the direction of blood flow to prevent appreciable underestimation of pressure gradients. The few available studies using Doppler ultrasound to assess valve function *in vivo* have shown a reasonably good correlation with results obtained at cardiac catheterisation and would therefore suggest that in most cases this does not present a major problem.³⁻⁵

Further *in vivo* studies are necessary to validate the technique in the clinical situation, but we have shown that Doppler ultrasound can accurately measure pressure differences *in vitro*, and the potential therefore exists to provide a non-invasive haemodynamic assessment of bioprosthetic function *in vivo*.

References

- 1 Walker DK, Scotten LN, Modi VI, Brownlee RT. In vitro assessment of mitral valve prostheses. *J Thorac Cardiovasc Surg* 1980;79:680-8.
- 2 Angelsen BAJ, Brubakk AD. Transcutaneous measurement of blood flow velocity in the human aorta. *Cardiovasc Research* 1976;10:368-79.
- 3 Holen J, Simonsen S, Froysaker T. An ultrasound Doppler technique for the noninvasive determination of the pressure gradient in the Bjork-Shiley mitral valve. *Circulation* 1979;59:436-42.
- 4 Holen J, Simonsen S, Froysaker T. Determination of pressure gradient in the Hancock mitral valve from noninvasive ultrasound Doppler data. *J Clin Lab Invest* 1981;41:177-83.
- 5 Nitter-Hauge S. Doppler echocardiography in the study of patients with mitral disc valve prostheses. *Br Heart J* 1984;51:61-9.
- 6 Yoganathan AP, Woo YR, Williams FP, Stevenson DM, Franch RH, Harrison EC. In vitro fluid dynamic characteristics of Ionescu-Shiley and Carpentier-Edwards tissue bioprostheses. *Artif Organs* 1983;7:459-69.
- 7 Halle L, Brubakk A, Tromsdal A, Angelson B. Non-invasive assessment of pressure drop in mitral stenosis by Doppler ultrasound. *Br Heart J* 1978;40:131-40.
- 8 Holen J, Aaslid R, Landmark K, Simonsen S, Ostrem T. Determination of effective orifice area in mitral stenosis from noninvasive ultrasound Doppler data and mitral flow rate. *Acta Med Scand* 1977;201:83-8.

A comparison of experience with the Hancock and Ionescu-Shiley low-profile pericardial bioprostheses

I. J. Reece, J. Fisher, B. Sethia, K. J. MacArthur, and D. J. Wheatley

Department of Cardiac Surgery, Royal Infirmary, Glasgow (Scotland)

The evolution and refinement of the design and construction of bioprosthetic heart valves have progressed so rapidly that the surgical community has been unable to keep pace in terms of clinical evaluation. While porcine valves with improved haemodynamics (6), lower profile (9) and zero pressure chemical fixation (2, 3, 7) represent one path of development, the introduction of the pericardial bioprosthesis (8) and, more recently, its low profile variants represents another (13). The arguments for and against bioprostheses as opposed to mechanical valves are not considered in this discussion, rather, this paper addresses the questions: 1. Is there any significant difference in early clinical results obtained with the low-profile Ionescu-Shiley and the Hancock pericardial valves in the first two years and, 2. Does the early performance of these valves indicate possible advantages over other clinical types of bioprostheses?

The surgeons of the University Department of Cardiac Surgery at the Glasgow Royal Infirmary, Scotland, began a prospective evaluation of the low profile Ionescu-Shiley pericardial bioprosthesis (LPIS) in February 1982. This valve was selected for evaluation because of its low gradients at small annulus diameter, its uniform full open orifice and the symmetrical characteristics of cusp movement. It was felt that this valve offered some advantages over the Carpentier-Edwards porcine and Standard Ionescu-Shiley valves then in use, in particular in terms of haemodynamics, thromboembolic rates and ease of insertion. Some six months later a programme of evaluation of the Hancock pericardial bioprosthesis (HP) was begun, for the reasons stated above and to compare the results of these two valves in similar groups of patients over a similar time frame in the same unit. At about the same time we began using new porcine bioprostheses and the results obtained with these three valves form the basis of this study. All patients were followed closely and were reviewed regularly. In addition,

patients completed a comprehensive questionnaire at regular intervals and were contacted directly if there were any unresolved problems or difficulties with interpretation of questionnaire responses. Follow-up closed at the end of November 1984.

Mortality

Low profile Ionescu-Shiley group

Between February 1982 and September 1984, 98 LPIS valves were implanted in 86 patients. Patient data are given in Table 1 and the operations performed in Table 2.

In the LPIS group there were four hospital deaths (within 30 days) (4.7%). Three of these deaths were non-valve-related: one from septicaemia, one from low cardiac output and possible allergic reaction and one renal failure and gastro-intestinal haemorrhage. However, the fourth death was secondary to

Table 1. Patient data of implantation of low profile Ionescu-Shiley (LPIS) and Hancock pericardial (HP) bioprostheses.

	LPIS	HP
Patients	86	81
Mean age	54.8 ± 10.8	57 ± 11.2
Age range	26-72	21-75
M:F ratio	0.95:1	0.84:1
Total follow-up	146 pt. years	69.3 pt. years
Mean follow-up	1.8 yrs/pt	0.89 yrs/pt

Table 2. Operations performed.

	LPIS	HP
Mitral replacement	36 (42%)	41 (51%)
Aortic replacement	37 (43%)	31 (38%)
Mitral & aortic replacement	12 (14%)	9 (11%)
Tricuspid replacement	1 (1%)	0
Replacement + revascularisation	11 (13%)	8 (10%)
Aortic replacement requiring patch annuloplasty	4/9 (8%)	3/40 (7.5%)

a stroke at four days post-operatively and is considered embolic, though post mortem was inconclusive and the mitral prosthesis and atrium were free of thrombus. Late death occurred in four patients (4.9% of hospital survivors). Death was considered to be valve-related in three cases (2.1%/patient year). Two deaths occurred at reoperation, one for removal of centrally regurgitant aortic and mitral prostheses at three months and the other for prosthetic endocarditis at 32 months.

One patient died with cardiogenic shock from infarction. No post mortem was obtained and this death was assumed to be valve-related. The fourth patient died from a subdural haematoma following a fall, four months postoperatively.

Hancock pericardial group

Between November 1982 and September 1984, 90 HP valves were implanted in 81 patients. Patient data are given in Table 1 and operations performed in Table 2.

There were three hospital deaths (3.7%). None of these were considered valve-related. One patient died from left ventricular rupture during mitral replacement, one from respiratory failure and another from respiratory failure and gastro-intestinal haemorrhage. Late death occurred in three patients (3.8% of hospital survivors). Two of these deaths were considered to be valve-related (2.9% patient year). One patient died of cerebral embolism secondary to prosthetic endocarditis at one month, another from syncope and cardiac failure at one month. Post mortem was not obtained. The third death was due to arrhythmia at two months.

Comparison of mortality

While both groups of patients have an acceptably low hospital mortality with only one "valve-related" death in the LPIS group, the valve-related late mortality has also proved to be similar at 2.8%/patient year for the HP group and 2.1% patient year for the LPIS group. This difference is not statistically significant and is very similar to results obtained with the new porcine valve in Glasgow in the same time-frame (1.7%/patient year) and with bioprostheses reported from other centres (1, 10, 11).

Complications

Low profile Ionescu-Shiley group

Over the follow-up period, five episodes of endocarditis occurred in five patients (3.4%/patient year), three required reoperation (2.1%/patient year) and one patient died. In two patients, (both aortics) endocarditis was controlled medically and valve function remains satisfactory. If the one patient in whom late endocarditis occurred is excluded (32 months), all other episodes occurred within

three months of operation. The actuarial freedom from endocarditis was 96% at 30 months.

Thromboembolism occurred in three patients (three episodes) all within three months of operation. One episode occurred at four days after mitral replacement and was fatal; another six weeks after mitral replacement and the other one month after mitral replacement. These last two patients have made a satisfactory recovery. All patients were anticoagulated at the time of the embolism. The incidence of thromboembolism was 2.1%/patient year and the incidence of fatal thromboembolism 0.7%/patient year. Actuarial freedom from thromboembolism was 96% at 30 months. The incidence of haemorrhagic, anticoagulant-related episodes is considered by many to be a valve-related complication and is included here for completeness. This complication occurred in three patients (2.1% patient year) and episodes were minor in all cases. Paravalvular leak occurred in four patients (4.9% of hospital survivors) and required reoperation in three. One patient had paravalvular leak associated with recurrent endocarditis three weeks after aortic replacement, another developed a leak three months after aortic replacement and one patient had a mitral paravalvular leak and underwent reoperation at one year. In one other patient with an aortic implant, the leak is haemodynamically unimportant at present.

Valve failure not related to endocarditis but requiring reoperation was observed in three patients (four valves). In one patient documented prosthetic aortic and mitral leaks, presumed to be transvalvular, were observed at three months. This patient was in cardiac failure and at reoperation, from which he did not recover, no paravalvular leaks were found. Both valves were explanted and replaced with Björk-Shiley valves but he died in low-output. These valves were examined thoroughly but did not appear to be regurgitant. In the second patient, one leaflet of the 29 mm mitral valve was torn and prolapsed at 27 months (Figures 1a and b).

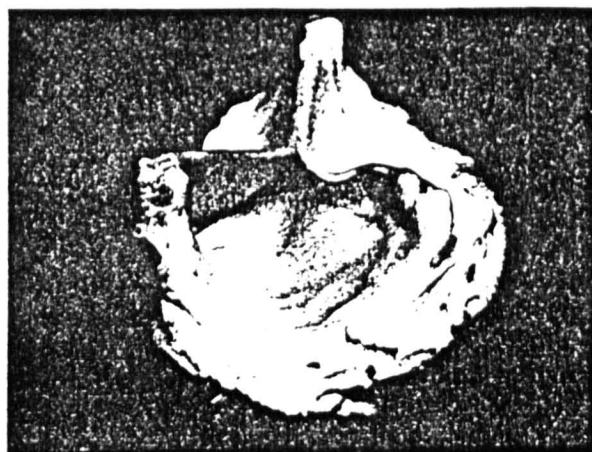


Fig. 1a. 29 mm LPIS mitral valve excised at 27 months with a torn cusp. Other cusp attachments appeared satisfactory.

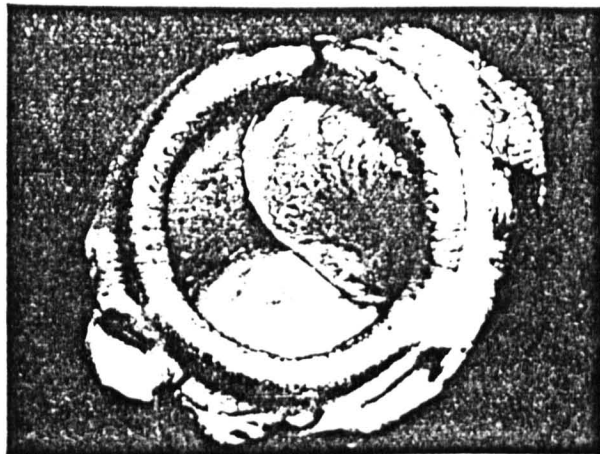


Fig. 1b. Leaflet prolapse producing major mitral regurgitation in the same valve.

This tear was similar to those observed with the Standard Ionescu-Shiley valve and reported by Gabbay et al. (5). In the third patient, tears at both posts produced a prolapsed leaflet and smaller tears were visible in one attachment of each of the other leaflets (Figures 2a and b). This patient was known

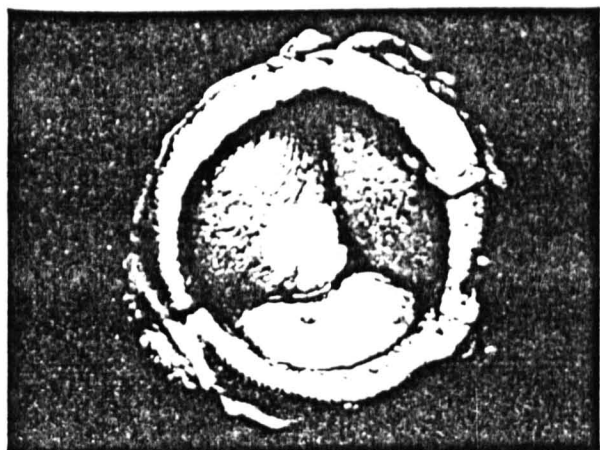


Fig. 2a. Similar prolapse in a 29 mm LPIS mitral valve explanted at 32 months.



Fig. 2b. In this case (see 2a) symmetrical tears were found on each side of the prolapsed leaflet and on one attachment of each of the other leaflets.

to have mitral prosthetic regurgitation at 14 months but required urgent operation when sudden deterioration occurred at 32 months. The incidence of valve failure was therefore 2.1%/patient year and freedom from valve failure 96% at 30 months.

In the LPIS group of patients, mean NYHA Functional Class improved from 2.7 ± 0.6 (60% of patients in Class III or IV) to 1.3 ± 0.2 postoperatively and only one patient in Class III (none in Class IV). Event-free survival was 85% at 20 months.

Hancock pericardial group

Four patients developed endocarditis in the follow-up period (5.7%/patient year). Reoperation was required in one patient at three months following aortic replacement. This patient presented with cerebral embolism. In two other patients, early endocarditis (at two and three months) was successfully treated medically but one other patient died from septic cerebral embolism one month after aortic and mitral replacement. One of the medically-treated patients also had an embolism to the femoral artery requiring operative removal. The incidence of endocarditis requiring re-replacement was therefore 1.4% patient years but in three of the four patients, endocarditis was associated with embolism (4.3% patient year). The incidence of fatal endocarditis was 1.4% patient year. Actuarial freedom from endocarditis was 94% at 30 months.

Thromboembolism occurred in four patients (5.7% patient year) but was associated with endocarditis in three instances. The only non-endocarditis-related episode occurred three months after mitral replacement. One patient died of cerebral thromboembolism and endocarditis (1.4% patient year incidence of fatal thromboembolism). Actuarial freedom from thromboembolism was 94% at 30 months. Haemorrhagic complications were not seen in the HP group. Paravalvular leak was observed in four patients (5% of hospital survivors) though none have yet required reoperation.

There have been no valve failures in the Hancock group though the total follow-up is still small and the period where tissue failure may begin to occur has yet to be reached for the majority of patients.

Mean preoperative Functional Class was 2.6 ± 0.6 (60% of patients in Class III or IV) and this improved to a mean post-operative value of 1.2 ± 0.3 with only one patient in Class III. Actuarial event-free survival was 87% at 20 months.

Comparison of results

Table 3 summarises the results for both the pericardial valves a new porcine bioprosthesis in use since December 1982 (12). There was no statistical-

Table 3. Summary of results.

	LPIS	HP	Wessex
Operative mortality	4.7%	3.7%	6.5%
Late mortality	4.9%*	3.8%*	4%*
Valve related late mortality	2.1%**	2.9%**	1.2%**
Role of thromboembolism (TE)	2.1%**	5.8%**	3.3%**
Actuarial freedom from TE	96%	94%	96.5%
Rate of endocarditis	3.4%**	5.8%**	1.7%**
Actuarial freedom from endocarditis	96%	94%	98%
Rate of reoperation	4.8%**	2.9%**	2%**
Actuarial freedom from reoperation	94%	96%	98%
Event-free survival	85%	87%	93%

* % of hospital survivors
** % per patient year

ly significant differences in the rates of endocarditis, endocarditis requiring reoperation, paravalvular leak, thromboembolism, or event-free survivals. Not only did the two pericardial valves exhibit similar satisfactory early results but we could demonstrate no difference between these values and the Wessex porcine valve. Similarly, in those patients who have undergone recatheterisation, gradients obtained were similar in all groups (Table 4) though numbers were too small for statistical analysis.

Table 4. Post-operative catheterization data.

	LPIS		HP		Wessex porcine	
	size mm	gradient mmHg	size mm	gradient mmHg	size mm	gradient mmHg
AVR					23	10
					25	7
MVR	29	6	29	2	31	0
	33	6	31	2-5	31	8
	29	0	29	6	33	2
	29	5				
	31	3				
	29	4				
	29	7				
	29	5*				

* this valve was excised with a torn and prolapsed leaflet at 34 months.

Obvious differences in results obtained with the two pericardial valves were observed in the rate of thromboembolism and tissue failure. Thromboembolism appeared to occur at a much higher rate (2.1% LPIS: 5.8% HP) in the HP patients and was associated with endocarditis in three of the four patients in whom it occurred. However, this rate is not significantly higher than the rate for the LPIS

group and is probably a manifestation of the shorter follow-up interval which tends to increase the rate of those complications which tend to occur early. The tendency for endocarditis to be associated with thromboembolism is well-known but was only manifest in the HP group. This association is of considerable interest and was not observed in the porcine valve patients. Rather surprisingly, all those patients with endocarditis and thromboembolism had aortic rather than mitral prostheses in situ. In those patients in the ISLP group who had endocarditis, three out of five had aortic replacements but none presented with thromboembolism. Only further observation over an extended period will determine whether this is a real problem or a manifestation of short follow-up and limited numbers.

The second obvious difference between the two pericardial valves is the occurrence of tissue failure only in the LPIS group. The two mitral valves with torn leaflets in the LPIS group are similar in character to those sometimes seen with the Standard Ionescu-Shiley valve (1, 5) and appeared to arise near the top of the posts. The mean time to failure of these valves was just over 30 months. No tissue failures were seen in either the HP or Wessex groups. Obviously, the difference in follow-up duration has a major influence on the rate of such complications and few patients with HP or Wessex mitral valves have reached the 30 month point. The recent withdrawal of the Hancock pericardial mitral prosthesis followed five episodes of tissue failure (4) with a mean follow-up of just over two years. The similar nature of the tissue failures in the LPIS mitral valves reported herein must lead to the conclusion that these valves should be used with some caution and implanted only in centres where detailed follow-up is maintained.

Actuarial event-free survival is not significantly different between the three groups and indicates excellent level of survival and freedom from complications in the early period. It would therefore appear that in the early period of these studies, i.e., within the first two to three years, there is no detectable difference in the results between the porcine valve and the low profile pericardial valves and the two different pericardial valves. It will be of considerable interest to follow these groups to determine the possible emergence of such differences.

Addendum

Since the preparation of this manuscript, additional important complications have occurred. One patient in the LPIS group, known to have a diastolic murmur one year after aortic replacement, required urgent reoperation after rapid deterioration. The explanted valve had tears similar to those seen in the mitral explants mentioned. The interval from implantation to explantation was 34 months.

In addition, one patient in the HP group has required reoperation for mitral paravalvular leak. This valve was in excellent condition with no evidence of leaflet tears at two years.

References

1. Brais MP, Bedard JP, Goldstein W, Koshal A, Keon WJ (1985) Ionescu-Shiley pericardial xenograft: Follow-up of up to six years. *Ann Thorac Surg* 39: 105-111
2. Broom ND, Thomson FJ (1979) Influence of fixation conditions on the performance of glutaraldehyde-treated porcine aortic valves: towards a more scientific basis. *Thorax* 34: 166-176
3. Broom ND, Marra D (1982) Effects of glutaraldehyde fixation and valve constraint conditions on porcine aortic valve leaflet co-aptation. *Thorax* 37: 620-626
4. Extracorporeal Inc, Anaheim California. Personal Communication, November 1984
5. Gabbay S, Bortolotti U, Wasserman F et al (1984) Fatigue induced failure of the Ionescu-Shiley pericardial xenograft in the mitral position: in vivo and in vitro correlation and a proposed classification. *J Thorac Cardiovasc Surg* 87: 836-841
6. Henrks FFA, Turina M, Huysmans HA (1982) In vitro and in vivo assessment of the flow characteristics of the Xenomedica porcine xenograft. In: Cohn LH, Gallucci V (eds) *Cardiac Bioprostheses*. Yorke Medical Book Publisher, New York, pp 469-478
7. Imamura E, Ishihara S, Ohteki H, Aomi S, Koyanagi H (1984) Open-position fixation of bioprostheses for more physiological performance. *J Thorac Cardiovasc Surg* 88: 114-121
8. Ionescu MI, Tandon AP, Mary DAS, Abid A. (1977) Heart valve replacement with the Ionescu-Shiley pericardial xenograft. *J Thorac Cardiovasc Surg* 73: 31-34
9. Liotta D, Bracco D, Ferrari H, Bertolozzi E, Pisanu A, Donato O (1977) Low profile bioprosthesis for cardiac valve replacement. Early clinical results. *Cardiovascular Diseases Bulletin, Tex Heart Inst*
10. Oyer PE, Stinson EB, Reitz BA, Miller OC, Rossiter SJ, Shumway NE (1979) Longterm evaluation of the porcine xenograft bioprosthesis. *J Thorac Cardiovasc Surg* 78: 343-350
11. Pelletier C, Chaitman BR, Baillet R, Guiteras P, Bonan R, Dyrda I (1982) Clinical and haemodynamic results with the Carpentier-Edwards porcine bioprosthesis. *Ann Thorac Surg* 34: 612-623
12. Reece JJ, Wheatley DJ, Munro JL et al (1985) Early results with the Wessex Porcine Bioprosthesis. Presented to the International Symposium on Cardiac Bioprostheses, London 1985
13. Walker DK, Scotten LN, Brownlee RT (1984) New generation tissue valves: Their in vitro function in the mitral position. *J Thorac Cardiovasc Surg* 88: 573-582

Authors' address:

I. J. Reece M.D., Department of Cardiac Surgery, Royal Infirmary, Alexandra Parade, Glasgow G 3 7 ER, Scotland

REFERENCES

1. Wheatley DJ. Heart valves. In: McAinsh TF, ed. Encyclopaedia of physics in medicine and biology. Oxford: Pergamon Press, 1986; 379-84.
2. Hufnagel CA. Basic concepts in the development of cardiovascular prostheses. Am J Surg 1979; 137: 285-300.
3. Gibbon JH. Mechanical heart and lung apparatus. Minnesota Medicine 1954; 37: 171-85
4. Harken DE, Soroff HS, Taylor WJ, Lefemure AA, Gupta SK, Lunzer S. Partial and complete prostheses in aortic insufficiency. J Thorac Cardiovasc Surg 1960; 40: 744-62.
5. Starr A, Edwards ML. Mitral valve replacement: Clinical experience with the ball valve prosthesis. Ann Surg 1961; 154: 726-37.
6. Ross DN. Homograft replacement of the aortic valve. Lancet 1962; 2: 487.
7. Barrett-Boyce BG, Lowe IB, Cole DS, Kelly DT. Homograft replacement for aortic valve disease. Thorax 1965; 20: 495-504.
8. Bjork VO. A new tilting disc valve prosthesis. Scan J Thorac Cardiovasc Surg 1969; 3: 1-10.
9. Emery RW, Nicoloff DM. St Jude Medical cardiac valve prosthesis. J Thorac Cardiovasc Surg 1979; 78: 269-76.
10. Ionescu MI, Pabraski BC, Holden MP, Mary DAS, Wooler GH. Results of aortic valve replacement with frame supported fascia lata and pericardial grafts. J Thorac Cardiovasc Surg 1972; 64: 340-55.

11. Jones EL. Haemodynamic and clinical evaluation of the Hancock xenograft bioprosthesis for aortic valve replacement. *J Thorac Cardiovasc Surg* 1975; 75: 300-08.
12. Ionescu MI, Tandon AP, Mary DAS, Abid A. Heart valve replacement with the Ionescu-Shiley pericardial xenograft. *J Thorac Cardiovasc Surg* 1977; 73: 31-42.
13. Wheatley DJ. Valve prostheses. In: Jamieson SW, Shumway ME, eds. *Operative surgery cardiac surgery*, 4th Ed. London: Butterworths, 1986; 415-24.
14. Starr A. Ball valve prosthesis: a perspective after 22 years. In: Debakey ME, ed. *Advances in cardiac valves*. New York: Yorke Medical Books, 1983: 1-13.
15. Bjork VO. Improved Bjork-Shiley tilting disc valve prosthesis. *Scan J Thorac Cardiovasc Surg* 1978; 12: 81-4.
16. Bjork VO, Herze A. Ten years experience with the Bjork-Shiley tilting disc valve. *J Thorac Cardiovasc Surg* 1979; 78: 331-42.
17. Yoganathan AP, Chaux A, Gray RJ, Robertis MD, Matloff JM. Flow characteristics of the St Jude prosthetic valve. An in vitro and in vivo study. *Art Organs* 1982; 6: 288-94.
18. Debakey ME. Experience with 366 St Jude valve prosthesis in 346 patients. In: Debakey ME, ed. *Advances in cardiac valves*. New York: Yorke Medical Books, 1983: 13-21.
19. Black MM, Drury PJ, Tindale WB. Twenty-five years of heart valve substitutes: a review. *J Roy Soc Med* 1983; 76: 667-80.
20. Carpentier A, Deloche A, Pellard J, Dubost C. Valvular xenograft and valvular bioprosthesis. In: Kalmanson D, ed. *The mitral valve: a pluradisciplinary approach*. London: Edward Arnold, 1976: 527-40.

21. Broom ND. The stress strain and fatigue behaviour of glutaraldehyde-preserved heart valve tissue. *J Biomech* 1977; 10: 707-24.
22. Gallucci V, Valfre C, Mazzucco A et al. Heart valve replacement with the Hancock bioprosthesis. In: Cohn LH, Gallucci V, eds. *Cardiac bioprostheses*. New York: Yorke Medical Books, 1982: 9-24.
23. Jamieson WRE, Pelletier LC, Janusz MT, Chaitman BR, Tyers GFO, Miyagishima RT. Five year evaluation of the Carpentier-Edwards porcine bioprosthesis. *J Thorac Cardiovasc Surg* 1984; 88: 324-33.
24. Wright JTM, Eberhardt CE, Gibbs ML, Saul T, Gilpin CB. Hancock II: an improved bioprosthesis. In: Cohn LH, Gallucci V, eds. *Cardiac Bioprostheses*. New York: Yorke Medical Books, 1982: 425-44.
25. Bartek IT, Holden MP, Ionescu MI. Frame mounted tissue heart valves: technique of construction. *Thorax* 1974; 29: 51-5.
26. Becker RM, Strom J, Frishman W et al. Hemodynamic performance of Ionescu-Shiley valve prostheses. *J Thorac Cardiovasc Surg* 1980; 80: 613-20.
27. Ionescu MI, Tandon AP, Saunders NR, Chidambaram M, Smith DR. Clinical experience of the pericardial xenograft: 11 years experience. In: Cohn LH, Gallucci V, eds. *Cardiac Bioprostheses*. New York: Yorke Medical Books, 1982; 42-60.
28. Gabbay S, Bortolotti U, Wasserman F et al. Longterm follow-up of the Ionescu-Shiley mitral pericardial xenograft. *J Thorac Cardiovasc Surg* 1984; 88: 758-63.

29. Brais MP, Bedard JP, Goldstein W, Koshal A, Keon WJ. Ionescu-Shiley pericardial xenograft: follow-up of up to six years. *Ann Thorac Surg* 1985; 39: 105-11.
30. Cosgrove DM, Lytle BW, Gill CC et al. In vivo hemodynamic comparison of porcine and pericardial valves (Discussion by Rainer WG). *J Thorac Cardiovasc Surg* 1985; 89: 358-68.
31. Roberts WC. Choosing a substitute cardiac valve, type, size and surgeon. *Am J Cardiol* 1976; 38: 633-45.
32. Bonchek LI. Current status of cardiac valve replacement, selection of prostheses and indications of operations. *Am Heart J* 1981; 101: 96-106.
33. Carpentier A, Dubost C, Lane E et al. Continuing improvements in valvular prostheses. *J Thorac Cardiovasc Surg* 1982; 83: 27-42.
34. Lentz DJ, Pollock EM, Olsen DB, Andrews EJ, Murashita J, Hastings WL. Inhibition of mineralization of glutaraldehyde-fixed Hancock bioprosthetic valves. In: Cohn LH, Galluci V, eds. *Cardiac Bioprostheses*. New York: Yorke Medical Books, 1982; 306-19.
35. Carpentier A, Nashref A, Carpentier S et al. Prevention of tissue calcification by chemical techniques. In: Cohn LN, Gallucci V, eds. *Cardiac Bioprostheses*. New York: Yorke Medical Books, 1982; 320-27.
36. Reece IJ, Anderson JD, Wain WH et al. A new porcine prosthesis: in vitro and in vivo evaluation. *Life Support Systems* 1985; 3: 207-27.

37. Weinhold CH, Reichart B, Schoff J, Hammer C. Preliminary results of a new kangaroo aortic valve prostheses in the stage of development. *Life Support Systems* 1984; 2 (Suppl): 78-81.
38. Ionescu MI, Silverton NP. Longterm durability of the pericardial valve. In: Yacoub M, Bodnar E, eds. *Cardiac Bioprostheses*. New York: Yorke Medical Books, 1986 (In Press).
39. Walker DT, Scotten LN, Brownlee RT. New generation tissue valves: their in vitro performance in the mitral position. *J Thorac Cardiovasc Surg* 1984; 88: 573-78.
40. Reece IJ, Fisher J, Sethia B, MacArthur KJD, Wheatley DJ. A comparison of experience with the Hancock and Ionescu-Shiley low profile pericardial bioprostheses. *Z Kardiol* 1986; 75 Suppl. 232-236.
41. Reece IJ, Sethia B, MacArthur KJD, Wheatley DJ. Early results with two low profile pericardial bioprostheses. In: Yacoub M, Bodnar E, eds. *Cardiac Bioprostheses*. New York: Yorke Medical Books, 1986 (In Press).
42. Bailly P, Sauer M, Vouche P et al. Experience of four surgical centres with the Hancock pericardial valve. In: Yacoub M, Bodnar E, eds. *Cardiac Bioprostheses*. New York: Yorke Medical Books, 1986 (In Press).
43. Deverall PH, Revuelta JM, Gometza B, Duran CG. Early results of the Mitroflow valve. In: Yacoub M, Bodnar E, eds. *Cardiac Bioprostheses*. New York: Yorke Medical Books, 1986 (In Press).
44. Cosgrove DM, Lytle BN, Williams GW. Haemodynamic performance of the Carpentier-Edwards pericardial valve in the aortic position in vivo. *Circulation* 1985; 72 Suppl II: 146-52.

45. Swanson J, Perier P, Takriti A, Chachques JC, Chauvaud S, Carpentier A. Early results with the Carpentier-Edwards pericardial valve. In: Yacoub M, Bodnar E, eds. Cardiac Bioprostheses. New York: Yorke Medical Books, 1986 (In Press).
46. Gabbay S, Bortollotti U, Wasserman F et al. Fatigue-induced failure of the Ionescu-Shiley pericardial xenograft in the mitral position. J Thorac Cardiovasc Surg 1984; 87: 836-44.
47. Gabbay S. Ionescu-Shiley pericardial xenograft: follow-up up to six years. Ann Thorac Surg 1985; 39: 101-02.
48. Clarke RE, Swanson WM, Kardos JL, Hagen RW, Beauchamp RA. Durability of prosthetic heart valves. Ann Thorac Surg 1978; 26: 323-35.
49. Nugent AH, Scotten LN, Walker DK, Brownlee RT. Accelerated fatigue tests on heart valves: a preliminary database. Proc ACEMB 1984; 37:149.
50. Walker DK, Scotten LN, Nugent AH, Brownlee RT. In vitro assessment of the Ionescu-Shiley III, Mitral Medical and Edwards Pericardial valves. In: Yacoub M, Bodnar E, eds. Cardiac Bioprostheses. New York: Yorke Medical Books, 1986 (In Press).
51. Martin TRP, Van Noort R, Black MM, Morgon J. Accelerated fatigue tests of biological tissue heart valves. Proc ESAO 1980; 7: 315-18.
52. Ionescu MI, Lenker JA, Rosenbluth RF. Low profile prosthetic xenograft heart valve. European Patent Application 813051224, 1981.

53. Thubrikar MJ, Skinner JR, Nolan SP. Design and stress analysis of bioprosthetic valves in vivo. In: Cohn LH, Galluci, eds. Cardiac Bioprostheses. New York: Yorke Medical Books, 1982; 445-55.
54. Ionescu MI. The pericardial xenograft valve. Mode of failure and remedial developments. In: Yacoub M, Bodnar E, eds. Cardiac Bioprostheses. New York: Yorke Medical Books, 1986 (In Press).
55. Black M, Drury PJ, Tindale WB. A construction technique for minimising valve leaflet failure in pericardial valves. Life Support Systems 1984; 2 Suppl: 89-91.
56. Walker DK, Scotten LN, Hewgill DE, Racca RG, Brownlee RT. Development and in vitro assessment of a new two leaflet replacement heart valve designed using computer generated bubble surfaces. Med Biol Eng Comput 1983; 21: 31-38.
57. Gabbay S, Bortolotti U, Capolletti G et al. The Meadox Unicusp pericardial bioprosthetic heart valve. Ann Thorac Surg 1984; 37: 448-56.
58. Gabbay S, Bortolotti U, Wasserman F, Frater RWM. Prediction of bioprosthetic valve durability by accelerated fatigue tests. Proc AAMI 1984; 18: 95.
59. Swanson WM. Failure modes in biological tissue valves. Proc AAMI 1984; 39: 99.
60. Walker DK, Scotten LN, Modi V, Brownlee RT. In vitro assessment of mitral valve prostheses. J Thorac Cardiovasc Surg 1980; 79: 680-88.

61. Gabbay S, Frater RWM. In vitro comparison of the new generation of mitral valve prostheses. *Trans Am Soc Artif Intern Organs* 1982; XXVIII: 143-47.
62. Tindale WB, Trowbridge EA. Evaluation in vitro of prosthetic heart valves: pulsatile flow through a compliant aorta. *Life Support Systems* 1983; 1: 173-83.
63. Yoganathan AP, Chaux A, Gray RJ et al. Bileaflet, tilting disc and porcine aortic valve substitutes: in vitro hydrodynamic characteristics. *JACC* 1984; 3: 313-20.
64. Bruss K, Reul H, Van Gilse J, Knott E. Pressure drop and velocity fields at four mechanical heart valve prostheses: Bjork-Shiley Standard, Bjork-Shiley concave-convex, Hall-Kaster, and St Jude Medical. *Life Support Systems* 1983; 1: 3-22.
65. Rainer WG, Christopher RA, Sadler TR, Hilgenberg AD. Dynamic behaviour of prosthetic aortic tissue valves as viewed by high speed cinematography. *Ann Thorac Surg* 1979; 28: 274-80.
66. Kasagi Y, Wada J. Haemodynamics of the St Jude medical valve in a mock circulation. *J Thorac Cardiovasc Surg* 1981; 81: 202-09.
67. Lewis JMO, Macleod N. A blood analogue for experimental study of flow related thrombosis at prosthetic heart valves. *Cardiovascular Res* 1983; 17: 466-75.
68. Jones M, Barnhart GR, Chavez AM et al. Experimental evaluation of bioprosthetic valves in sheep. In: Cohn LH, Gallucci V, eds. *Cardiac Bioprostheses*. New York: Yorke Medical Books, 1982; 276-92.
69. Calvert G, Drabble J, Serafin R, Temple RJ. An aortic pulse duplicator of simple design. *J Thorac Cardiovasc Surg* 1964; 47: 633-43.

70. Starkey WL, Sirak HD, Collins JA, Hagan BT. Design and development of a cardiac simulator for the evaluation of heart valve prosthesis. *J Thorac Cardiovasc Surg* 1963; 46: 207-212.
71. Elzinga G, Westerhof N. How to quantify pump function of the heart. *Circulation Research* 1979; 44: 303-09.
72. Swanson WM, Clarke RE. A simple cardiovascular system simulator: design and performance. *J Bioeng* 1976; 1: 135-45.
73. Scotten LN, Walker DK, Brownlee RT. Construction and evaluation of a hydromechanical simulation facility for the assessment of mitral valve prostheses. *J Med Eng Technol* 1979; 3: 11-18.
74. Wright JTM. Hydrodynamic evaluation of tissue valves. In: Ionescu MI, ed. *Tissue heart valves*. London: Butterworths, 1979; 31-87.
75. Duff WR, Fox RW. Prosthetic cardiac valves: an in vitro study. *J Thorac Cardiovasc Surg* 1972; 63: 131-42.
76. Bjork VO, Olin C. A hydrodynamic evaluation of the new tilting disc valve for mitral valve replacement. *Scan J Cardiovasc Surg* 1970; 4: 37-43.
77. Martin TRP, Tindale WB, Van Noort R, Black MM. In vitro heart valve evaluation: fact or fantasy. *Trans Am Soc Artif Organs* 1981; XXVII: 475-499.
78. Scotten LN, Walker DK, Smith DN, Brownlee RT. A versatile pump for simulating physiological fluid flows. *Proc AAMI* 1983; 18: 108.
79. Weiting DW. Dynamic flow characteristics of heart valves. PhD Dissertation. University of Texas, Austin, 1969.

80. Yoganathan AP, Corcoran WH, Harrison EC. Pressure drops across prosthetic aortic heart valves under steady and pulsatile flow: in vitro measurements. *J Biomechanics* 1979; 12: 153-64.
81. Cornhill JF. An aortic left ventricular pulse duplicator used in testing prosthetic aortic heart valves. *J Thorac Cardiovasc Surg* 1977; 73: 550-58.
82. Mohnhaupt A, Affeld K, Mohnhaupt R, Bucherl ES. A comparative performance analysis of heart valve prostheses. *Proc ESAO* 1975; II: 39-45.
83. Reul H. Cardiovascular simulation models. *Life Support Systems* 1984; 2: 77-98.
84. Martin TRP, Black MM. Problems of in vitro testing of heart valve replacements. *Proc ESAO* 1976; III: 131-37.
85. Knight CJ, Julian DG, Macleod N, Taylor DEM, Wade D. An artificial heart with independently variable pulse parameters. *Trans Am Soc Art Int Organs* 1971; XVII: 433-36.
86. Gentle CR. The role of simulation studies in cardiac valve prosthesis design. *Eng in Med* 1978; 7: 101-06.
87. Gabbay S, McQueen DM, Yellin EL, Becker RM, Frater RWM. In vitro hydrodynamic comparison of mitral valve prostheses at high flow rates. *J Thorac Cardiovasc Surg* 1978; 76: 771-86.
88. Swanson WM. Comparison of in vitro valve pressure drop results from different investigators. *Med Inst* 1984; 18: 115-18.
89. Reul H. In vitro evaluation of artificial heart valves. In: Ghista DN, ed. *Adv Cardiovasc Phys* 5 (Part IV). Basle: Karger, 1983; 16-30.

90. Kohler J, Ehrentraut G, Stormer B. Hemodynamics of four new prosthetic heart valves. *Proc ESAO* 1981; 8: 361-68.
91. Westerhof N, Elzinger G, Sipkema P. An artificial arterial system for pumping hearts. *J Appl Physiol* 1971; 31: 776-81.
92. Martin TRP, Palmer JA, Black MM. A new apparatus for the in vitro study of aortic valve mechanics. *Eng in Med* 1978; 1: 229-30.
93. Murgo JP, Westerhof N, Giolma JP, Altobelli A. Aortic input impedance in normal man: relationships to pressure flow waveforms. *Circulation* 1980; 62: 105-16.
94. Chandran KB, Khalighi B, Chen JG, Falsetti HL, Yearwood TL, Hiratzka LF. Effect of valve orientation on flow development post aortic valve prosthesis in a model human aorta. *J Thorac Cardiovasc Surg* 1983; 85: 893-901.
95. Reul H, Tesch B, Schoenmackers J, Effert S. Hydromechanical simulation of systemic circulation. *Med Biol Eng* 1984; 12: 431-36.
96. Walker DK, Scotten LN, Racca RG, Brownlee RT. Acquisition and analysis of data obtained from the in vitro testing of heart valves. *Proc AAMI* 1983; 18: 130.
97. Wright JTM, Brown MC. A method of measuring the mean pressure gradient across prosthetic heart valves under in vitro pulsatile flow conditions. *Med Instrumentation* 1977; 11: 110-13.
98. Yellin EL, McQueen P, Gabbay S, Strom JA, Becker RM, Frater RWM. Pressure flow relations and energy losses across prosthetic mitral valves. In: Baun J, Arntzerius AC, Yellin EL, eds. *Cardiac dynamics*. The Hague: Martinus Nijhoff, 1980; 509-19.

99. Tindale WB, Martin TRP, Van Noort R, Black MM. Problems of measurement in aortic valve in vitro evaluation. Proc ESAO 1981; 356-60.
100. Tindale WB, Black MM, Martin TRP. In vitro evaluation of prosthetic heart valves: anomalies and limitations. Clin Phys Physiol Meas 1982; 3: 115-30.
101. Reul H. Velocity fields at bioprosthetic heart valves measured by laser doppler anemometry. Life Support Systems 1984; 2 Suppl: 72-7.
102. Bousquet A, Bellet D, Boccalon H, Puel P. Flows nearby heart valve prosthesis. Proc ESAO 1982; VIII: 369-73.
103. Yoganathan AP, Corcoran WH, Harrison EC, Carl JR. In vitro velocity measurements in the near vicinity of the Bjork-Shiley aortic prosthesis using a laser doppler anemometry. Med Biol Eng Comp 1979; 17: 453-59.
104. Massey BS. Mechanics of fluids. 4th Edition. New York: Van Nostrand Reinhold, 1979; 95.
105. Gorlin R, Gorlin SG. Hydraulic formulae for calculation of the area of stenotic mitral valve, other cardiac valves and central circulatory shunts. Am Heart J 1951; 41: 1-29.
106. Cohen MV, Gorlin R. Modified orifice equation for mitral valve area. Am Heart J 1972; 84: 839-40.
107. Yellin EL, Peskin CS. Large amplitude pulsatile water flow across an orifice. Trans ASME 1975; 92-5.
108. Peskin C. The fluid dynamics of heart valves: experimental, theoretical and computational methods. Am Rev Fluid Mech 1982; 14: 235-59.

109. Bellhouse B, Bellhouse F. Fluid mechanics of model normal and stenosed aortic valves. *Circ Res* 1969; XXV: 693-704.
110. Clarke C. The fluid mechanics of aortic stenosis: theory and steady flow experiment. *J Biomechanics* 1979; 521-28.
111. Reul H, Talukder N, Muller EW. Fluid mechanics of the natural mitral valve. *J Biomechanics* 1981; 14: 361-72.
112. Talukder N, Reul W, Muller EW. Fluid mechanics of the natural aortic valve. *Cardiovasc Dynamics. Inserm-Euromech* 92, 1977; 71: 335-50.
113. Bellhouse BJ, Bellhouse FH. Mechanics of closure of the aortic valve. *Nature* 1969; 217: 86-7.
114. Bellhouse BJ. Fluid mechanics of the aortic valve. In: Ionescu MI, Wooler GH, eds. *Biological tissue valves in heart valve replacement*. London: Butterworths, 1972; 23-47.
115. Fisher J, Jack GR, Wheatley DJ. Design of a function test apparatus for prosthetic heart valves. Initial results in the mitral position. *Clin Phys Physiol Meas* 1986; 6: 63-73.
116. Macdonald I, Fisher J, Evans AL, Wheatley DJ. A computerised data acquisition system for a heart valve test apparatus. *J Med Eng Technol* 1986 (In Press)
117. Simpson I, Fisher J, Reece IJ, Houston AB, Wheatley DJ. In vitro comparison of bioprosthetic valve function using Doppler ultrasound. *Cardiovascular Research* 1986; 20: 317-21.
118. Fisher J, Reece IJ, Wheatley DJ. The in vitro evaluation of six mechanical and six bioprosthetic heart valves. *Thoracic and Cardiovasc Surgeon* 1986; 37: 157-64.

119. Quinton WE, Ofstun MS, Leyser M et al. An accelerated fatigue pump for testing prosthetic aortic valves. In: Merendino KA, (ed). Prosthetic valves for cardiac surgery. Springfield, Illinois: Thomas CC, 1961; 234-41.
120. Steinmetz GP, May KJ, Mueller V, Anderson HW, Meredino KA. An improved accelerated fatigue machine and pulse simulator for testing and developing prosthetic cardiac valves. J Thorac Cardiovasc Surg 1964; 47: 186-98.
121. Haussinger G, Reul H. Design and construction of a fatigue test unit for prosthetic heart valves. Biomed Technol 1981; 26: 13-18.
122. Black MM. Development and testing of prosthetic heart valves: cardiovascular simulation and life support systems. In: Kennedy RM, ed. Perspectives in biomedical engineering. London: MacMillan, 1973; 21-28.
123. Thubrikar M, Nolan SP. Mechanism of opening of the aortic valve. J Thorac Cardiovasc Surg 1970; 77: 863-70.
124. Swanson WM, Clarke RE. Aortic valve leaflet motion during systole: numerical and graphical determination. Circ Res 1973; XXXII: 42-49.
125. Swanson WM, Clarke RE. Dimensions and geometric relationships of human aortic valve as a function of pressure. Circulation Res 1974; 35: 871-82.
126. Broom ND, Thomson FJ. Influence of fixation conditions on the performance of glutaraldehyde-treated porcine aortic valves. Thorax 1979; 34: 166-76.

127. Clarke RE, Gould PL, Swanson WM et al. Design and fabrication of prosthetic heart valve leaflets. *Biomat Med Dev Art Org* 1974; 2: 379-85.
128. Missirilis YF, Chong M. Aortic valve mechanics I: material properties of natural porcine aortic valves. *J Bioeng* 1978; 2: 287-300.
129. Lee MJ, Courtman DW, Boughner DR. The glutaraldehyde stabilised porcine aortic valve I: tensile visco-elastic properties of fresh leaflet material. *J Biomed Mat Res* 1984; 18: 61-77.
130. Clarke RE, Sutura SP. Methods of design of leaflet valvular prostheses I: stresses in the mitral valve leaflets in health and disease. *J Thorac Cardiovasc Surg* 1973; 65: 890-96.
131. Chong KP, Weiting DW, Hwang NH, Kennedy JH. Stress analysis of normal human aortic valve leaflets during diastole. *Biomat Med Dev Art Org* 1973; 13: 307-21.
132. Missirilis YF, Armeniades CD. Stress analysis of aortic valve during diastole. Important parameters. *J Biomechanics* 1976; 9: 477-80.
133. Gould PL, Cataloglu A, Dhatt G, Chattapodhyay A, Clarke RE. Stress analysis of the human aortic valve. *Comp Struct* 1973; 3: 377-84.
134. Cataloglu A, Clarke RE, Gould PL. Stress analysis of aortic valve leaflets with smoothed geometrical data. *J Biomechanics* 1977; 10: 153-58.
135. Christie CW, Medland IC. A non-linear finite element stress analysis of bioprosthetic heart valves. In: Gallagher RH, Simon BR, Johnson PC, Cross JF, eds. *Finite elements in biomechanics*. London: John Wiley & Sons; 1982, 153-79.

136. Christie CW. Analysis of mechanics of bioprosthetic heart valves. PhD Thesis, University of Auckland, 1982.
137. Thubrikar M, Piepgrass WC, Deck DJ, Nolan SP. Stresses of natural versus prosthetic aortic valve leaflets. *Ann Thorac Surg* 1980; 30: 230-39.
138. Thubrikar M, Skinner JR, Eppink RT, Nolan SP. Stress analysis of porcine bioprosthetic heart valves in vivo. *J Biomed Mat Res* 1982; 16: 811-26.
139. Thubrikar M, Skinner JR, Aouad J, Finkelmeier BA, Nolan SP. Analysis of the design and dynamics of aortic bioprostheses in vivo. *J Thorac Cardiovasc Surg* 1982; 84: 181-90.
140. Ghista DN. Towards an optimum prosthetic bileaflet aortic valve design. *Med Biol Eng Comput* 1976; 5: 122-25.
141. Ghista DN, Reul H. Optimal prosthetic aortic leaflet valve. *J Biomech* 1977; 10: 313-24.
142. Corry AE, Corry RL. Improvements in or relating to support frames for use in cardiac operations. British Patent 1264471, 1968.
143. Batten RJ. Tricuspid tissue prosthetic heart valve. United States Patent 4172295, 1979.
144. Ionescu MI. Improvements to support frames for use in cardiac operations. UK Patent 47204169, 1969.
145. Reul H. Artificial heart valve. UK Patent 1443221, 1973.
146. Davis RB, Skelton J, Clarke RE, Swanson WM. United States Patent 4, 297749, 1981.
147. Black MM, Drury PJ, Tindale WB. Heart valve replacements. European Patent Application 0116236, 1983.

148. Reis RL, Hancock WD, Yarbrough JW, Glancy DL, Morrow AG. The flexible stent. *J Thorac Cardiovasc Surg* 1971; 62: 683-89.
149. Wheatley DJ, Fisher J, Reece IJ, Spyt T. Mechanism of failure in pericardial heart valves. *J Thorac Cardiovasc Surg* 1986 (In Press).
150. Fisher J, Reece IJ, Wheatley DJ. Laboratory evaluation of the design, function and durability of four pericardial heart valves. *Proc Seminar Heart Valve Engineering, I MechE, London* 1986 (In Press).
151. Fung YCB. Elasticity of soft tissue in simple elongation. *Am J Physiol* 1967; 213: 1532-44.
152. Hildebrandt J, Fukaya H, Martin CJ. Stress-strain relations of tissue sheets undergoing uniform two dimensional stretch. *J App Physiol* 1969; 27: 758-62.
153. Evans JH, Barbenel JC. Structural and mechanical properties of tendon related to function. *Equine Vet J* 1975; 7: 1-8.
154. Clark RE, Finke EH. Scanning and light microscopy of human aortic leaflets in stressed and relaxed states. *J Thorac Cardiovasc Surg* 1974; 67: 792-804.
155. Clark RE. Stress-strain characteristics of fresh and frozen human aortic and mitral leaflets and chordal tendae. *J Thorac Cardiovasc Surg* 1973; 66: 202-08.
156. Broom ND. Stress/strain and fatigue behaviour of glutaraldehyde-preserved heart valve tissue. *J Biomechanics* 1977; 10: 707-24.
157. Broom ND. The observation of collagen and elastin structures in wet whole mounts of pulmonary and aortic leaflets. *J Thorac Cardiovasc Surg* 1978; 75: 121-30.

158. Broom ND. Simultaneous morphological and stress-strain studies of fibrous components in wet heart valve leaflet tissue. *Conn Tiss Res* 1978; 6: 37-50.
159. Broom ND, Thomson FJ. Influence of fixation conditions on the performance of glutaraldehyde-treated porcine aortic valves: towards a more scientific basis. *Thorax* 1979; 34: 166-76.
160. Broom ND. Fatigue-induced damage in glutaraldehyde-preserved heart valve tissue. *J Thorac Cardiovasc Surg* 1978; 76: 202-11.
161. Broom ND. An in vitro study of mechanical fatigue in glutaraldehyde-treated porcine aortic valve tissue. *Biomaterials* 1980; 1: 3-8.
162. Broom ND. Effect of glutaraldehyde fixation and valve constraint conditions on porcine aortic valve leaflets. *Thorax* 1980; 37: 620-26.
163. Thomson FJ, Barret-Boyce BG. The glutaraldehyde treated heterograft valve. *J Thorac Cardiovasc Surg* 1977; 74: 317-321.
164. Lee MJ, Boughner DR, Courtman DW. The glutaraldehyde stabilised porcine aortic valve xenograft. Effect of fixation with or without pressure on the tensile visco-elastic properties of the leaflet material. *J Biomed Mat Res* 1984; 18: 79-98.
165. Ishihara T, Ferrans VJ, Jones M et al. Histological and ultrastructural features of normal human parietal pericardium. *Am J Cardiol* 1980; 46: 744-53.
166. Ishihara T, Ferrans VJ, Jones M et al. Structure of bovine parietal pericardium and of unimplanted Ionescu-Shiley pericardial valvular bioprostheses. *J Thorac Cardiovasc Surg* 1981; 81: 747-57.

167. Eyre DR. Collagen, molecular diversity in the body's protein scaffold. *Science* 1980; 207: 1315-22.
168. Lee JM, Boughner DR. Tissue mechanics of canine pericardium in different test environments. *Circulation Research* 1981; 49: 533-544.
169. Dunn G, Silver FH. Visco-elastic behaviour of human connective tissues. Relative contributions of viscous and elastic components. *Conn Tiss Res* 1983; 12: 59-70.
170. Yin FCP, Chew PH, Shumf RK et al. Biaxial stress-strain properties of myocardium and pericardium. In: *Proceedings of the Meeting on Material Properties and Stress Analysis in Biomechanics*. Institute of Physics Publications 1985; 3-7.
171. Van Noort R, Yates SP, Martin TRP et al. A study of the effects of glutaraldehyde and formaldehyde on the mechanical behaviour of bovine pericardium. *Biomaterials* 1982; 3: 21-26.
172. Reece IJ, Van Noort R, Martin TRP et al. Physical properties of bovine pericardium: a study of the effects of stretching during chemical treatment in glutaraldehyde. *Ann Thorac Surg* 1981; 33: 480-5.
173. Trowbridge EA, Lawford PV, Crofts CE et al. The mechanical properties of natural and chemically modified bovine pericardium. In: *Proceedings of the Meeting of Material Properties and Stress Analysis in Biomechanics*. Institute of Physics Publications 1985; 9-14.
174. Trowbridge EA, Black MM, Daniel CL. The mechanical response of glutaraldehyde fixed pericardium to uniaxial load. *J Mat Sci* 1985; 20; 114-40.

175. Trowbridge EA, Roberts KM, Crofts CE, Lawford PV. Pericardial heterografts: towards better quality control of the mechanical properties of glutaraldehyde fixed leaflets. *J Thorac Cardiovasc Surg* 1986 (In Press).
176. Weigner AW, Bing OHL. Mechanical and structural properties of canine pericardium. *Circ Res* 1981; 49: 807-14.
177. Trowbridge EA, Crofts CE. The standardisation of gauge length: its influence on the relative extensibility of natural and chemically-modified pericardium. *J Biomechanics* 1986 (In Press).
178. Elias H, Boyd JL. Notes on the anatomy, embryology and histology of pericardium. *Journal of New York College of Medicine* 1960; 2: 50-78.
179. Barbenel JC, Zioupos P, Fisher J. The mechanical properties of bovine pericardium. *Proceedings of Seminar in Heart Valve Engineering*. London: Institute of Mechanical Engineers; 1986 (In Press).
180. Carpentier A, Ladislas R, Lemaigre G et al. Biological factors affecting long-term results of valvular heterografts. *J Thorac Cardiovasc Surg* 1969; 58: 467-483.
181. Carpentier A, Dubost C. From xenograft to bioprosthesis. In: Ionescu MI, Ross DN, Weaver DH, eds. *Biological tissue in heart valve replacement*. London: Butterworths, 1972; 515-41.
182. Nose Y, Inai Y, Tajima Y et al. Cardiac prostheses utilizing biological material. *J Thorac Cardiovasc Surg* 1971; 62: 714-24.
183. Picha GJ, Gibbons DF. Glutaraldehyde on pericardium. In: Williams D, ed. *Biocompatibility of implant materials*. Kent, England: Sector Publishing, 1976; 193-201.

184. Bowes JH, Cater CW. The reaction of glutaraldehyde with proteins and other biological materials. *J Royal Micros Soc* 1966; 50: 193-200.
185. Woodroof EA. The chemistry and biology of aldehyde-heated tissue heart valve xenografts. In: Ionescu MI, ed. *Tissue heart valves*. London: Butterworths, 1979; 349-62.
186. Hadat MA. Fixation. In: *Principles and Techniques of Electromicroscopy: Biological Applications*, 1981; 32-55.
187. Gillet R, Gull K. Glutaraldehyde: its stability and purity. *Histochem* 1972; 30: 162-67.
188. Richards FM, Knowles JR. Glutaraldehyde as a protein crosslinking agent. *J Mol Biol* 1968; 37: 231-233.
189. Hardy FM, Nicholls AC and Rydon HN. The nature of crosslinking of proteins by glutaraldehyde. *J Chem Soc* 1976; I: 958-62.
190. Cheung DT, Nimni ME. Mechanism of crosslinking of proteins I. *Conn Tiss Res* 1982; 10: 187-99.
191. Cheung DT, Nimni ME. Mechanism of crosslinking of proteins II. *Conn Tiss Res* 1982; 10: 201-16.
192. Cheung DT, Perelman N, Ellen CK, Nimni ME. Mechanism of crosslinking of proteins III. *Conn Tiss Res* 1984; 13: 109-115.
193. Gavilanes JG, De Buitrago GG, Lizarbe MA, Municio AM, Olmo N. Stabilisation of pericardial tissue by glutaraldehyde. *Conn Tiss Res* 1984; 13: 37-44.
194. Lelous M, Allain JC, Cohen-Solal L et al. Hydrothermal isometric tension curves from different connective tissue. *Conn Tis Res* 1983; 11: 199-206.
195. Lawford PV, Stoves JL, Barker AT. *Life Support Systems I*, 1983; 243-5.

196. Gekko K, Koga S. Increased thermal stability of collagen in the presence of sugars and polyols. *J Biochem* 1983; 199-205.
197. Lelous M, Flandin F et al. Influence of collagen denaturation on the chemorheological properties of skin assessed by differential scanning calorimetry and hydrothermal isometric tension measurements. *Biochemica et Biophysica* 1982; 717: 295-300.
198. Black MM, Drury PJ, Tindale WB. A bicuspid bioprosthetic mitral valve. *Proc ESAO* 1982; 9: 116-119.
199. Imamura E, Ishihara H, Isubui T et al. Open versus closed fixation position of bioprostheses. *J Thorac Cardiovasc Surg* 1982; 83: 610-17.
200. Love JM. Rapid intraoperative fabrication of an autogenous tissue heart valve. A new technique. In: Yacoub M, Bodnar E, eds. *Cardiac Bioprostheses*. New York: Yorke Medical Books, 1986 (In Press).
201. Love JM. A tricuspid prosthetic tissue heart valve. *American Patent* 41470,157, 1984.
202. Hayashi K. Fundamental and applied studies of mechanical properties of living tissue. *Biorheology* 1982; 19: 425-36.
203. Barnhart GR, Ishihara T, Ferrans VJ, Jones M, McIntosh CL, Roberts WC. Intracuspals hematomas in bioprosthetic valves: pathological findings and clinical implications. *Circulation* 1982; 66 Suppl I: 167-71.
204. Barnhart GR, Jones M, Ishihara I et al. Degeneration and calcification of bioprosthetic cardiac valves - animal model: bioprosthetic tricuspid valve implantation in sheep. *Am J Pathol* 1982; 106: 136-42.

205. Deck JD, Thurbrakar MJ, Nolan SP, Aouad J. Role of mechanical stress in calcification of bioprostheses. In: Cohn LN, Gallucci V. Role of mechanical stress in calcification of bioprostheses. New York: Yorke Medical Books, 1982; 293-305.
206. Lawford PV, Roberts K, Drury PJ, Black MM. Valve failure - a pathological and physical study of explanted bioprosthetic valves. Proc ESAO 1986 (In Press).

APPENDIX III

A MICROCOMPUTER-BASED DATA ACQUISITION SYSTEM
FOR A PROSTHETIC HEART VALVE TEST APPARATUS

I MacDonald
J Fisher*
AL Evans
DJ Wheatley*

Department of Clinical Physics and Bioengineering,
West of Scotland Health Board,
and
*Department of Cardiac Surgery,
Royal Infirmary, Glasgow
Scotland

Address for correspondence:
Mr John Fisher
Senior Physicist
Department of Cardiac Surgery
Royal Infirmary, Glasgow G31 2ER
Scotland

Key words: microcomputer, heart, valve

ABSTRACT

The hydrodynamic testing of prosthetic heart valves in the laboratory under pulsatile flow conditions remains the only way of obtaining detailed information about valve function. Test procedures have become increasingly sophisticated with a variety of different test conditions and detailed analysis of the pressure and flow signals.

A computerised data acquisition system has been developed for use with the Glasgow pulsatile flow test apparatus. The computer collects seven signals from the test rig over a period of 20 seconds, and calculates the average waveform for each signal. Standard parameters, such as mean pressure differences, mean flows, regurgitant volumes and energy losses, are calculated automatically. The complexity of the analysis and the need for standardised documentation makes computerisation essential. The system has been used extensively for function tests on over 160 prosthetic heart valves.

INTRODUCTION

Although prosthetic heart valves have been used clinically for over 25 years, the ideal heart valve has not yet been developed. Hydrodynamic testing of prosthetic heart valves under pulsatile flow conditions in the laboratory remains the only way of assessing valve function prior to implantation for evaluation in animals or clinical trials in patients. The tests provide detailed information which cannot be obtained clinically. Valve test methods have become increasingly sophisticated in recent years (1-3) and the pressure and flow signals measured in the apparatus require detailed analysis. As each valve has to be tested in different sizes, and under a range of flow conditions, a computerised data acquisition system is an essential feature of any valve test facility.

The valve test apparatus developed in Glasgow has been described elsewhere (4-6). A diagram of the system is shown in Figure 1. The valve under test can be positioned in either the aortic or mitral position, and a standard control valve is placed in the other position. Essentially it consists of a servocontrolled piston pump (Superpump, Cardiac Development Laboratories) - (2), driven by a programmable waveform generator. Two separate test chambers are used (aortic and mitral) in which the pressure difference across, and flows through, the valve under test can be measured directly. A standard afterload and atrial reservoir complete the apparatus.

The computerised data acquisition system was required to perform the following operations:

- i Monitor seven signals from the test rig (three direct pressure signals, the differential pressure and flow signal for the valve under test, and the displacement and velocity signals from the pump) and display them in real time.
- ii Collect data from the seven signals over a period of 20 seconds, store the data and calculate an average waveform for each signal.
- iii Store the average waveforms on disk and produce graphical printouts of the waveforms.
- iv Calculate from the average waveforms, the mean pressure difference, the mean and the root mean square flows, the volume of fluid displaced through the valve under test, the energy loss and the effective orifice areas (EOA) for different time intervals in the cycle.

Description of the System:

i Computer hardware

The Apple II microcomputer system includes a 12" colour monitor, dual disk drives and Anadex printer (Figure 2). The seven signals to be monitored are connected to a 16 channel 8 bit ADC Card (Interactive structures A1). Timing for the data acquisition is controlled by a clock card which generated an interrupt every one millisecond. Each channel of the ADC card was read 200 times a second (every 5 ms). The ADC gives a resolution of 0.2 mmHg on the differential pressure signal, 1 mmHg on the three direct pressure signals and 2 or 6 ml s⁻¹ on the low or high range for the flow signal. This is similar to the accuracy quoted for the transducers.

ii Software

The programs are menu-driven and are divided up into sections with each section of the program being loaded separately from disk.

The various modes selectable from the menu are:

- i Calibration
- ii Display and acquisition
- iii Graphs
- iv Calculations

In the calibration mode each signal can be calibrated by either entering a predetermined conversion factor or by calibrating the transducer with reference signals. This mode also allows reconfiguration of the signal inputs when changing from the mitral to aortic test positions. Calibration is carried out before each valve is tested and the zero reset on the pressure and flow channels immediately before the data is acquired in an attempt to eliminate drift in the transducers. Calibration factors are stored on the program disk.

In the display mode the monitor displays any three signals in real time along with a digital display of the pump rate, the stroke volume of the pump, and the mean aortic pressure. These are the critical parameters in setting the test conditions. In a test run, data is acquired over a period of twenty seconds and is stored in a temporary file. The variation in the period of the cycle is calculated over the acquisition period and the average cycle period is calculated from the displacement signal of the pump. The data

from each signal is processed automatically to calculate an average waveform. The time reference point for each cycle is taken from the pump displacement signal. When the data from all seven signals has been processed the average waveforms are stored on a data disk file.

In the print graphs mode, any of the seven average waveforms can be plotted on the Anadex printer. Examples of the pressure and flow waveforms are shown in Figure 3. Both the x and y axis scales can be varied for the printouts.

In the calculation mode, the differential pressure waveform and the flow waveform are displayed consecutively on the screen in order to set the time intervals over which the analysis is carried out. On the flow waveform a vertical cursor is placed automatically at the start of forward flow (point 1), the end of forward flow (point 4) and the end of the closing regurgitation (point 5) (see Figure 3). The cursor position can also be moved from the keyboard. For the differential pressure waveform the start of positive pressure (point 2) and the end of positive pressure (point 3) are also determined (Figure 3). In addition, the peak differential pressure and forward flow are identified with horizontal cursors. These reference points are stored in the memory and the following parameters are calculated: the rate and stroke volume of the pump, and the volumes displaced through the valve during forward flow (points 1 to 4), during the closing regurgitation (points 4 to 5) and during the period the valve was closed (points 5 to 1). Four time intervals during forward flow are defined (points 1 to 3, 1 to 4, 2 to 3, and 2 to 4) and the mean pressure difference, mean and root mean square (RMS) forward flow through the valve, and the effective orifice area of the open valve

(3) are calculated for each interval. In addition, the energy loss associated with the flow through the valve is calculated for each of the time intervals. An example of a printout of the results of these calculations is shown in Figure 4.

The system takes approximately 15 minutes to acquire and process the data, print the graphs and carry out the calculations.

Most of the programs are written in BASIC with assembly language routines to speed up the data acquisition and display, the calculation of averages, and graph plotting on the printer. A Basic Interface Area with resident variables is defined in memory to allow communication between the program segments that are loaded from disc.

DISCUSSION

Evaluation of the hydrodynamic function of prosthetic heart valves under pulsatile flow conditions requires detailed analysis of the flow and pressure signals associated with the fluid flow through the valves. This involves calculating an average waveform over several cycles, calculating mean and root mean square values for the signals, and integrating the signals to obtain the volume displaced and the energy loss. Although real time displays can be obtained on oscilloscope or analogue printers and the calculation carried out manually, the complexity of the analysis and the need for standardised documentation makes computerisation necessary. The system which has been developed has been extensively used with function tests carried out on over 60 different commercial valves, over 100 prototype valves of a new design of prosthetic valve, and a series of explanted

clinical prosthetic valves. The important parameters which are determined during these function tests are the mean pressure difference across the valve during forward flow and its effective orifice area, the volume of regurgitation passing back through the valve during closure, the leakage backflow through the closed valve, and the energy losses associated with both forward and reverse flow phases of the cycle.

The main advantages of the system are rapid calculation and analysis, compared with manual processing, efficient storage of data with easy access, and the production of standardised documentation of results and graphs. The real time displays and calibration modes simplified the operation of the test apparatus.

Although the system has the disadvantage of limited memory and graphics handling facilities, it represents good value for money and performs efficiently and reliably.

This software is freely available for Health Service users.

REFERENCES

1. Tindale WB, Trowbridge EA (1983). Evaluation in vitro of prosthetic heart valves: pulsatile flow through a compliant aorta. *Life Support Systems*, 1, pp 173-83.
2. Scotten LN, Walker DK, Brownlee RT (1979). Construction and evaluation of a hydromechanical simulation facility for the assessment of mitral valve prosthesis. *J Med Eng Technol*, 3, pp 1-18.
3. Yoganathan AP, Corcoran WH, Harrison EC (1979). Pressure drops across prosthetic aortic heart valves under steady and pulsatile flow in vitro. *J Biomechanics*, 12, pp 153-64.
4. Fisher J, Jack GR, Wheatley DJ (1986). Design of a function test apparatus for prosthetic heart valves. Initial results in the mitral position. *Clin Phys Physiol Meas*, 7, pp 63-73.
5. Simpson I, Fisher J, Reece IJ et al (1986). In vitro comparison of bioprosthetic valve function using Doppler ultrasound. *Cardiovascular Research*, 20, pp 317-21.
6. Fisher J, Reece IJ, Wheatley DJ (1986). In vitro evaluation of six mechanical and six bioprosthetic valves. *Thorac Cardiovasc Surg*, 37, pp 157-64.

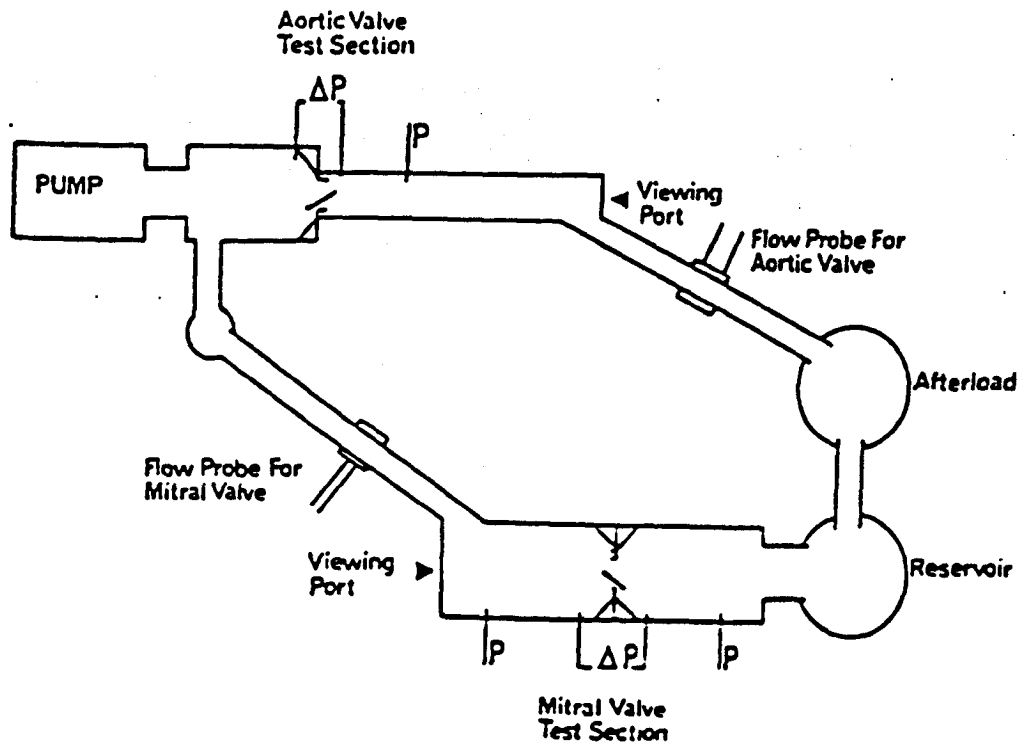


Figure 1: Diagram of the pulsatile flow test apparatus. P shows the position of the direct pressure measurements, ΔP shows the position of the differential pressure transducer for either the aortic or the mitral position.

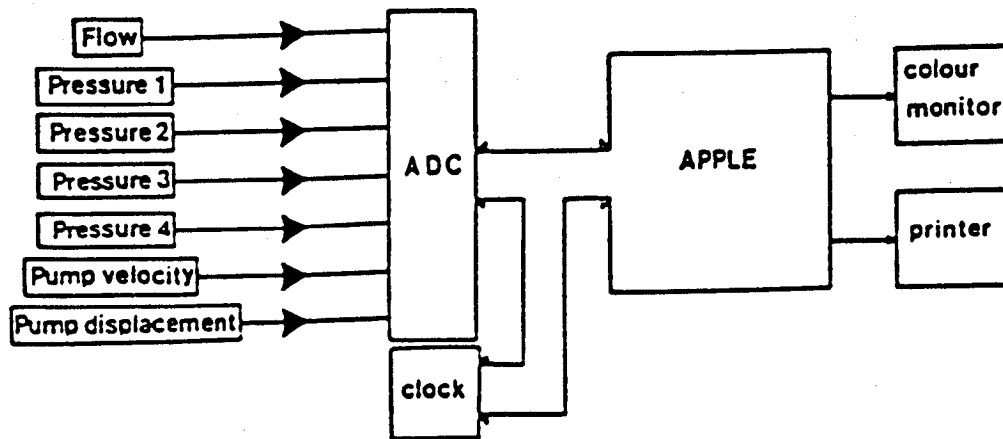


Figure 2: Schematic diagram of the computer system.

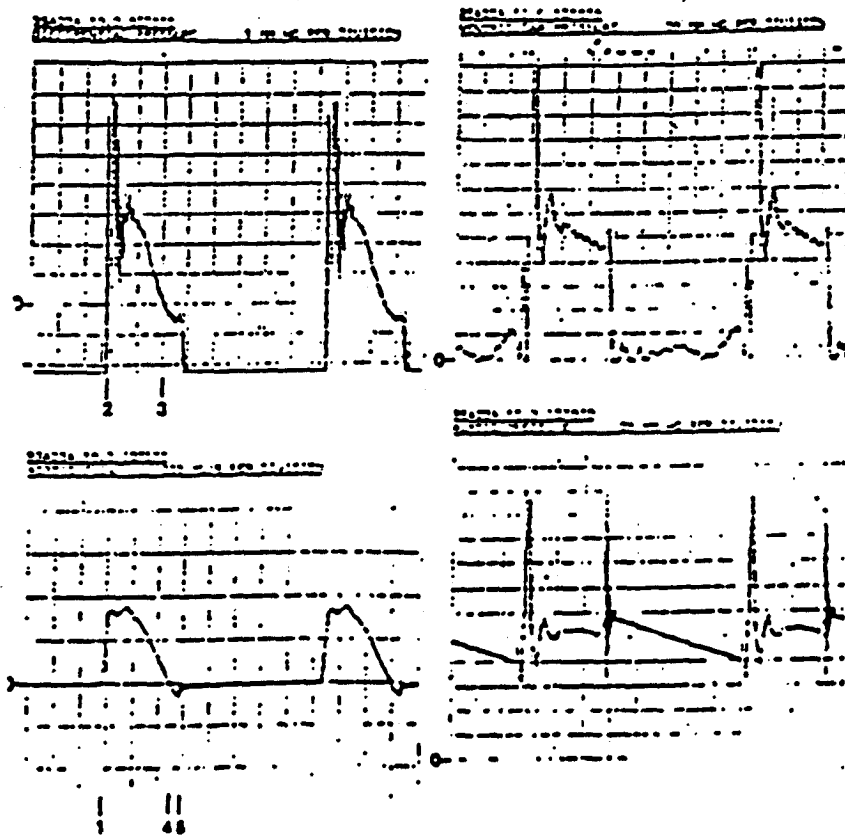


Figure 3: Examples of the print-outs for the average waveforms for the differential pressure aortic flow, ventricular pressure and aortic pressure. The time scale on the x axis is 100 ms per division.

JUL23A 50.0 027070
 ACQUIRED 4/7/85
 MEAN PERIOD = 949.7 MS (S.D. = 4.7 MS)
 RATE = 70.6/MIN
 DATA ACQUIRED OVER 25 CYCLES
 TIMES:
 START OF FORWARD FLOW = 225 MS
 START OF FORWARD PRESSURE = 280 MS
 END OF FORWARD PRESSURE = 500 MS
 START OF RECIRCITANT FLOW = 545 MS
 START OF LEAKAGE FLOW = 590 MS
 (TOTAL PERIOD OF CYCLE = 850 MS)

	FORWARD	RECIRC.	LEAKAGE
PER. (MS)	260	45	245
VOL. (ML)	60.32	-1.72	-6.15

ZERO POINTS	PRESS. (MM HG)	FLOW (ML/S)	RMS FLOW (ML/S)	EOA (CM ²)
FLOW	9.92	232	255.2	1.57
PRESS.	12.22	261.5	275	1.53
PR,FL	9.9	227.5	253.1	1.56
FL,PR	12.3	267.2	275.2	1.54

ENERGIES (MILLIJOULES):
 255-279 (245MS): 272.22 MJ 72.45 ML
 280-499 (220MS): 98.4 MJ 27.52 ML
 500-544 (45MS): -0.35 MJ 2.79 ML
 545-589 (45MS): 1.04 MJ -1.73 ML
 590-824 (235MS): 73.11 MJ -6.15 ML

PEAK FLOW = 354.7 ML/S
 PEAK PRESSURE = 17.27 MM HG
 EOA = 1.74 CM²

Figure 4: An example of the computer print-out of the calculation and analysis which gives the valve reference number and date of test; the reference times for different phases of the cycle; the time period (PER) in milliseconds (MS) and volume (VOL) in millilitres (ML); the mean pressure (PRESS), mean flow (FLOW), root mean square flow (RMS FLOW), and effective orifice area (EOA) calculated for four time periods during forward flow defined by zero points of the flow waveform (FLOW), pressure waveforms (PRESS), start of the pressure and end of the flow (PR, FL), and start of the flow and end of the pressure (FL, PR); the energy loss in millijoules (MJ) and volume passing through the valve are also given; REGURG defines the period of closure of the valve and LEAKAGE the period when the valve is closed.

APPENDIX IV

CALCULATION OF ENERGY LOSS

The energy loss is calculated from the product of the pressure difference across the valve, and flow through the valve, integrated with respect to time during each phase of the cycle (39). During forward flow the energy loss is calculated from the differential pressure signal and flow signal digitised at 5 mS intervals on the computer (115,116). During reverse flow the reverse pressure difference is much greater and is outwith the range of the differential pressure transducer. During the closing and closed phases of the cycle the computer calculates the pressure differences from the two direct pressure measurements on either side of the valve which are digitised at 5 mS intervals. This is multiplied by the flow through the valve at each time interval to give the power loss, which is then integrated with respect to time during each phase of the cycle. During closing regurgitation there is little energy loss until the reverse pressure increases rapidly just before the valve is fully closed. At this point there is a peak in the power loss curve (39) as the pressure rises rapidly and the flow reduces rapidly. In tissue valves, where the valve and leaflets are compliant, energy is stored in the valve as the leaflets and frame are displaced under the back pressure. This can make it difficult to define the precise point at which the valve has closed to distinguish between the closing and closed regurgitant energy losses. In addition the rapid rise in pressure and pressure oscillations which are dependent on the compliance of the valve under test make it difficult to determine

the exact time when the valve is fully closed.

The loss of energy calculated is in effect the loss of potential energy between the two pressure measurement points. Most of this is converted into kinetic energy. In the mitral position this kinetic energy is dissipated downstream of the valve so the loss of potential energy measured is the total energy loss. In the aortic valve, pressure recovery can occur which results in the recovery of potential energy beyond the downstream pressure measurement point. The fraction recovered is dependent on the geometry and dimensions of the aorta. This is not calculated in my system. During regurgitant flow it is assumed that all the kinetic energy is dissipated, so the loss of potential energy is the total energy loss.

Care has to be taken in interpreting energy loss calculations. In the mitral position reverse flow energy losses are due to work carried out by the left ventricle, while high forward flow energy losses are a consequence of high pressures in the left atrium. Clinically it may be more important to minimise the forward flow energy losses in prosthetic mitral valves. In the aortic position energy losses during forward and reverse flow are due to work carried out by the left ventricle. During closing regurgitation the pressure difference across the valve and, consequently, energy loss is small. However, if the energy loss was calculated as the additional work needed to move the equivalent volume of fluid forward through the valve to compensate for the regurgitation it would be much greater.

